

**NUMERICAL STUDY OF HELICAL SAVONIUS ROTOR IN
URBAN AREAS**

SAIF ZEYAD MUSTAFA

**DISSERTATION SUBMITTED IN PARTIAL FULFILMENT
OF THE REQUIREMENTS FOR
THE DEGREE OF MASTER OF ENGINEERING**

**FACULTY OF ENGINEERING
UNIVERSITY OF MALAYA
KUALA LUMPUR**

JUNE 2011

ABSTRACT

Wind energy has a huge role in the production of free electricity in urban areas. Usage of helical wind turbine as a power producer is low cost compare to other horizontal wind turbines. Helical savonius wind turbine has a wide range of mechanical design parameters to meet the numerous design requirements. A total of 10 prototypes have been designed using the pro engineer program which are divided into a few mechanical design considerations like aspect ratio, separation gap and Bach cross-section profile, in order to study the behavior of the rotor through using a numerical analysis program like cfdesign. Therefore, this study introduce a new mechanical design considerations to improve the performance over ($c_p=0.2$) using computational fluid dynamics (CFD) and analyze the results, helical rotor found to have ($c_p=0.26$) with a Bach cross-section of (90° to 20°), considering the wind resources in Malaysia.

ABSTRAK

Tenaga angin memainkan peranan yang sangat besar dalam pengeluaran kuasa percuma di kawasan bandar. Penggunaan Turbin Angin Helical (“Helical Wind Turbine”) sebagai pengeluar kuasa adalah rendah kosnya berbanding dengan turbin angin mendatar (“Horizontal Wind Turbines”) yang lain. Turbin Angin Helical Savonius (“Helical Savonius Wind Turbine”) mempunyai pelbagai macam rekacipta parameter mekanik untuk memenuhi keperluan lain-lain jenis rekaan/ciptaan. Sebanyak 10 prototaip telah direkacipta menggunakan program Pro Engineer (“pro engineer program”) yang kemudian dibahagikan menjadi beberapa pertimbangan desain mekanikal seperti aspek nisbah, jurang pemisahan dan profil penampang Bach (“Bach cross-section profile”), untuk mengkaji perilaku rotor melalui penggunaan program analisis berangka seperti “cfdesign”. Oleh kerana itu, berdasarkan sumber-sumber angin di Malaysia, pengajian ini memperkenalkan reka bentuk mekanikal yang baru untuk meningkatkan prestasi di atas ($c_p=0.26$) menggunakan komputer dinamik bendalir (“computational fluid dynamics” – CFD) dan apabila dianalisa hasilnya, didapati rotor helical mempunyai ($c_p=0.26$) dengan penampang Bach (90° to 20°).

ACKNOWLEDGMENT

First, I would Like to thank god, for giving me the strength courage to endlessly pursue what is so called knowledge.

I would like to express my sincere gratitude and deepest appreciation to my supervisor Prof. Dr. Zahari Taha for his attention to every work I have done at each project phase. He provides lots of useful opinions, suggestions, guidance and comments regarding to this thesis. with his support, kind assistance and encouragement during all the stages, I am able to complete my project.

I would like to express my special thanks and extremely grateful to my family starting by my father Mr. Zeyad Mustafa and my mother Mrs. Muaad who support me throughout this research and my brother Mr. Mustafa for the courage to finish this dissertation with them deepest love.

Also I wish to thank Wan Faudziah for all her support and assistance and my dear friends Mr. Zaid Esam and Mr. Ahmed Al-ani for them help through my study and listening to my complaints, and my extremely grateful to all my friends in UM who have supplied me with unlimited encouragement and friendship throughout my period of study.

TABLE OF CONTENTS

| | Page | |
|---|--|------------|
| ABSTRACT | | Ii |
| ABSTRAK | | Iii |
| ACKNOWLEDGMENTS | | Iv |
| TABLE OF CONTENTS | | V |
| LIST OF FIGURES | | X |
| LIST OF TABLES | | Xiv |
| LIST OF SYMBOLS AND ABBREVIATION | | Xv |
| CHAPTER ONE : INTRODUCTION | | |
| 1.1 | Background | 1 |
| 1.2 | General | 1 |
| 1.3 | Historical Development | 2 |
| 1.4 | Wind Turbine Configuration | 4 |
| 1.4.1 | Drag-Type Wind Turbines | 4 |
| 1.4.2 | Lift-Type Wind Turbines | 5 |
| 1.4.3 | Magnus Effect Wind Machines | 8 |
| 1.4.4 | Vortex Wind Machines | 8 |
| 1.5 | Wind Turbine Types | 9 |
| 1.5.1 | Wind Turbines with Horizontal Rotor Axis | 9 |
| 1.5.1.1 | System Components | 9 |

| | | |
|--|---|----|
| 1.5.2 | Wind Turbines with Vertical Rotor Axis | 11 |
| 1.6 | Commercial Applications of Wind Turbines | 11 |
| 1.6.1 | Stand-Alone Applications | 11 |
| 1.6.2 | Small grids with Diesel Generators and Wind Turbines | 12 |
| 1.6.3 | Wind Turbines Interconnected with Large Utility Grids | 12 |
| 1.7 | Problem Statement | 12 |
| 1.8 | Objectives | 13 |
| 1.9 | Chapters Layout | 13 |
| CHAPTER TWO : LITERATURE REVIEW | | 14 |
| 2.1 | Background | 14 |
| 2.2 | Basic Concept of Wind Energy Converters | 15 |
| 2.3 | Physical Principles of Wind Energy Conversion | 17 |
| 2.3.1 | Betz's Elementary Momentum Theory | 17 |
| 2.3.2 | Power Extracted from the Wind | 18 |
| 2.3.3 | Rotor Swept Area | 21 |
| 2.3.4 | Wind Energy Converters Using Aerodynamic Drag or Lift | 22 |
| | 2.3.4.1 Drag Devices | 23 |
| | 2.3.4.2 Rotors using Aerodynamic Lift | 27 |
| 2.4 | Types of Wind Turbine | 28 |
| 2.4.1 | Horizontal Axis Wind Turbine | 29 |
| 2.4.2 | Vertical Axis Wind Turbine | 31 |
| | 2.4.2.1 H-Rotors | 32 |
| | 2.4.2.2 Darrieus Wind Turbines | 33 |
| | 2.4.2.3 Savonius Wind Turbine | 35 |
| 2.5 | Horizontal Axis Versus Vertical Axis | 39 |

| | | |
|---------|--|----|
| 2.6 | Savonius Wind Turbine Characteristics | 40 |
| 2.6.1 | The Rotor Aspect Ratio | 40 |
| 2.6.2 | The Rotor Overlap Ratio | 42 |
| 2.6.3 | The Rotor Twisted Angle | 43 |
| 2.6.4 | The Rotor Blades Number | 44 |
| 2.6.5 | The Separation Gap | 45 |
| 2.6.6 | Cross-section Profile | 46 |
| 2.7 | Wind Turbine Performance Parameters | 47 |
| 2.8 | Wind Turbines in Commercial Stand Alone Applications | 47 |
| 2.8.1 | Autonomous Power Supply and Storage Problems | 48 |
| 2.8.2 | Residential Heating | 50 |
| 2.8.3 | Pumping Water | 51 |
| 2.8.4 | Desalination of Sea Water | 52 |
| 2.9 | Conclusions | 53 |
| | CHAPTER THREE : METHODOLOGY | 54 |
| 3.1 | Introduction | 54 |
| 3.2 | Wind Data Collection | 56 |
| 3.3 | Data collection and analysis | 56 |
| 3.4 | Computational Fluid Dynamic (CFD) | 57 |
| 3.4.1 | Material Selection | 57 |
| 3.4.2 | Boundary Conditions | 58 |
| 3.4.3 | Mesh Generation | 58 |
| 3.4.4 | Turbulence Method | 58 |
| 3.4.4.1 | The Continuity Equation | 59 |
| 3.4.4.2 | The Momentum Equation | 60 |

| | | |
|---|---|-----------|
| 3.4.4.3 | K-E Two-Equation Model | 61 |
| CHAPTER 4: RESULTS AND DISCUSSIONS | | 63 |
| 4.1 | Wind Speed | 63 |
| 4.2 | Wind Speed Comparison | 66 |
| 4.3 | Mean Wind Speed and Standard Deviation | 67 |
| 4.4 | Prototyping | 68 |
| 4.4.1 | Aspect Ratio | 68 |
| 4.4.1.1 | Aspect Ratio (3:1) | 69 |
| 4.4.1.2 | Aspect Ratio (4:1) | 70 |
| 4.4.1.3 | Aspect Ratio (5:1) | 71 |
| 4.4.2 | Separation Gap (20mm Minus and 20 mm Plus) | 72 |
| 4.4.2.1 | Separation Gap 20mm Minus | 72 |
| 4.4.2.2 | Separation Gap 20mm Plus | 72 |
| 4.4.3 | Bach Shape for the Blade | 73 |
| 4.4.3.1 | Bach Shape with Outer Edge of 20° and Inner Edge of 90° | 73 |
| 4.4.3.2 | Bach Shape with Outer Edge of 40° and Inner Edge of 70° | 74 |
| 4.4.3.3 | Bach Shape with Outer Edge of 60° and Inner Edge of 40° | 75 |
| 4.4.3.4 | Bach Shape with Outer Edge of 80° and Inner Edge of 30° | 76 |
| 4.4.3.5 | Bach Shape with Outer Edge of 90° and Inner Edge of 20° | 77 |
| 4.5 | Grid and Meshing | 78 |
| 4.6 | Wind Distribution Over The Rotor | 79 |
| 4.7 | Coefficient of Power | 80 |
| 4.7.1 | Coefficient of Power for Different Aspect Ratio | 81 |

| | | |
|---|---|----|
| 4.7.2 | Coefficient of power for different separation gap | 82 |
| 4.7.3 | Coefficient of power for Bach Cross-Section Profile with different inner and outer edge Angle | 83 |
| 4.8 | Coefficient of Torque | 84 |
| 4.8.1 | Coefficient of Torque for Different Aspect Ratio | 84 |
| 4.8.2 | Coefficient of torque for different separation gap | 85 |
| 4.8.3 | Coefficient of Torque for Bach Cross-Section Profile with different inner and outer edge Angle | 86 |
| 4.9 | Output power | 87 |
| 4.9.1 | Output Power for Different Aspect Ratio | 87 |
| 4.9.2 | Output Power for Different Separation Gap | 88 |
| 4.9.3 | Output Power for Bach Cross-section Profile with Different Inner and Outer Edge Angle | 89 |
| CHAPTER 5: CONCLUSIONS AND RECOMMENDATIONS | | 91 |
| 5.1 | Conclusions | 91 |
| 5.2 | Recommendations for Further Work | 92 |
| REFERENCES | | |

LIST OF FIGURES

| No | Description | Page |
|-----|--|------|
| 1.1 | A2-bucket Wind Turbine(Aldo Vieira da Rosa, 2005) | 5 |
| 1.2 | Air Flow in a Savonius (Aldo Vieira da Rosa, 2005) | 5 |
| 1.3 | A horizontal axis (propeller) type turbine, and two vertical axis machines- a "gyromill" and a darrieus (Aldo Vieira da Rosa, 2005) | 7 |
| 1.4 | Diagram of Magnus Effect (Vaughn Nelson, 2009) | 8 |
| 1.5 | Section through the Stall-controlled TW600 Wind Generator (600 kW Change-pole Asynchronous Generator, 43 m Rotor Diameter, 50–70 m Hub Height) (Volker Quaschnig, 2005) | 10 |
| 1.6 | rotors with vertical axis (Volker Quaschnig, 2005) | 11 |
| 2.1 | Typical New Power Capacity Installed in 2008 | 15 |
| 2.2 | Rotor Efficiency Versus V_0/V ratio has Single Maximum. Rotor efficiency is The Fraction of available Wind Power extracted by The Rotor and fed to the Electrical Generator (Mukund R. Patel,1999) | 21 |
| 2.3 | Rotor efficiency versus tip speed ratio for rotors with different numbers of blades. Two-blade rotors have the highest efficiency (Eldridge, 1975).Typical Photography for Filler Types | 22 |
| 2.4 | Drag Coefficients for Various Shapes (Volker Quaschnig, 2005) | 24 |
| 2.5 | Model of Cup Anemometer for the Calculation of Power (Volker Quaschnig, 2005) | 26 |
| 2.6 | Aerodynamic Forces acting on an Airfoil exposed to an Air Stream. (Erick Hau, 2006) | 27 |
| 2.7 | Orientation of the axis of rotation of a horizontal-axis wind turbine | 28 |

| | | |
|------|--|----|
| | In comparison to a vertical-axis wind turbine. (Frank Scheurich, 2009) | |
| 2.8 | Typical Horizontal Wind Turbine Components | 30 |
| 2.9 | Typical Horizontal Wind Turbine Types | 30 |
| 2.10 | H-Rotor-type Vertical axis Wind Turbine (Mazharul Islam, 2008) | 33 |
| 2.11 | Typical Photograph of Curved-Blade Darrieus Wind Turbine | 35 |
| 2.12 | Illustration of positive Torque and Negative Torque (U. K. Saha, 2008) | 36 |
| 2.13 | Savonius-type Vertical axis Wind Turbine (Mazharul Islam, 2008) | 38 |
| 2.14 | Typical Photograph of Helical Savonius Wind Turbine | 39 |
| 2.15 | Aspect Ratio (Ibrahim Al-Bahadly, 2009) | 41 |
| 2.16 | Overlap Ratio (Ibrahim Al-Bahadly, 2009) | 42 |
| 2.17 | Four types Helical Rotor with Different Twist Angle (Zhenzhou Zhao, 2010). | 44 |
| 2.18 | The Fluid Field of Two and Three Blades Rotor (Zhenzhou Zhao, 2010) | 45 |
| 2.19 | Separation Gap (Ibrahim Al-Bahadly, 2009) | 46 |
| 2.20 | Cross-section Profile (Ibrahim Al-Bahadly, 2009) | 46 |
| 2.21 | Flywheel storage system developed by Enercon(Erick Hau, 2006) | 50 |
| 2.22 | Wind-supported irrigation system with an Aeroman wind turbine and two underwater electric well pumps (Erick Hau, 2006) | 52 |
| 3.1 | Flow chart for the Helical Wind Turbine Design and Analysis | 55 |
| 4.1 | Histogram of frequency of wind speed at kuala Terengganu station | 63 |
| 4.2 | Histogram of frequency of wind speed at Kota Bharu station | 66 |
| 4.3 | Graph of comparison of Wind speed | 67 |
| 4.4 | Front and Top View of Helical Wind Turbine with 3:1 Aspect Ratio | 69 |
| 4.5 | Schematic of the Helical Wind Turbine 3:1 Aspect Ratio Top View | 69 |
| 4.6 | Front and Top View of Helical Wind Turbine with 4:1 Aspect Ratio | 70 |
| 4.7 | Schematic of the Helical Wind Turbine 4:1 Aspect Ratio Top View | 70 |

| | | |
|------|---|-----|
| 4.8 | Front and Top View of Helical Wind Turbine with 5:1 Aspect Ratio | 71 |
| 4.9 | Schematic of the Helical Wind Turbine 5:1 Aspect Ratio Top View | 71 |
| 4.10 | Front and Top View of Helical Wind Turbine with Minus Separation Gap | 72 |
| 4.11 | Front and Top View of Helical Wind Turbine with plus Separation Gap | 73 |
| 4.12 | Front and Top View of Helical Wind Turbine with Bach Shape 20 to 90 | 74 |
| 4.13 | Schematic of the Helical Wind Turbine with Bach 20 to 90 | 74 |
| 4.14 | Front and Top View of Helical Wind Turbine with Bach Shape 40 to 70 | 75 |
| 4.15 | Schematic of the Helical Wind Turbine with Bach Shape 40 to 70 | 75 |
| 4.16 | Front and Top View of Helical Wind Turbine with Bach Shape 60 to 40 | 76 |
| 4.17 | Schematic of the Helical Wind Turbine with Bach Shape 60 to 40 | 76 |
| 4.18 | Front and Top View of Helical Wind Turbine with Bach Shape 80 to 30 | 77 |
| 4.19 | Schematic of the Helical Wind Turbine with Bach Shape 80 to 30 | 77 |
| 4.20 | Front and Top View of Helical Wind Turbine with Bach Shape 90 to 20 | 78 |
| 4.21 | Schematic of the Helical Wind Turbine with Bach Shape 90 to 20 | 78 |
| 4.22 | Mesh Generation for the Wind Tunnel for the Helical Wind Turbine by cfdesign Program | 79 |
| 4.23 | Wind Disturbution Over Bach rotor with with (90°-20°) | 80 |
| 4.24 | the performance curve of rotor with different aspect ratio | 82 |
| 4.25 | The Preformance Curve of Rotor with Diffrnet Sepration Gap | 83 |
| 4.26 | The Preformance Curve of Rotor with Diffrnet Bach Shape | 84 |
| 4.27 | The Coefficient of Torque for Rotor with different Aspect Ratio | 85 |
| 4.28 | The Coefficient of Torque for Rotor with different Separation gap | 86 |
| 4.29 | The Coefficient of torque for Rotor with Diffrnet Bach Shape | 87 |
| A1 | Pressure Distribution for Bach with (90o-20o) | 98 |
| A2 | Pressure Distribution for Bach with (90°-20°) | 99 |
| A3 | Pressure Distribution for Bach with (90°-20°) | 100 |

| | | |
|----|---|-----|
| A4 | Pressure Distribution for Bach with (90°-20°) | 101 |
| B1 | velocity Distribution with wind direction for Bach with (90°-20°) (Top View) | 103 |
| B2 | velocity Distribution with wind direction for Bach with (90°-20°) (Top View) | 104 |
| B3 | velocity Distribution with wind direction for Bach with (90°-20°) (side View) | 105 |
| B4 | velocity Distribution with wind direction for Bach with (90°-20°) (side View) | 106 |

LIST OF TABLES

| No | Description | Page |
|-----------|--|-------------|
| 4.1 | frequency of wind speed for Kuala Terengganu station | 64 |
| 4.2 | frequency of wind speed for Kota Bharu station | 65 |
| 4.3 | Mean wind speed and standard deviation for all stations | 68 |
| 4.4 | Coefficient of Power for different Mechanical Design Considerations Energy | 80 |
| 4.5 | Power Production for Helical Savonius with Different Aspect Ratio | 88 |
| 4.6 | Power Production for Helical Savonius with Different Separation Gap | 89 |
| 4.7 | Power Production for Helical Savonius with Different Inner and Outer Edge Angle for Bach Cross-section Profile | 90 |
| C.1 | Raw data from Kuala Terengganu station 1/1/2006-30/1/2006 | 108 |
| C.2 | Raw data from Kota Bharu station 1/1/2006-30/1/2006 | 109 |

LIST OF SYMBOLS AND ABBREVIATION

| | |
|---------------|--|
| A | Cross- section Area (m^2) |
| C_D | Drag Coefficient |
| C_p | Coefficient of Power |
| $C_{P,OPT,D}$ | Optimum Power |
| C_T | Coefficient of Torque |
| D | Rotor Diameter (m) |
| E | Kinetic Energy (Joules) |
| ϵ | Turbulent Dissipation rate |
| F_D | Drag Force (kg.m) |
| HAWT | Horizontal Axis Wind Turbine |
| M | Mass flow (kg/s) |
| M | Air Mass (kg/s) |
| P | Air Density (kg/m^3) |
| P | Power (watt) |
| P_{fc} | Body Force per unit Volume ($watt/m^3$) |
| P_o | Mechanical Power extracted by the rotor (watt) |
| R | Rotor radius (m) |
| Re | Reynolds Number |
| RPM | Revolution per minute |
| S_{ij} | Strain- rate Tansor (kg/m.s) |
| τ | Viscous Stress Tensor |
| T_{ij}^f | Favre-averaged Turbulent Stresses |

| | |
|------------|--|
| TSR | Tip Speed Ratio |
| u | A Speed of Object move by Influence of the Wind (m/s) |
| v | Velocity (m/s) |
| V | Volume (m^3) |
| V_o | Down Stream Wind velocity at Exit of rotor blade (m/s) |
| VAWT | Vertical Axis Wind Turbine |
| ϵ | Explicit Wall Term |
| λ | Ratio of the circumferential speed to the Wind speed |

CHAPTER ONE

INTRODUCTION

In Malaysia, wind energy conversion is a serious consideration. The potential for wind energy generation in Malaysia depends on the availability of the wind resources that varies with location. Understanding the site-specific nature of the wind is a critical step in planning a wind energy project. Detailed knowledge of wind on-site is needed to estimate the performance of a wind energy project. The first step requires a general assessment of the wind energy potential nationwide.

1.1 Background

The Energy of the wind has been utilized for more than 3000 years. Until the early twentieth century wind power was used to generate mechanical power to pump water or to grind grain. At the starting of modern industrialization, the use of the fluctuating wind energy resource was substituted by fossil fuel fired engines or the electrical grid, which provided a more consistent power source (Thomas Ackermann, 2005).

1.2 General

Wind is a free, clean, and inexhaustible energy source. It has benefited mankind well for many centuries by propelling ships and driving wind turbines to grind grain and pump water. Interest in wind power lagged, however, when cheap and plentiful petroleum products became easy after World War II. The high capital costs and the uncertainty of

the wind placed wind power at an economic disadvantage. Then in 1973, the Arab nations placed an embargo on petroleum. The days of cheap and plentiful petroleum were drawing to an end. People began to realize that the world's oil supplies would finish soon and that remaining supplies should be conserved for the petrochemical industry (Gary L. Johnson, 2006). Wind generators go by several names: wind turbines, wind machines, and wind plants. All Residential wind generators large and small have the same three basic components (Dan Chiras, 2006):

- A blade assembly, commonly referred to as a rotor, that turns in the wind
- A shaft that connects to the rotor and rotates when the blades turn
- A generator, a device that produces electricity

1.3 Historical Development

The use of wind energy dates back to ancient times when it was employed to propel sailboats. Extensive application of wind turbines seems to have originated in Persia where it was used for grinding wheat. The Arab conquest spread this technology throughout the Islamic world and China. In Europe, the wind turbine made its appearance in the eleventh century. Two centuries later it had become an important tool, especially in Holland. The development of the American West was aided by wind-driven pumps and sawmills (Aldo Vieira da Rosa, 2005).

The first wind turbine designed especially for the generation of electricity was built by Charles Brush in Cleveland, Ohio. It operated for 12 years, from 1888 to 1900

supplying the needs of his mansion. Charles Brush was a mining engineer who made a fortune with the installation of arc lights to illuminate cities throughout the United States. His wind turbine was of the then familiar multi-vane type (it sported 144 blades) and, owing to its large solidity, rotated rather slowly and required gears and transmission belts to speed up the rotation by a factor of 50 so as to match the specification of the electric generator. The wind turbine itself had a diameter of 18.3 meters and its hub was mounted 16.8 meters above ground. The tower was mounted on a vertical metal pivot so that it could orient itself to face the wind. The whole contraption massed some 40 tons. Owing to the intermittent nature of the wind, electric energy had to be stored in this case in 400 storage cells. Although the wind is free, the investment and maintenance of the plant caused the cost of electricity to be much higher than that produced by steam plants. Consequently, the operation was discontinued in 1900 and from then on the Brush mansion was supplied by the Cleveland utility (Aldo Vieira da Rosa, 2005).

In 1939, construction of a large wind generator was started in Vermont. This was the famous Smith-Putnam machine, erected on a hill called Grandpa's Knob. It was a propeller-type device with a rated power of 1.3 MW at a wind speed of 15 m/s. Rotor diameter was 53 m. The machine started operation in 1941, feeding energy synchronously directly into the power network. Owing to blade failure, in March 1945, operation was discontinued. It ought to be mentioned that the blade failure had been predicted but during World War II there was no opportunity to redesign the propeller hub (Aldo Vieira da Rosa, 2005).

After World War II, the low cost of oil discouraged much of the alternate energy research and wind turbines were no exception. The 1973 oil crises re-spurred interest in

wind power as attested by the rapid growth in federal funding. This led to the establishment of wind farms that were more successful in generating tax incentives than electric energy. Early machines used in such farms proved disappointing in performance and expensive to maintain. Nevertheless, the experience accumulated led to an approximately 5-fold reduction in the cost of wind-generated electricity. In the beginning of 1980, the cost of 1 kWh was around 25 cents; in 1996 it was, in some installations, down to 5 cents. To be sure, the determination of energy costs is, at best, an unreliable art. Depending on the assumptions made and the accounting models used, the costs may vary considerably (Aldo Vieira da Rosa, 2005).

1.4 Wind Turbine Configuration

Several wind turbine configurations have been proposed, including:

1.4.1 Drag-Type Wind Turbines

In a drag-type turbine, the wind exerts a force in the direction it is blowing that is, it simply pushes on a surface as it does in a sailboat sailing before the wind. Clearly, the surface on which the wind impinges cannot move faster than the wind itself. The bucket wind turbine, sketched in Figure 1.1, is another vertical-axis drag-type device. It rotates because the convex surface offers less wind drag than the concave one. This device can be cheaply built by amateurs using an oil barrel cut along its vertical axis. It operates indecently.

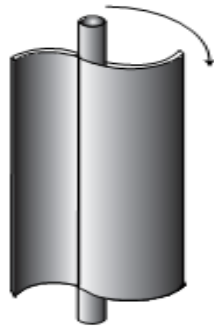


Figure 1.1: A2-bucket Wind Turbine(Aldo Vieira da Rosa, 2005)

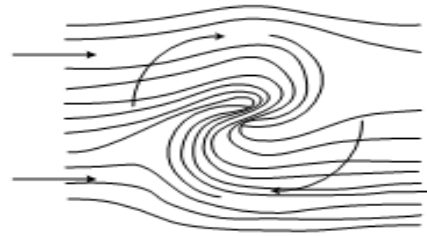


Figure 1.2: Air Flow in a Savonius (Aldo Vieira da Rosa, 2005)

Improved performance can be obtained by keeping a gap between the blades as shown in Figure 1.2. The air is accelerated as it passes the gap reducing the front drag of the convex bucket. It is then blown on the reverse side of the bucket aiding in the creation of torque. This type of device is called a Savonius rotor and actually uses a certain amount of lift (in addition) to drag. Savonius turbines cannot compete in efficiency with pure lift-type machines, but they are easy to build and find application as sensors in anemometers and eolergometers and as starters for vertical-axis lift-type machines (Aldo Vieira da Rosa, 2005).

1.4.2 Lift-Type Wind Turbines

A lift device can produce on the order of 100 times the power per unit surface area of blade versus a drag device (Vaughn Nelson, 2009). In a lift-type machine, the wind generates a force perpendicular to the direction it is blowing. The familiar propeller wind turbines are of the horizontal-axis, lift-type. All lift-type turbines are analogous to sailboats sailing cross wind. The sailboat (or the blade of the turbine) can move substantially faster than the wind itself. Figure 1.3 shows such turbines. Notice that the

propeller-driven shaft that delivers the collected energy is high above ground level. This usually forces one of two solutions: either the electric generator is placed on top of the tower next to the propeller, or a long shaft, with associated gears, is used to bring the power to a ground-level generator. The first solution, although requiring reinforced towers, is the preferred one because of the cost and difficulties of transmitting large mechanical power over long shafts. Mounting the generator on top of the tower increases the mass of that part of the system that has to swivel around when the wind changes direction (Aldo Vieira da Rosa, 2005).

Some wind turbines have the propeller upstream from the generator and some downstream. It has been found that the upstream placement reduces the noise produced by the machine. A propeller wind turbine that employs a ground-level generator but avoids the use of a long shaft is the suction-type wind turbine. It resembles a conventional wind turbine but the rotating blades act as a centrifugal pump. The blades are hollow and have a perforation at the tip so that air is expelled by centrifugal action creating a partial vacuum near the hub. A long pipe connects the hub to an auxiliary turbine located at ground level. The in-rushing air drives this turbine. The system does not seem promising enough to justify further development. One wind turbine configuration not only allows placing the generator on the ground but also avoids the necessity of reorienting the machine every time the wind changes direction. It is the vertical-axis lift-type wind turbine. The one illustrated in the center of Figure 1.3 is a design that was proposed by McDonnell-Douglas and was called Gyromill. It would have been capable of generating 120 kW, but it was never commercialized.

One obvious disadvantage of the gyromill is the centrifugal force that causes the wings to bend outward, placing considerable stress on them. An elegant way to avoid centrifugal stresses is to form the wings in the shape assumed by a rotating rope loosely attached to the top and bottom of the rotating shaft. This leads to the familiar "egg beater" shape and, of course, causes the wing to work only in tension. The shape of such a rotating rope is called a troposkein and resembles closely a catenary (Aldo Vieira da Rosa, 2005).

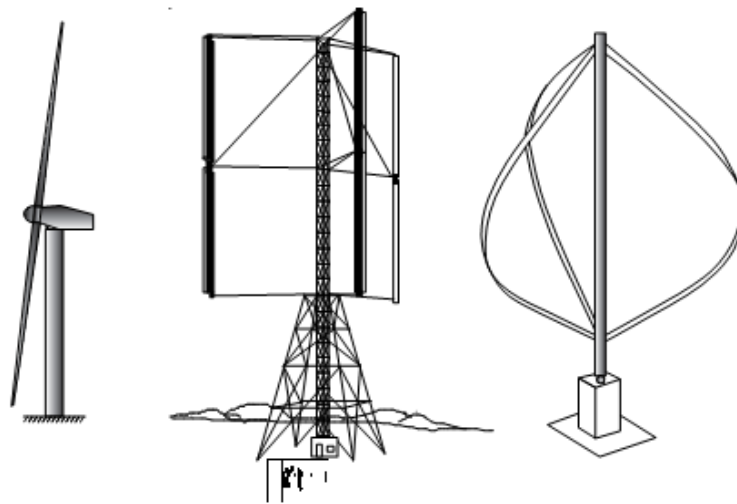


Figure 1.3: from left to right: a horizontal axis (propeller) type turbine, and two vertical axis machines-a "gyromill" and a darrieus (Aldo Vieira da Rosa, 2005)

There is, however, a difference. The catenary is the shape assumed by a perfectly flexible inextensible cord of uniform density and cross-section hanging freely from two fixed points." Each unit length of the cord is subject to the same (gravitational) force. In the case of the troposkein, the force acting on each section of the cord depends on the distance of the section from the axis of rotation. The troposkein wing (right-hand drawing of Figure 1.3) was first suggested by a French engineer called Darrieus after whom this type of wind turbine is named (Aldo Vieira da Rosa, 2005).

1.4.3 Magnus Effect Wind Machines

Magnus effect machines have been proposed but look unpromising. This effect is the one responsible for, among other things, the “curve” in baseball. When a pitcher throws a curve, he causes the ball to spin creating an asymmetry: one side of the ball moves faster with respect to the air than the other and, consequently, generates the “lift” that modifies the trajectory of the ball. An identical effect occurs when a vertical spinning cylinder is exposed to the wind. The resulting force, normal to the wind direction, has been employed to move sailboats and wind machines like in figure 1.4 (Aldo Vieira da Rosa,2005).

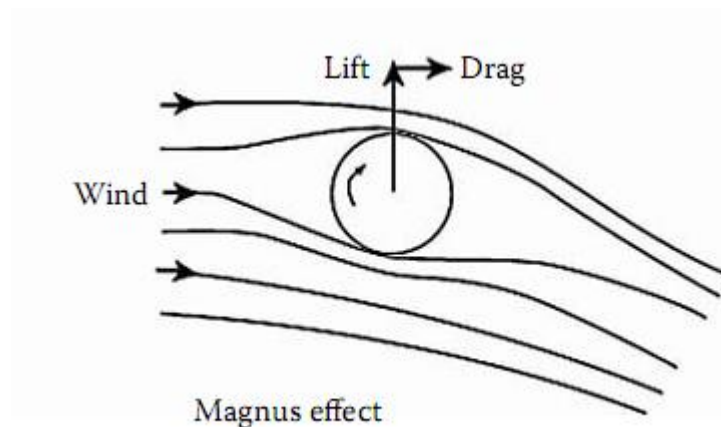


Figure 1.4: Diagram of Magnus Effect (Vaughn Nelson, 2009)

1.4.4 Vortex Wind Machines

Finally, it is possible to abstract energy from the wind by making it enter tangentially through a vertical slit into a vertical hollow cylinder. As a result, the air inside is forced

to gyrate and the resulting centrifugal force causes a radial pressure gradient to appear. The center of this air column, being at lower than atmospheric pressure, sucks outside air through openings at the bottom of the cylinder. The in rushing air drives a turbine coupled to a generator. The spinning air exits through the open top of the cylinder forming a vortex continuously swept away by the wind. This type of machine has been proposed by Gruman (Aldo Vieira da Rosa, 2005).

1.5 Wind Turbine Types

The previous section explained in general how drag and lift devices can utilize wind power. This section describes technical solutions for this utilization. In the past, wind energy was mainly converted to mechanical energy; some modern wind pumping systems also use the mechanical energy directly. However, today the generation of electricity is in higher demand; therefore, a wind rotor drives an electrical generator (Volker Quaschnig, 2005).

1.5.1 Wind Turbines with Horizontal Rotor Axis

1.5.1.1 System Components

Most wind turbines generating electricity today are horizontal axis machines. It is predominantly medium-sized enterprises that have pushed wind market developments. Wind power plants have reached a high technical level and current systems reach powers up to several megawatts, whereas the wind generators of the 1980s were in the

power range below 100 kW. A horizontal axis wind turbine generally consists of the following components see Figure 1.5 (Volker Quaschnig, 2005):

- Rotor blades, rotor hub, rotor brake and if need be, a pitch mechanism
- Electrical generator and if need be, a gearbox
- Wind measurement system and yaw drive (azimuth tracking)
- Nacelle, tower and foundation
- Control, substation and mains connection.

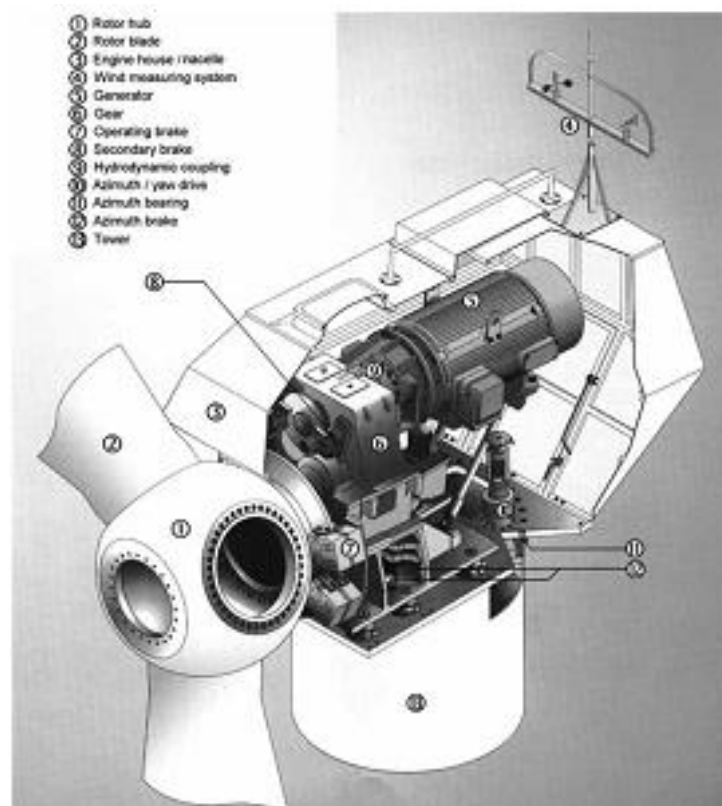


Figure 1.5: Section through the Stall-controlled TW600 Wind Generator (600 kW Change-pole Asynchronous Generator, 43 m Rotor Diameter, 50–70 m Hub Height)

(Volker Quaschnig, 2005)

1.5.2 Wind Turbines with Vertical Rotor Axis

Wind wheels and windmills with vertical axes are the oldest systems to exploit the wind. For more than 1000 years drag devices with vertical axes have been constructed. Today there are some modern wind generator concepts that also have vertical axes as shown in Figure 1.6. Rotor concepts with vertical axis are (Volker Quaschnig, 2005):

- The Savonius rotor
- The Darrieus rotor and
- The H rotor.

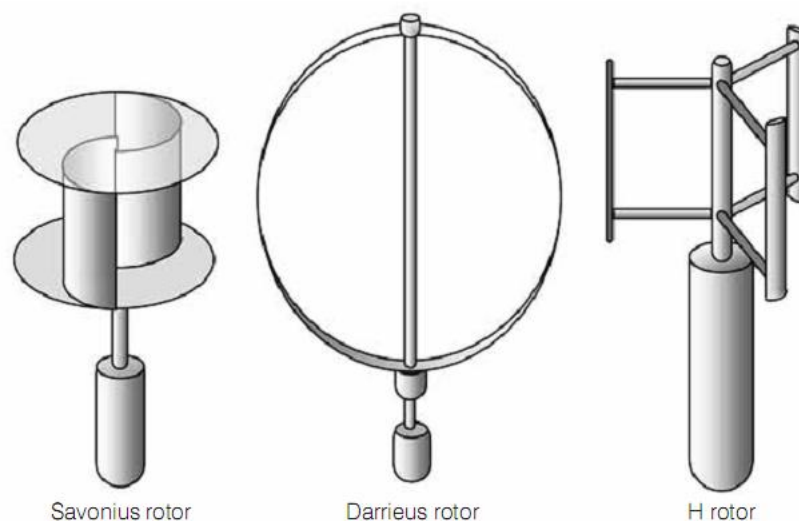


Figure 1.6: rotors with vertical axis (Volker Quaschnig, 2005)

1.6 Commercial Applications of Wind Turbines

1.6.1 Stand-Alone Applications

The first attempts of generating electric current with the help of wind energy were almost always directed at providing independent electrical energy in remote areas without connection to the grid. As long as a few hundred watts of direct current were enough to cover this modest need of electrical energy, generally only for lighting, this object could be achieved with comparatively simple technical means by using a small wind turbine and a storage battery (Erick Hau, 2006) and these applications are:

- Autonomous Power Supply and Storage Problems
- Residential Heating
- Pumping Water
- Desalination of Sea Water

1.6.2 Small grids with Diesel Generators and Wind Turbines

1.6.3 Wind Turbines Interconnected with Large Utility Grids

1.7 Problem Statement

The force of the wind can be very strong and there have been numerous efforts to benefit from this clean power and increase its rate in power generation all over the world. In his study the design of the savonius wind turbine is discussed and reported. The study is required to fulfill the need of clean energy to save the earth and supply cheap energy for Malaysia.

1.8 Objectives

The goal of this study is to determine the feasibility of developing a high efficiency helical type vertical axis wind turbine by modifying the rotor shape with the following objectives:

1. To study and the effect of different separation gap for the rotor and optimize the separation gap.
2. To study the effect of the Bach cross-section with different inner and outer edge angle and optimize the cross section.
3. To study the effect of different aspect ratio for the rotor and optimize the aspect ratio.
4. To increase the efficiency of the vertical axis wind turbine design by applying computational fluid dynamics (CFD) software to optimize the helical shape.

1.9 Chapters Layout

In this thesis, the first chapter explains the wind turbine history, types, uses, the problem statement, objectives and chapter layout; the second chapter explains the researcher's work in this field. The next chapter explains the experimental work and methodology of this project through the design stage and the numerical analysis. Chapter four shows the discussion and results of this study. The fifth contains the conclusion of all the results obtained from the test.

CHAPTER TWO

LITERATURE REVIEW

2.1 Background

The power of the wind is gaining increasing importance throughout the world. This fast development of wind energy technology and of the market has large implications for a number of people and institutions: for instance, for scientists who research and teach future wind power, and electrical engineers at universities; for professionals at electric utilities who really need to understand the complexity of the positive and negative effects that wind energy can have on the power system; for wind turbine manufacturers; and for developers of wind energy projects, who also need that understanding in order to be able to develop feasible, modern and cost-effective wind energy projects (Thomas Ackermann,2005).

The beginning of the twenty-first century is an exciting time for wind energy. With the changes in technology, policy, environmental concern and electricity industry structure which have occurred in recent years, the coming decade offers an unparalleled opportunity for wind energy to emerge as a viable mainstream electricity source and a key component of the world's environmentally sustainable development path. Yet the challenges facing wind energy remain both substantial and complex (Robert Y. Redlinger, 2002).

How much of the world's electricity needs could actually be met using wind energy? This is a question of fundamental importance. Detractors of wind energy, and of renewable energy in general, often assert that modern renewable energy will never contribute more than a few per cent of world energy demand and is therefore not worthy of serious consideration (Robert Y. Redlinger,2002).

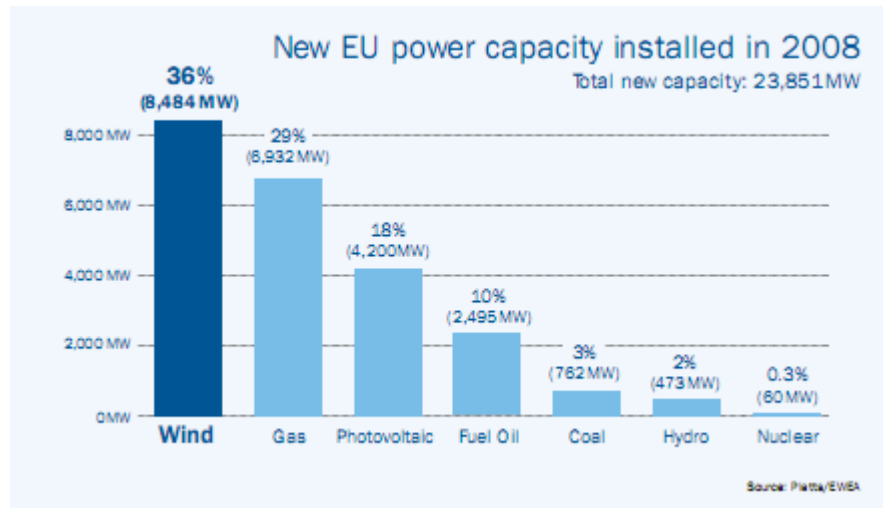


Figure 2.1: Typical New Power Capacity Installed in 2008

2.2 Basic Concept of Wind Energy Converters

There are many different ways in which devices convert the kinetic energy contained in an air stream into mechanical work can be realized and the most bizarre concepts have been proposed. Museums and patent are filled to the rafters with more or less promising inventions of this type. In most cases, however, the practical applicability of these “wind power plants” falls far behind the inventors’ expectations. An attempt to develop an orderly and systematic classification of wind energy converter types is certainly an interesting task, but it brings little reward as the number of significant designs is drastically limited by their practical usefulness. When speaking of varying designs one

should be aware of the fact that primarily varying designs of the wind energy converter, the wind rotor, are meant. But the wind rotor is not the only component of a wind turbine. Other components for the mechanical-electrical energy conversion such as gearbox, generator, control systems and a variety of auxiliary units and items of equipment are just as necessary for producing usable electric energy from the wind rotor's rotational motion. Many inventors of novel wind rotors, however, do not seem to be aware of this fact when they are hoping that their invention of a different rotor design will improve everything (Erick Hau, 2006).

Wind energy converters can be classified firstly in accordance with their aerodynamic function and, secondly, according to their constructional design. The rotor's aerodynamic function is characterized by the fact of whether the wind energy converter captures its power exclusively from the aerodynamic drag of the air stream acting on rotor surfaces, or whether it is able to utilize the aerodynamic lift created by the flow against suitably shaped surfaces. Accordingly, there are so-called "drag-type rotors" and "rotors which make use of the aerodynamic lift". Occasionally, the aerodynamic "tip-speed ratio" is used to characterize wind rotors and one speaks of "low-speed and high-speed rotors" in this case. These characteristics, however, are of little significance to modern wind turbines. Apart from the American wind turbine, almost all other wind turbines designs are of the high-speed type. Classification according to constructional design aspects is more practicable for obvious reasons and thus more common. The characteristic which most obviously meets the eye is the position of the axis of rotation of the wind rotor. Thus, it is important to make a distinction between rotors which have a vertical axis of rotation, and those with a horizontal axis of rotation (Erick Hau, 2006).

2.3 Physical Principles of Wind Energy Conversion

The wind turbine captures the wind's kinetic energy in a rotor consisting of two or more blades mechanically coupled to an electrical generator. The turbine is mounted on a tall tower to enhance the energy capture. Numerous wind turbines are installed at one site to build a wind farm of the desired power production capacity. Obviously, sites with steady high wind produce more energy over the year (Mukund R. Patel, 1999).

The credit for having recognized this principle is owed to Albert Betz. Between 1922 and 1925, Betz published writings in which he was able to show that, by applying elementary physical laws, the mechanical energy extractable from an air stream passing through given cross-sectional area is restricted to a certain fixed proportion of the energy or power contained in the air stream. Moreover, he found that optimal power extraction could only be realized at a certain ratio between the flow velocity of air in front of the energy converter and the flow velocity behind the converter (Erick Hau, 2006).

2.3.1 Betz's Elementary Momentum Theory

The kinetic energy of an air mass m moving at a velocity v can be expressed as:

$$E = \frac{1}{2} m v^2 \quad (\text{Nm}) \quad (2.1)$$

Considering a certain cross-sectional area A , through which the air passes at velocity v , the volume \dot{V} flowing through during a certain time unit, the so-called volume flow, is:

$$\dot{V} = v A \quad (\text{m}^3/\text{s}) \quad (2.2)$$

And the mass flow with the air density ρ is:

$$\dot{m} = \rho v A \quad (\text{kg/s}) \quad (2.3)$$

The equations expressing the kinetic energy of the moving air and the mass flow yield the amount of energy passing through cross-section A per unit time. This energy is physically identical to the power P (Erick Hau, 2006):

$$P = \frac{1}{2} \rho v^3 A \quad (\text{W}) \quad (2.4)$$

2.3.2 Power Extracted from the Wind

The actual power extracted by the rotor blades is the difference between the upstream and the downstream wind powers.

$$P_o = \frac{1}{2} \text{mass flow rate per second} \cdot \{V^2 - V_o^2\} \quad (2.5)$$

Where P_o = mechanical power extracted by the rotor, i.e., the turbine output power

V = upstream wind velocity at the entrance of the rotor blades

V_o = downstream wind velocity at the exit of the rotor blades.

The air velocity is discontinuous from V to V_o at the “plane” of the rotor blades in the macroscopic sense. The mass flow rate of air through the rotating blades is, therefore, derived by multiplying the density with the average velocity (Mukund R. Patel, 1999).

That is:

$$\text{mass flow rate} = \rho \cdot A \cdot \frac{V + V_o}{2} \quad (2.6)$$

The mechanical power extracted by the rotor, which is driving the electrical generator, is therefore:

$$P_o = \frac{1}{2} \left[\rho \cdot A \cdot \frac{(V + V_o)}{2} \right] \cdot (V^2 - V_o^2) \quad (2.7)$$

The above expression can be algebraically rearranged:

$$P_o = \frac{1}{2} \rho \cdot A \cdot V^3 \frac{\left(1 + \frac{V_o}{V}\right) \left[1 - \left(\frac{V_o}{V}\right)^2\right]}{2} \quad (2.8)$$

The power extracted by the blades is customarily expressed as a fraction of the upstream wind power as follows:

$$P_o = \frac{1}{2} \rho \cdot A \cdot V^3 \cdot C_p \quad (2.9)$$

$$C_p = \frac{\left(1 + \frac{V_o}{V}\right) \left[1 - \left(\frac{V_o}{V}\right)^2\right]}{2} \quad (2.10)$$

Where Coefficient of power of modified Savonius rotor is a function of the shape of the rotor and Reynolds number. This is expressed in dimensionless form as in Equation (2.11) :

$$C_p = f(m/D, H/D, \psi, p/q, Do/D, Re) \quad (2.11)$$

The first five parameters depend on the geometry of the rotor and the Reynolds number depends on the wind velocity and the rotor diameter (M.A.Kamoji, 2009). The C_p is the fraction of the upstream wind power, which is captured by the rotor blades. The remaining power is discharged or wasted in the downstream wind. The factor C_p is called the power coefficient of the rotor or the rotor efficiency. For a given upstream wind speed, the value of C_p depends on the ratio of the downstream to the upstream wind speeds, that is (V_o/V) . The plot of power coefficient versus (V_o/V) shows that C_p is a single, maximum-value function Figure 2.2. It has the maximum value of 0.59 when the (V_o/V) is one-third. The maximum power is extracted from the wind at that speed ratio, when the downstream wind speed equals one-third of the upstream speed. Under This condition (Mukund R. Patel,1999):

$$P_{\max} = \frac{1}{2} \rho \cdot A \cdot V^3 \cdot 0.59 \quad (2.12)$$

The theoretical maximum value of C_p is 0.59. In practical designs, the maximum achievable C_p is below 0.5 for high-speed, two-blade turbines, and between 0.2 and 0.4 for slow speed turbines with more blades (Figure 2.3). If we take 0.5 as the practical maximum rotor efficiency, the maximum power output of the wind turbine becomes a

Simple expression (Mukund R. Patel, 1999):

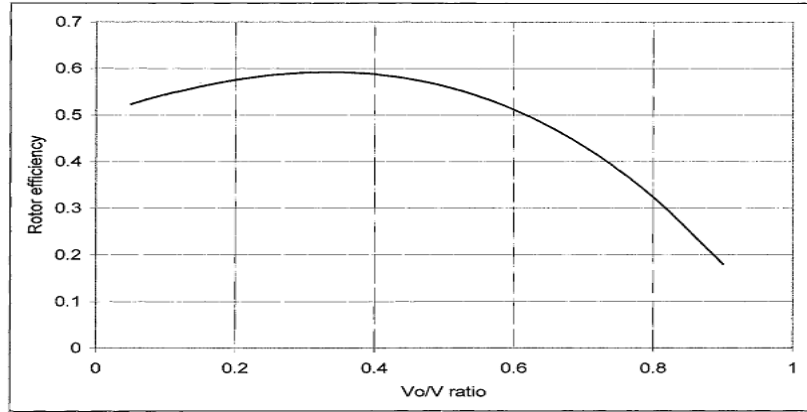


Figure 2.2: Rotor Efficiency Versus V_0/V ratio has Single Maximum. Rotor efficiency is The Fraction of available Wind Power extracted by The Rotor and fed to the Electrical Generator (Mukund R. Patel,1999)

2.3.3 Rotor Swept Area

As seen in the power equation, the output power of the wind turbine varies linearly with the rotor swept area. For the horizontal axis turbine, the rotor swept area is given by:

$$A = \frac{\pi}{4} D^2 \quad \text{where } D \text{ is the rotor diameter.} \quad (2.13)$$

For the Darrieus vertical axis machine, determination of the swept area is complex, as it involves elliptical integrals. However, approximating the blade shape as a parabola leads to the following simple expression for the swept area (Mukund R. Patel,1999):

$$A = \frac{2}{3} \cdot (\text{Maximum rotor width at the center}) \cdot (\text{Height of the rotor}). \quad (2.14)$$

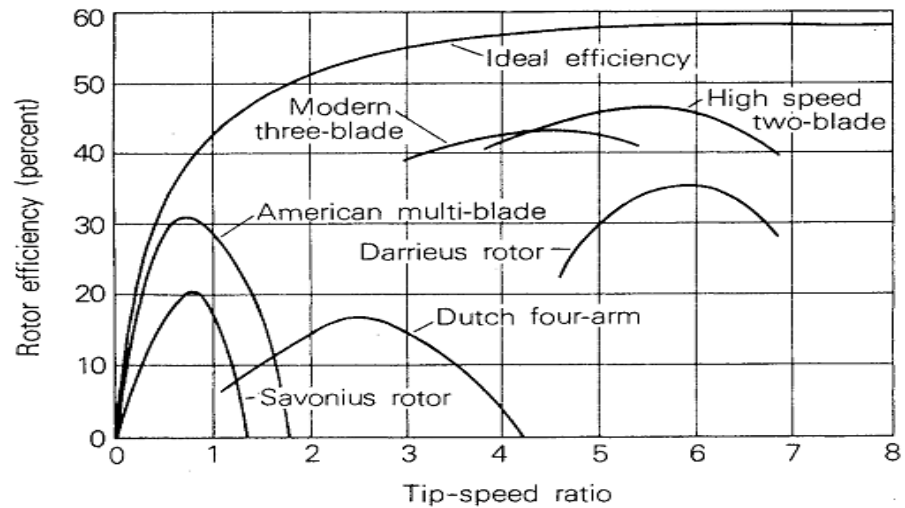


Figure 2.3: Rotor efficiency versus tip speed ratio for rotors with different numbers of blades. Two-blade rotors have the highest efficiency (Eldridge, 1975).

The wind turbine efficiently intercepts the wind energy flowing through the entire swept area even though it has only two or three thin blades with solidity between 5 to 10 percent. The solidity is defined as the ratio of the solid area to the swept area of the blades. The modern 2-blade turbine has low solidity ratio. Hence, it requires little blade material to sweep large areas (Mukund R. Patel, 1999).

2.3.4 Wind Energy Converters Using Aerodynamic Drag or Lift

The momentum theory by Betz indicates the physically based, ideal limit value for the extraction of mechanical power from a free-stream airflow without considering the design of the energy converter. However, the power which can be achieved under real conditions cannot be independent of the characteristics of the energy converter. The real power coefficients obtained vary greatly in dependence on whether aerodynamic drag or aerodynamic lift is used (Erick Hau, 2006).

2.3.4.1 Drag Devices

If an object is set up perpendicularly to the wind, the wind exerts a force F_D on the object. The wind speed v , the effective object area A and the drag coefficient c_D , which depends on the object shape, define the drag force:

$$F_D = c_D \cdot \frac{1}{2} \cdot \rho \cdot A \cdot v^2 \quad (2.15)$$

Figure 2.4 shows drag coefficients for various shapes. With $P_D = F_D \cdot v$, the power to counteract the force becomes:

$$P_D = c_D \cdot \frac{1}{2} \cdot \rho \cdot A \cdot v^3 \quad (2.16)$$

If an object moves with speed u by the influence of the wind in the same direction as the wind, the drag force is:

$$F_D = c_D \cdot \frac{1}{2} \cdot \rho \cdot A \cdot (v - u)^2 \quad (2.17)$$

And the power used is:

$$P_T = c_D \cdot \frac{1}{2} \cdot \rho \cdot A \cdot (v-u)^2 \cdot u \quad (2.18)$$

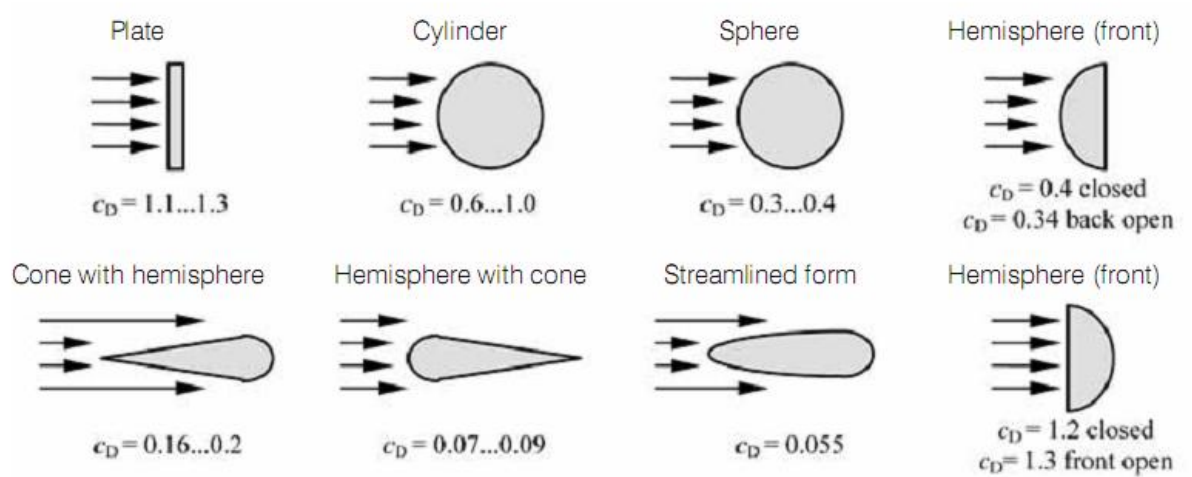


Figure 2.4: Drag Coefficients for Various Shapes (Volker Quaschnig, 2005)

The following example calculates approximately the used power of a cup anemometer that is used for the measurement of the wind speed v . It consists of two open hemispherical cups that rotate around a common axis. The wind impacts the front of the first cup and the back of the second cup (Figure 2.5). The resulting force F consists of a driving and a decelerating component (Gasch and Twele, 2002).

$$F = c_{D1} \cdot \frac{1}{2} \cdot \rho \cdot A \cdot (v-u)^2 - c_{D2} \cdot \frac{1}{2} \cdot \rho \cdot A \cdot (v+u)^2 \quad (2.19)$$

The used power is:

$$P_T = \frac{1}{2} \cdot \rho \cdot A \cdot \left(c_{D1} \cdot (v-u)^2 - c_{D2} \cdot (v+u)^2 \right) \cdot u \quad (2.20)$$

The ratio of the circumferential speed u to the wind speed v is called the tip speed ratio λ :

$$\lambda = \frac{u}{v} \quad (2.21)$$

The tip speed ratio of drag devices is always smaller than one. Using the tip speed ratio, the power is (Volker Quaschnig, 2005):

$$P_T = \frac{1}{2} \cdot \rho \cdot A \cdot v^3 \cdot \left(\lambda \cdot \left(c_{D1} \cdot (1 - \lambda)^2 - c_{D2} \cdot (1 + \lambda)^2 \right) \right) \quad (2.22)$$

Hence, the power coefficient of the cup anemometer becomes:

$$c_P = \frac{P_T}{P_0} = \frac{P_T}{\frac{1}{2} \cdot \rho \cdot A \cdot v^3} = \lambda \cdot \left(c_{D1} \cdot (1 - \lambda)^2 - c_{D2} \cdot (1 + \lambda)^2 \right) \quad (2.23)$$

The maximum value of the power coefficient of the cup anemometer is about 0.073. This is much below the ideal Betz power coefficient of 0.593. The cup anemometer reaches its maximum power coefficient at a tip speed ratio of about 0.16, when the wind speed v is about six times higher than the circumferential speed u (Volker Quaschnig, 2005).

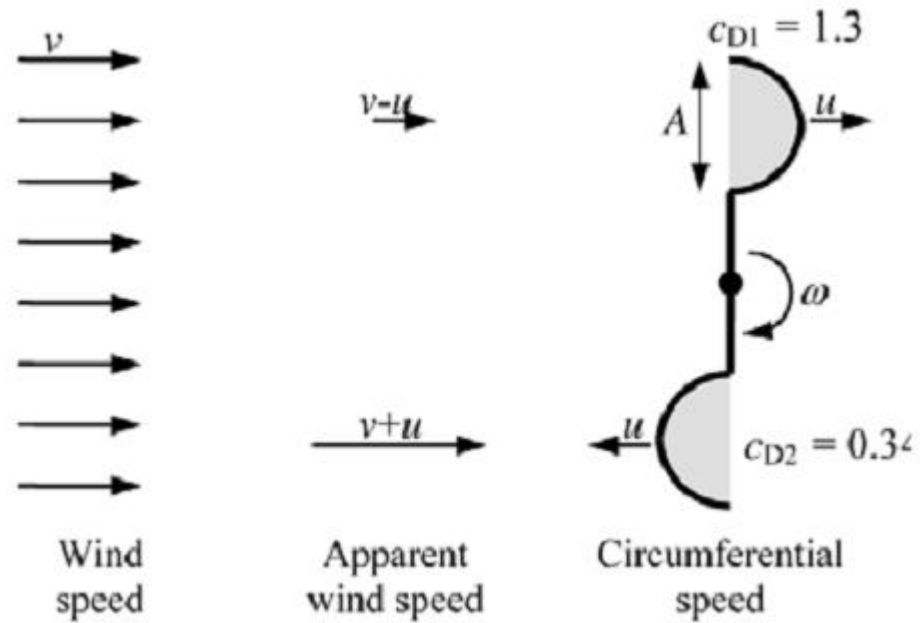


Figure 2.5: Model of Cup Anemometer for the Calculation of Power (Volker Quaschnig, 2005)

The optimal power coefficient $C_{P, \text{opt},D}$ of a drag device can be calculated using

$$c_p = \frac{P_T}{P_0} = \frac{\frac{1}{2} \cdot \rho \cdot A \cdot c_D \cdot (v-u)^2 \cdot u}{\frac{1}{2} \cdot \rho \cdot A \cdot v^3} = c_D \cdot \left(1 - \frac{u}{v}\right)^2 \cdot \frac{u}{v} \quad (2.24)$$

Using $u/v = 1/3$ as well as the maximum drag coefficient of $C_{D \text{ max}} = 1.3$, this gives (Volker Quaschnig, 2005):

$$C_{P, \text{opt},D} = 0.193 \quad (2.25)$$

The order of magnitude of the result becomes clear if it is taken into consideration that the aerodynamic drag coefficient of a concave surface curved against the wind direction can hardly exceed a value of 1.3. Thus, the maximum power coefficient of a pure drag-type rotor becomes (Erick Hau, 2006):

$$c_{P_{\max}} \approx 0,2 \quad (2.26)$$

It thus achieves only one third of Betz's ideal C_p value of 0.593. It must be pointed out that, Strictly speaking, this derivation only applies to a translatory motion of the drag surface (Erick Hau, 2006).

2.3.4.2 Rotors using Aerodynamic Lift

If the rotor blade shape permits utilization of aerodynamic lift, much higher power coefficients can be achieved. Analogously to the conditions existing in the case of an aircraft airfoil, utilization of aerodynamic lift considerably increases the efficiency Figure 2.6 (Erick Hau, 2006).

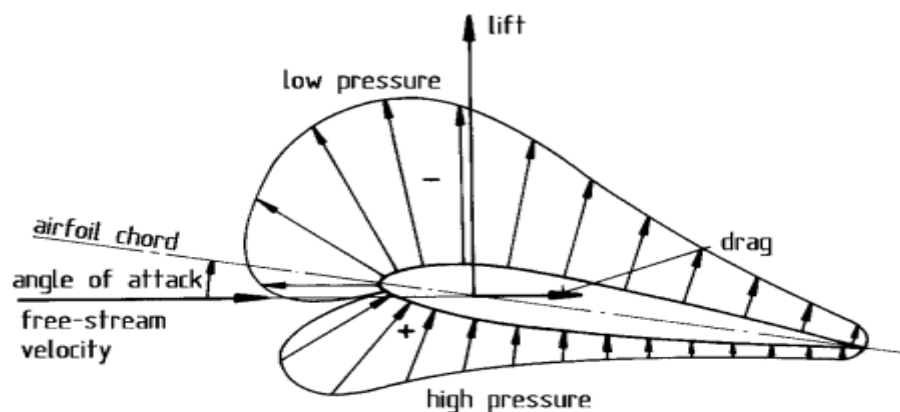


Figure 2.6: Aerodynamic Forces acting on an Airfoil exposed to an Air Stream. (Erick Hau, 2006)

2.4 Types of Wind Turbine

Wind turbines can be categorized according to the orientation of the axis of rotation with respect to the wind direction. Figure 2.7 shows a schematic representation of a vertical-axis wind turbine in comparison to a horizontal-axis wind turbine. In contrast to current on- and offshore wind farms where mostly large-scale horizontal-axis wind turbines are deployed, one of the strategies of harvesting wind energy in the urban environment is based on small-scale vertical-axis wind turbines with rotor diameters of only several meters. The application of vertical-axis wind turbines in cities is mainly due to their inherent advantage over horizontal-axis wind turbines in the built environment since vertical-axis wind turbines are, by design, insensitive to the wind direction. Horizontal-axis wind turbines, in contrast, have to be rotated into the wind each time the wind direction changes (Frank Scheurich, 2009).

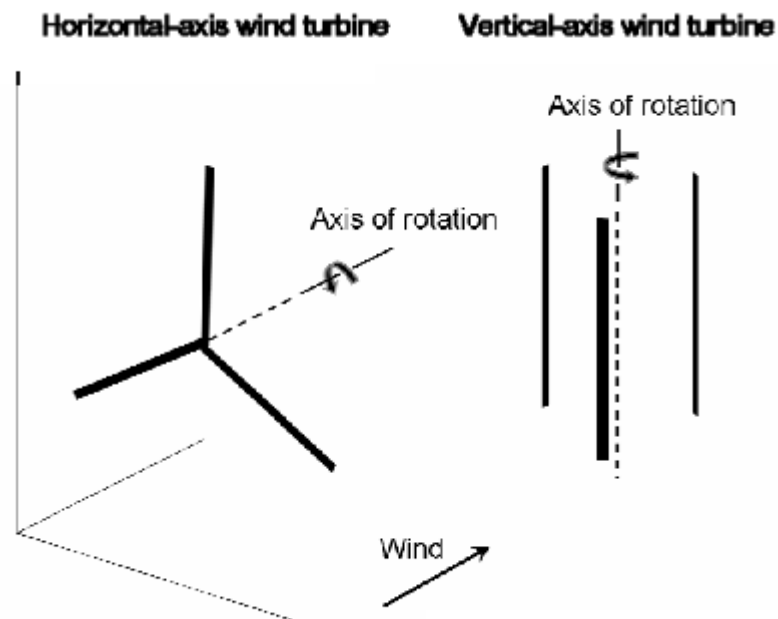


Figure 2.7: Orientation of the axis of rotation of a horizontal-axis wind turbine

In comparison to a vertical-axis wind turbine. (Frank Scheurich, 2009)

2.4.1 Horizontal Axis Wind Turbine

There are two main types of wind turbines. The horizontal axis wind turbine (HAWT) and the vertical axis wind turbine (VAWT) (Edwards, 1986). The HAWT has a rotor which moves perpendicular to the wind direction. Blades are mounted radially from the rotor and used to create a lift/drag differential which causes the rotor to rotate. The high speed two bladed HAWT can have efficiencies as high as 47% power extraction from the wind. They are generally grid connected for commercial use in electricity generation but smaller versions have been fabricated and sold commercially for small-scale applications (Ibrahim Al-Bahadly, 2009).

The advantages of the HAWT are that it can obtain a relatively high efficiency and that because they are typically tower mounted they have access to the higher undisturbed wind flows above ground level. With this advantage of being tower mounted there is also a trade-off. There is an increased capital cost incurred in the need for the tower and also the rotor and generator are more difficult to attend to for maintenance and repair than if the wind turbine was mounted on the ground. There is also a general need to orientate them into the wind by means of a tail or yaw mechanism. The final major disadvantage of this type of wind turbine is that there is a need for over-speed protection as they can rotate at velocities several times that of the wind speed.(Ibrahim Al-Bahadly,2009) A horizontal axis wind turbine generally consists of the following components(Volker Quaschnig,2005):

- Rotor blades, rotor hub, rotor brake and if need be, a pitch mechanism
- Electrical generator and if need be, a gearbox

- Wind measurement system and yaw drive (azimuth tracking)
- Nacelle, tower and foundation.
- Control, substation and mains connection.

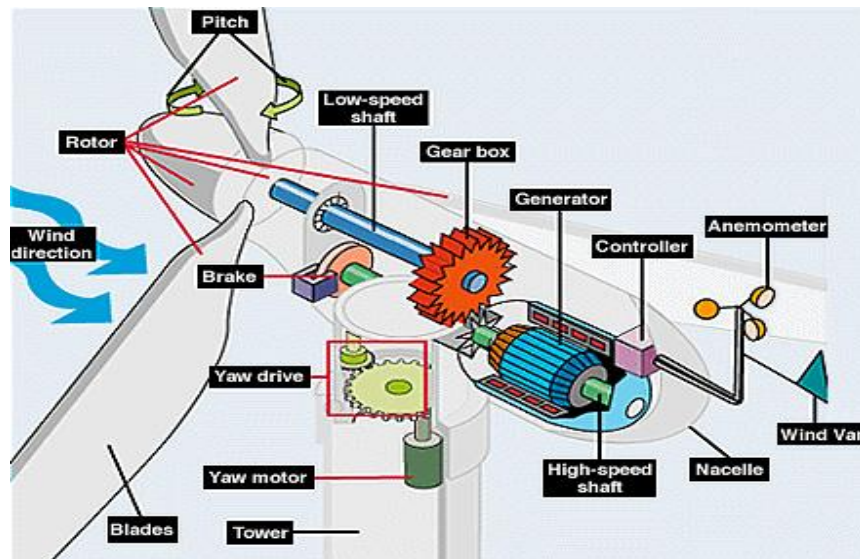


Figure 2.8: Typical Horizontal Wind Turbine Components

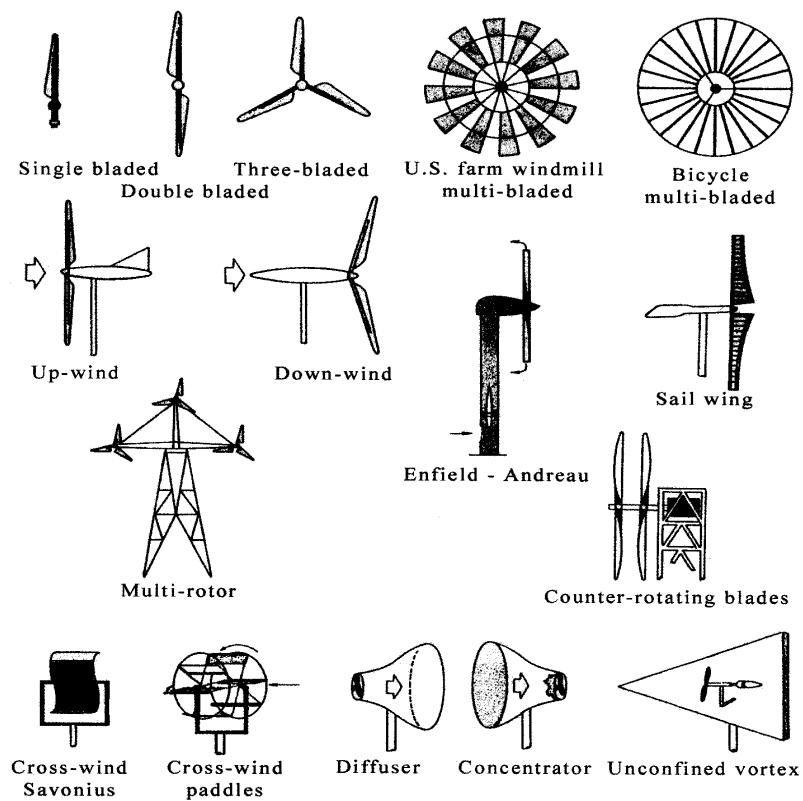


Figure 2.9: Typical Horizontal Wind Turbine Types

2.4.2 Vertical Axis Wind Turbine

It is evident that wind turbines can compete with conventional sources in niche markets, and lower costs make them affordable options in increasingly large markets. Environmentally benign Vertical axis wind turbines can be utilized for a range of applications, including:

- Electricity generation
- Pumping water
- Unifying and/or desalinating water by reverse osmosis
- Heating and cooling using vapor compression heat pumps;
- Mixing and Aerating water bodies
- Heating water by fluid turbulence.

In general, Vertical axis wind turbine can sensibly be used in any area with sufficient wind, either as a stand-alone system to supply individual households with electricity and heat, or for the operation of freestanding technical installations. If a network connection is available, the energy can be fed in, thereby contributing to a reduction in electricity costs. In order to maximize the security of the energy supply, different types of Vertical axis wind turbine can be supplemented by a photovoltaic system or a diesel generator in a quick and uncomplicated fashion (Mazharul Islam et al, 2008).

Through the combination of several Vertical axis wind turbines with other renewable energy sources and a backup system, local electrical networks can be created for the energy supply of small settlements and remote locations. In this modern time, there is

resurgence of interests regarding VAWTs as several universities and research institutions have carried out extensive research activities and developed numerous designs based on several aerodynamic computational models. These models are crucial for optimum design parameters and also for predicting the performance before fabricating the models or prototypes. There have been many designs of vertical axis windmills over the centuries and currently the vertical axis wind turbines can be broadly divided into three basic types, namely (Mazharul Islam et al, 2008):

- (1) Savonius type.
- (2) Darrieus type.
- (3) H-Rotor type.

2.4.2.1 H-Rotors

H rotor or H-Darrieus rotor. This rotor is also called the Heidelberg rotor after the company Heidelberg Motor. A permanent-magnet generator is directly integrated into the rotor structure and needs no gearbox. The three rotor blades of the H rotor are attached vertically. Supports to the vertical axis help the rotor maintain its shape. The very robust H rotor was designed for the extreme weather conditions existing in high mountains or in Antarctica (Volker Quaschnig, 2005).

H-Rotors, as shown in Figure 2.10, were developed in the UK though the research carried out during the 1970–1980s when it was established that the elaborated mechanisms used to feather the straight-bladed Darrieus VAWT blades were unnecessary. It was found out that the drag/stall effect created by a blade leaving the

wind flow would limit the speed that the opposing blade (in the wind flow) could propel the whole blade configuration forward. The H-Rotor was therefore self-regulating in all wind speeds reaching its optimal rotational speed shortly after its cut-in wind speed (Mazharul Islam et al, 2008).

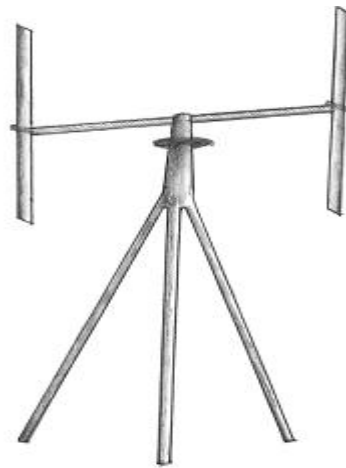


Figure 2.10: H-Rotor-type Vertical axis Wind Turbine (Mazharul Islam, 2008)

2.4.2.2 Darrieus Wind Turbines

The modern Darrieus Vertical axis Wind Turbine was invented by a French engineer George Jean Mary Darrieus. He submitted his patent in 1931 in the USA (Darrieus GJM, 1931) which included both the “Eggbeater (or Curved Bladed)” and “Straight-bladed” VAWTs. The Darrieus Wind Turbine shown in Figure 2.11. The Darrieus-type Vertical axis Wind Turbines are basically lift force driven wind turbines. The turbine consists of two or more aerofoil-shaped blades which are attached to a rotating vertical shaft. The wind blowing over the aerofoil contours of the blade creates aerodynamic lift and actually pulls the blades along. The troposkien shape eggbeater-type Darrieus VAWT, which minimizes the bending stress in the blades, was commercially deployed in California in the past (Mazharul Islam et al, 2008).

In the small-scale wind turbine market, the simple straight-bladed Darrieus VAWT, often called giromill or cyclo-turbine, is more attractive for its simple blade design. This configuration fall into two categories: fixed pitch and variable pitch. It has been found that fixed pitch Vertical axis Wind Turbines provide inadequate starting torque. Contemporary variable pitch blade configuration has potential to overcome the starting torque problem but it is overly complicated, rendering it impractical for smaller capacity applications. Majority of the previously conducted research activities on Vertical axis Wind Turbine focused on straight bladed Vertical axis Wind Turbines equipped with symmetric airfoils (like NACA) which were unable to self-start. This inability to self-start is due to several factors (like technical, inadequate research work & funding), and the most dominant ones are due to aerodynamic factors. According to an internet survey, there are a handfuls of commercial straight-bladed Vertical axis Wind Turbines products, but no reliable information could be obtained from an independent source regarding the performance of these products and the claims made by the manufacturers are yet to be authentically verified (Mazharul Islam et al, 2008).

At present, development of large-scale straight-bladed VAWT is limited, although large eggbeater Darrieus wind turbine had reached the market commercially in the past before disappearing away later. However, in the small-scale wind turbine market, the simple straight-bladed Darrieus seems to be more cost effective than the eggbeater Darrieus as few companies had marketed this type of wind turbine (Mazharul Islam, 2008). The efficiency of the Darrieus rotor is much above the efficiency of the Savonius rotor; however, it reaches efficiencies of only about 75 per cent of modern rotors with horizontal axes. A grave disadvantage of the Darrieus rotor is that it cannot start on its

own: it always needs an auxiliary starting system that can be a drive motor or a coupled Savonius rotor (Volker Quaschnig, 2005).



Figure 2.11: Typical Photograph of Curved-Blade Darrieus Wind Turbine

2.4.2.3 Savonius Wind Turbine

The Savonius-type VAWT, as shown in Figure 2.13, was invented by a Finnish engineer S.J. Savonius in 1929. Savonius wind rotor, having an S-shaped section field, consists of two half cylinders called the blade the centre of which has been slid symmetrical to each other and placed in between two horizontal discs. The wind hitting the Savonius wind rotor at a certain speed leads to a positive torque in the inner part of the cylinder forming the rotor and a negative torque in its outer part. Since the torque in its inner part is higher than the torque in the outer part, a rotation movement is secured. When the torque on the concave blade of the Savonius wind rotor is compared with the torque on the convex blade, the former appears to be higher because of the different

resistance coefficients of the blade surfaces .For this reason, the Savonius wind rotor rotates in the direction of the positive torque that forms on the concave blade (Burçin Deda Altan,2009).

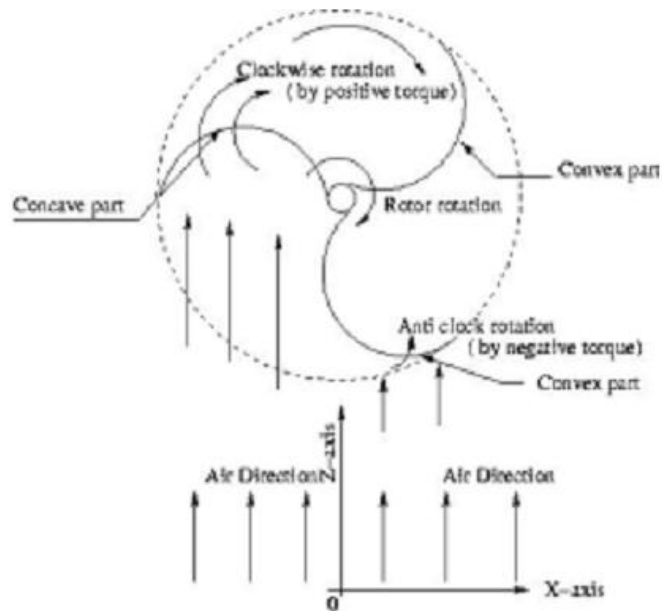


Figure 2.12: Illustration of positive Torque and Negative Torque (U. K. Saha and M. Jaya Rajkumar, 2008)

This process continues all the time the wind blows and the turning of the shaft is used to drive a pump or a small generator. Though typical values of maximum power coefficient for other types of wind turbines vary between 30% to 45%, those for the Savonius turbines are typically not more than 25% according to most investigators (Mazharul Islam et al, 2008). This type of turbine is suitable for low-power applications and they are commonly used for wind speed instruments (Volker Quaschnig, 2005).

The Savonius rotor vertical axis wind turbine definitely has a place in electricity generation. It has many advantages despite its relatively low efficiency. On other hand; small scale it is cheap, simple to design and construct and is also very robust. There are

a number of small-scale applications for which it would be suitable especially for tin likes of a small isolated homestead. As it is easily repairable and maintainable there would be little need for the services of a technician as almost any individual with an understanding of basic mechanics would be able to service it(I. Al-Bahadly,2009). It has been found out the previous research activities that the static torque coefficients at all the rotor angles for a helical Savonius rotors studied in this study are positive (Zhenzhou Zhao et al,2010) .However, for conventional Savonius rotor, there are several rotor angles at which static torque coefficient is negative(M.A. Kamoji,2008). The wind energy is transferred into mechanical energy Savonius rotor is also called S-type rotor for its S-shaped cross-section. Compared with other rotor, the Savonius rotor has many advantages:

- Its construction is simpler and cheaper
- Savonius rotor has a better starting torque at lower wind speeds, therefore can be used in Darrieus-type wind rotor as a starter.
- Independence of the wind direction
- Its generator and gear box can be installed over ground or under the wind rotor, so the maintenance gets more convenient and cheaper

But Savonius rotor has lower power performance $C_p=0.15$ than that of wind rotors with a horizontal axis $C_p=0.45$ and Darrieus-type rotor with a vertical axis $C_p=0.35$. Therefore the Savonius rotor is developed slowly and mainly applied in the urban family power supply in small scale (Zhenzhou Zhao et al, 2010).

At certain rotor angles, conventional Savonius rotors cannot start on their own as the coefficient of static torque is negative. Conventional Savonius rotor is having negative

torque for the rotor angles in the range of 135° – 165° and from 315° to 345° . The use of three bladed single stage rotor, with each blade at 120° also reduces the torque variation in a rotor cycle but the coefficient of power decreases that twisted three bladed Savonius rotor with a twist angle of 15° has a maximum coefficient of power of 0.14 (tip speed ratio of 0.65) compared to 0.11 for a three bladed conventional Savonius rotor (Zhenzhou Zhao et al, 2010). That all show the potential of the Savonius rotor with twisted blades in terms of smooth running, higher efficiency and self-starting capability as compared to that of the semicircular bladed rotor (U.K. Saha and M. Jaya Rajkumar, 2008) then it will call helical savonius wind turbine in figure 2.14.

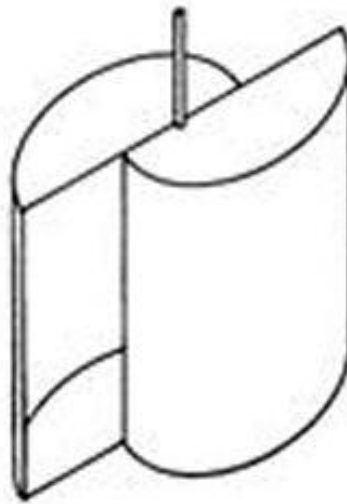


Figure 2.13: Savonius-type Vertical axis Wind Turbine (Mazharul Islam et al, 2008)



Figure 2.14: Typical Photograph of Helical Savonius Wind Turbine

2.5 Horizontal Axis Versus Vertical Axis

Most wind turbines built at present have a horizontal axis. The vertical axis Darrieus machine has several advantages. First of all, it is omnidirectional and requires no yaw mechanism to continuously orient itself toward the wind direction. Secondly, its vertical drive shaft simplifies the installation of the gearbox and the electrical generator on the ground, making the structure much simpler. On the negative side, it normally requires guy wires attached to the top for support. This could limit its applications, particularly for the offshore sites. Overall, the vertical axis machine has not been widely used because its output power cannot be easily controlled in high winds simply by changing the blade pitch. With modern low-cost, variable-speed power electronics emerging in the wind power industry, the Darrieus configuration may revive, particularly for large capacity applications (Mukund R. Patel, 1999).

2.6 Savonius Wind Turbine Characteristics

A number of scientists have experimentally and numerically examined the effects of various design parameters of Savonius wind rotor such as (Zhenzhou Zhao et al, 2010):

- (1) the rotor aspect ratio
- (2) The overlap ratio.
- (3) The number of blades.
- (4) The twisted angle.
- (5) The separation gap.
- (6) The cross-section profile.

2.6.1 The Rotor Aspect Ratio

Aspect ratio as shown in Fig. 2.15 is the ratio of the height of the rotor to the width. A large aspect ratio of around 4 to 5 provides the rotor with good torque and power characteristics (Ibrahim Al-Bahadly, 2009). The performance of the helical rotor with slim shape is better than that of the podgy shape one. Compared with the slim shape rotor, the podgy shape rotor has a bigger rotational diameter and produces a bigger torque but a lower rotational speed. On the contrary, the slim helical rotor can get higher rotational speed but lower torque for a small rotational diameter. In addition, if the diameter is too small, it would cause airflow to move in an eddy even to break away because of a fast swerving. This also leads to the performance dropping. Therefore,

there must exist an optimum aspect value with which the rotor has highest coefficient of power (Zhenzhou Zhao et al, 2010).

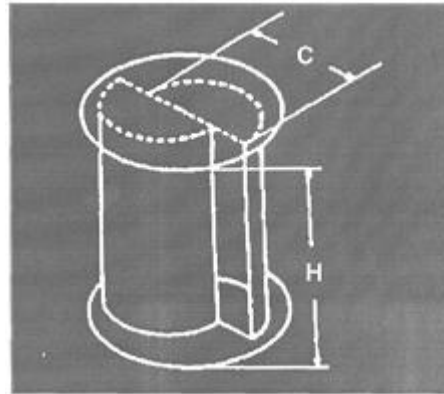


Figure 2.15: Aspect Ratio (Ibrahim Al-Bahadly, 2009)

But Kamoji in his study of the helical wind turbine, found that the Helical Savonius rotor with a lower aspect ratio of 0.88 shows a higher performance than rotors with an aspect ratio of 0.93 and 1.17 (M.A. Kamoji et al, 2009). Zhenzhou Zhao study the effect of aspect ratio on the coefficient of power for a helical Savonius rotor with a 180° twist angle, two blades and overlap ratio 0.3 and found. The performance of helical Savonius rotor with an aspect ratio of 6.0 is marginally higher ($C_{pmax}=0.20$ at a $TSR=0.75$) compared to the helical rotor with a rotor aspect ratio of 1.0, 3.0, 5.0 and 7.0. Helical Savonius rotor with a higher aspect ratio of 6.0 shows a higher performance than rotors with an aspect ratio of 1.0, 3.0, 5.0 and 7.0 (Zhenzhou Zhao et al, 2010). The aspect ratio α equation is (Md. Nahidul Islam Khan et al, 2009):

$$\alpha = \frac{H}{D} \quad (2.27)$$

2.6.2 The Rotor Overlap Ratio

Overlap ratio as shown in Fig. 2.16 is the ratio of the diameter of the rotor blade to the distance which the blades overlap. The buckets of semi-circular cross-section, the appropriate overlap ratio is 20 to 30 %.(Ibrahim Al-Bahadly, 2009).

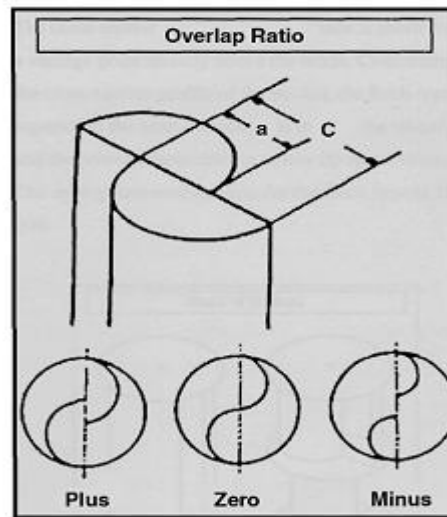


Figure 2.16: Overlap Ratio (Ibrahim Al-Bahadly, 2009)

The power coefficient of the Savonius rotor depends on the overlap distance. It was found that a higher pressure zone exists in either the upwind rotor because of heading-on the wind or the downwind rotor because of collecting the wind. It was observed that for the upwind rotor, the pressure of leeward side of blade is much lower than that of the opposite side, because of the lack of the air blowing. The bigger difference of pressure between the leeward side and the opposite side leads to the higher push counter-rotational direction on the upwind rotor, and the power coefficient getting lower. While, an air passage between two semi-circular buckets is constructed for an overlap structure, the air after working in the downwind rotor flows into the leeward side of upwind rotor and raises the leeward pressure (Zhenzhou Zhao et al, 2010).

Hence as the pressure difference of the two side of the upwind rotor gets smaller, the torque increases. The overlap ratio is a factor which determines the magnitude of the passage area. If ratio is too big to lead the air flow into the leeside of the downwind blade conducting little work in the upwind blade; while, if the ratio is too small to lead the little air flow into the leeside and raises the little pressure. So there must be an appropriate ratio value which leads to a maximum power coefficient. It may be seen that the tip speed ratio at which the maximum coefficient of power is observed decreases with the increase in the overlap ratio for helical Savonius rotors. Maximum coefficient of power for a helical Savonius rotor is around 0.181 for a 0.3 overlap ratio at a TSR of around 0.73 (Zhenzhou Zhao et al, 2010).

The overlap ratio β is given by the following equation (Md. Nahidul Islam Khan et al, 2009):

$$\beta = \frac{e}{d} \quad (2.28)$$

2.6.3 The Rotor Twisted Angle

For the twisted blade, the maximum force moves towards to the tip of the blade because of the twist in the blade, A larger twist angle is preferable in the lower wind velocity for producing maximum power and better starting characteristics (U.K. Saha et al, 2008) .The effect of twist angle on the performance of rotor is important. The coefficient of power studied for a two-bladed rotor with overlap ratio 0.3 and aspects ratio 2.0 at different twist angle. shows that the maximum coefficient of power 0.18 was found with

TSR=0.8 and 180° twist angle; while the worst one belongs to 90° twist angle, and 270° takes the second worst place. (Zhenzhou Zhao et al, 2010).



Figure 2.17: Four types Helical Rotor with Different Twist Angle (Zhenzhou Zhao et al, 2010).

2.6.4 The Rotor Blades Number

The number of blades that a rotor possesses has a direct effect on the performance of the rotor (figure 2.18). Rotors comprising of three or more blades are inferior to the two-blade rotor in both torque and power characteristics (Ibrahim Al-Bahadly, 2009). It is observed that the power coefficient of the rotor decreases when the number of blades increases from two to three. Form previous research by Zhenzhou Zhao, he found that for TSR=0.8, the power coefficient of two-bladed rotor equals 0.165 and bigger than that of conventional Savonius rotor, while that of three-bladed rotor is 0.12. He got the same results from experiment and explained that: when the number of blades was increased to three, the air which striked on one blade get reflected back on the following blade so that the following blade rotates in negative direction as compared to the succeeding blade. Hence, with an increase of number of blades, the rotor performance decreases. Figure 2.18 shows the simulation results of fluid field of both the three-bladed and the two-bladed rotor (Zhenzhou Zhao et al, 2010).

However, it can be found that the downwind pressure surface of the two-bladed is bigger than that of the three-bladed when both rotors are of the same rotor angle. Meanwhile, the upwind pressure surface gets bigger in three-bladed rotor because of following blade exiting. Both the bigger downwind surface and the smaller upwind surface lead to the better rotor performance. So, the performance of two-bladed rotor is better than that of the three (Zhenzhou Zhao et al, 2010).

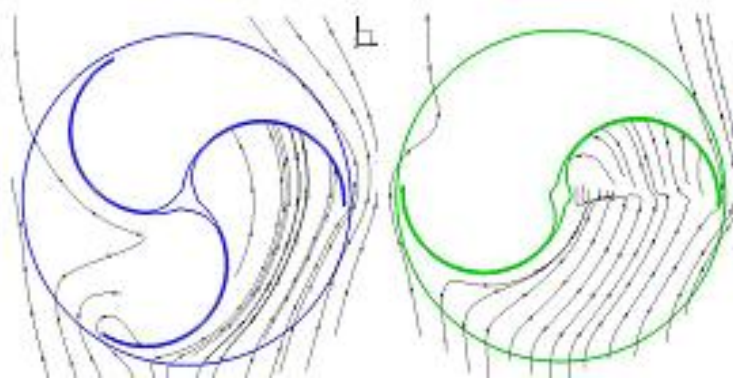


Figure 2.18: The Fluid Field of Two and Three Blades Rotor (Zhenzhou Zhao, 2010)

2.6.5 The Separation Gap

Separation gap as shown in Figure 2.19 is determined by the distance of the rotor blades from the vertical axis. An increase in the separation gap ratio results in a decrease in the torque coefficient and the power coefficient; a small negative gap is therefore preferable (Ibrahim Al-Bahadly, 2009).

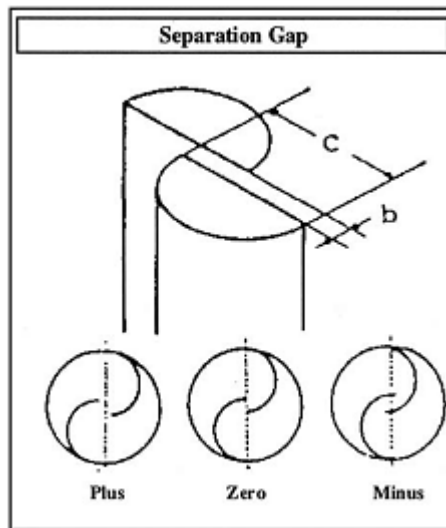


Figure 2.19: Separation Gap (Ibrahim Al-Bahadly, 2009)

2.6.6 Cross-section Profile

The cross-section profile of a rotor blade is taken from a vantage point directly above the blade Figure 2.20. Concerning the cross-section profile of the bucket, the Bach type is superior to the semi-circular type in both the torque and the power characteristics at low tip speed ratios. The appropriate overlap ratio for the Bach type is 10 to 30% (Ibrahim Al-Bahadly, 2009).

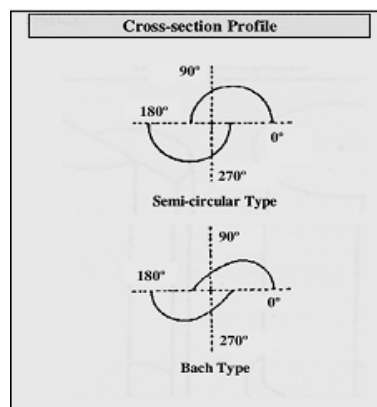


Figure 2.20: Cross-section Profile (Ibrahim Al-Bahadly, 2009)

2.7 Wind Turbine Performance Parameters

The measured quantities are combined in order to obtain the performance parameters commonly used in the Aerodynamics of Wind Turbines (V. D'Alessandro, 2010):

1. The torque coefficient.

$$C_T = 4T/PU^2D^2H \quad (2.29)$$

2. The power coefficient.

$$C_P = P_O/P \quad (2.30)$$

3. Both are evaluated as a function of the dimensionless parameter Tip-Speed Ratio (TSR).
4. Power output

$$RPM = (v/2\pi * r) * 60 \quad (2.31)$$

$$\text{Power (HP)} = (T * RPM) / 5252 \quad (2.32)$$

$$\text{Power (Watt)} = 745.5 * \text{Power (HP)} \quad (2.33)$$

2.8 Wind Turbines in Commercial Stand Alone Applications

The market for small scale commercially viable wind turbines is expanding from an economic standpoint and the social “going green” phenomena (David Olson and Ken Visser, 2008). Applications for the model designed and built are very limited due to the

fact that it has been built on such a small scale. To put things into perspective, with an average output of 0.65 kWh/day it would be able to run a small refrigerator. In order to be suitable for more practical applications the scale or size of the wind turbine would have to be increased. For an individual living with many of the modern luxuries such as TV the average usage of power per day is around 5 kWh/day. An individual living in an isolated environment and only requiring the basics should be able to get away with using around 2.7 kWh/day. There would realistically be a need for refrigeration, cooking and lighting at night. (Ibrahim Al-Bahadly, 2009).

2.8.1 Autonomous Power Supply and Storage Problems

Power supply in an isolated situation can only meet present-day requirements if a certain degree of security of supply is guaranteed. To put it more simply: Even if the wind does not blow, the lights must not go out. If wind is the sole source of energy, a means of energy storage is imperative. All efforts in striving for an autonomous energy supply system with the aid of renewable energy sources always end up with the problem of energy storage. The search for a cost effective energy storage is a theme pervading the whole range of these technologies. To exaggerate, one might say that as soon as an economically viable solution of storing energy has been found, all energy problems concerning the utilization of renewable energy sources, i.e. with solar energy, can be solved. However, there is no such technology of energy storage in existence at present. All storage methods which can be used in practice today have a very limited storage capacity and are very expensive. Moreover, they require complex conversion systems, as the energy is mostly stored in a form which is not suitable for the end user. Attempting to provide an overview of all possible methods of energy storage would be useless. The range of methods, patents and ideas relating to this subject is almost

inexhaustible .However, there are some energy storage methods which are frequently discussed in connection with wind energy utilization and these will be described in greater detail here. A wind turbine is a two-fold energy conversion system (Erick Hau, 2006):

Firstly, the rotor converts the kinetic energy of the moving air into mechanical energy, and secondly, the electrical generator converts the latter into electrical energy. There are, therefore, basically two ways of tackling the problem of energy storage. For one, it may be attempted to store the mechanical energy directly, which has the advantage of not requiring any further high-loss energy conversion. However, the choice of mechanical energy storage methods is narrow (Erick Hau, 2006).

The second possibility for energy storage is offered by the electrical energy generated. The capacity of storing electrical energy in conventional batteries is very limited. The storage capacities of even advanced batteries, for example nickel/cadmium- or silver/zinc-based batteries, are not enough to meet the electrical demand of some ten or even hundred kilowatts over a period of days. The economical use of batteries is therefore restricted to that as short term buffer storage batteries. For the more distant future, the continued advance in the development of the fuel cell gives rise to new hopes for a suitable long-term storage device (Erick Hau, 2006).



Figure 2.21: Flywheel storage system developed by Enercon (Erick Hau, 2006)

2.8.2 Residential Heating

There are a number of reasons why wind energy should be used for residential heating. Possibly the most important argument emerges when one looks at energy consumption patterns, for example for a country like Germany. At approximately 45%, the “households and small consumers” sector represents the highest percentage of overall primary energy consumption. About 6% of the energy requirement of this group is met by coal, about 16 % by gas and about 60% by oil. An overwhelming proportion of the energy consumed by this group is used for space heating. It accounts for 80% of the energy demand of a private household. This proportion is contrasted by only approximately 5% for lighting and power and approximately 15% for process heat (hot water for domestic use). Using a wind turbine for home heating would, therefore,

replace the primary energy sources of petroleum and natural gas particularly effectively (Erick Hau, 2006).

2.8.3 Pumping Water

Pumping water is one of the most ancient applications of wind power. From the last decades of the nineteenth century until today, the American (and Australian) wind turbine with its mechanically driven piston pump has become the second symbol for the utilization of wind energy, next to the European windmill. This technology is particularly well-suited to areas with moderate wind speeds and for the pumping of small amounts of water from a great depth, primarily for providing drinking water. For this application, the American wind pump has remained virtually unbeatable in its simplicity and reliability (Erick Hau, 2006).

However, modern irrigation technology has different requirements, especially in the agriculture of many developing countries. Here, large amounts of water are needed to be pumped, often from shallow depths. Moreover, it is frequently not possible to locate wind turbine and water pump in the same place. Under these circumstances, a conventional wind turbine for driving electrical water pumps becomes increasingly attractive, even though this technology is far more complicated. In many cases, the wind turbine is again set up as a hybrid system in combination with a diesel generator, or is integrated into an existing system. Its economic efficiency must then derive from the fuel saved in the diesel set (Erick Hau, 2006).

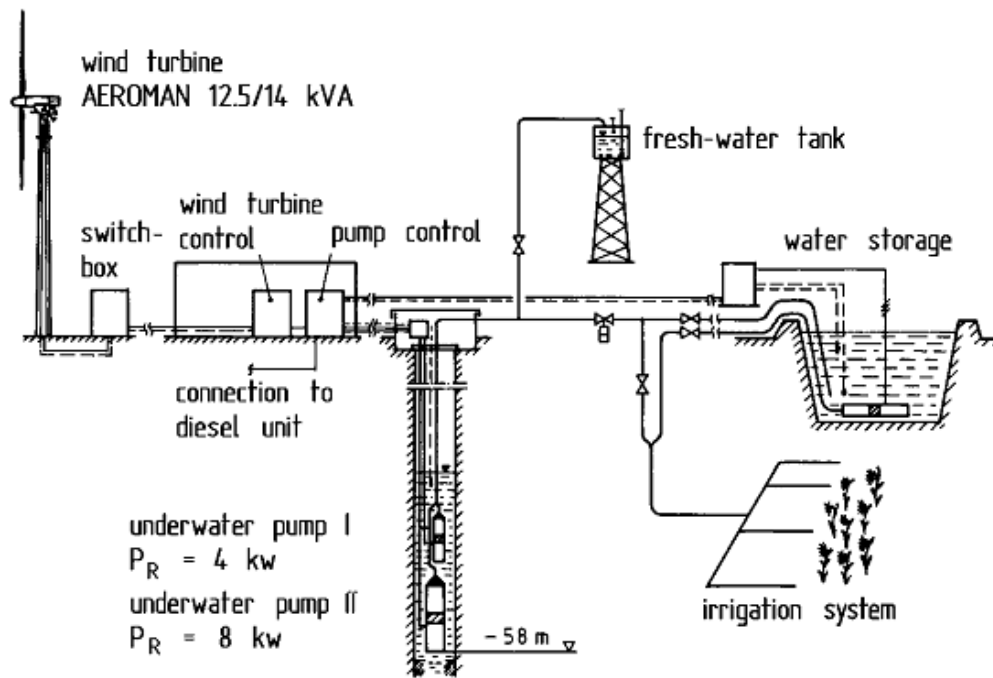


Figure 2.22: Wind-supported irrigation system with an Aeroman wind turbine and two underwater electric well pumps (Erick Hau, 2006)

2.8.4 Desalination of Sea Water

Quite a few experts predict that there will be a catastrophic world shortage of drinking water long before there will be a real energy crisis. This prediction is not so far-fetched for some Third World countries and it may even have become reality already in some regions. The only global solution seems to be the utilization of sea water for drinking water. Technical methods of sea-water desalination for use on board ships were developed as early as the 19th century. On land, sea-water desalination plants for supplying drinking water have only been in use for some decades. Desalination processes based either on distillation or on the separation of water and salt by semi-permeable membranes, have achieved practical significance (Erick Hau, 2006).

2.9 Conclusions

This chapter is an overview of all previous studies and to clarify the importance of the Wind energy which can be generated and used in a lot of industry applications.

CHAPTER THREE

METHODOLOGY

3.1 Introduction

A study was conducted to find the best parameters for a helical wind turbine as shown in the figure 3.1

In this chapter computational fluid dynamic is used to study the effect of parameters such as the aspect ratio (which is the ratio of the height to the radius of the blade), the Bach design for the turbine rotor and also the gap between the rotor in order to get the best performance of the helical wind turbine.

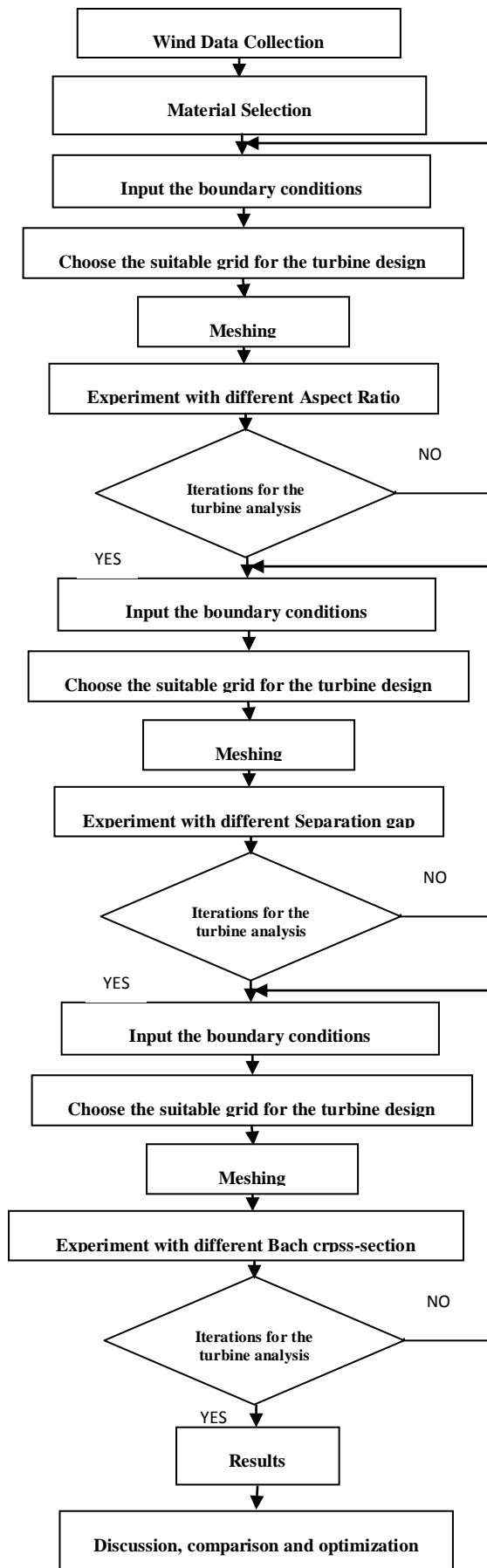


Figure 3.1: flow chart for the Helical Wind Turbine Design and Analysis

3.2 Wind Data Collection

There are data from 10 stations of which 10 years data are collected from each station. The data collected are wind speed frequency and wind direction frequency. The 10 stations are Kuala Terengganu, Alor Setar, Bayan Lepas, Ipoh, Kota Bahru, Kota Kinabalu, Kuantan, Kuching, Malacca and Petaling Jaya.

The result of the Kuala Terengganu station will be used as an example for the discussion of the frequency of wind speed in this study because of its high standard deviation. Apart from the overall results for standard deviation, mean wind speed energy density and the annual energy density for all the stations will be shown.

3.3 Data collection and analysis

Basically there are few stages to complete this study. The three stages are the material selection, wind data collection and prototyping with the use of the cfd programs. This stage consume a lot of time by studying the material for the wind turbine and come up with the best design focusing on the light material and the resistance for the environment effect especially the wind turbine which will be an outdoor device, then come up with the dimension for the wind turbine follow some mechanical considerations from previous studies. As for our study the weight effect a lot and its act a big factor effect direct the output. The data for mean wind speed was collected from the Malaysian metrological station (MMS). The data collected will be examined and analyzed and the results obtained will be used in the determining the type of the turbine being used in our study.

3.4 Computational Fluid Dynamic (CFD)

Using simulation tools that mathematically model fluid flow make assemblies become zero-cost prototypes that can reveal critical information not available from physical tests, Design changes can be made instantly and the results of which can be seen immediately using interactive flow bench ,thermal test and wind tunnel. There are several steps to be taken with a program like cfdesign which is a cfd program to analyze the aerodynamic aspects of the helical wind turbine.

3.4.1 Material Selection

There are two distinct material types in this analysis: fluids and solids. For the fluid air surrounds the helical wind turbine. For the rotor PVC was chosen as it has the following characteristics:

- 1- PVC is a Light Weight Material.
- 2- It is readily Formed.
- 3- It has Good resistance to the elements especial when installed in outdoor applications.
- 4- PVC is inexpensive.

3.4.2 Boundary Conditions

Boundary conditions are the physical significance of loads. Loads are divided into boundary conditions and internal conditions but in this thesis only the boundary conditions are defined which are the wind velocity in this case (10m/s) and the surrounding pressure.

3.4.3 Mesh Generation

The geometry has to be broken up into small, manageable pieces called elements. The corner of each element is called a node, and it is at each node that a calculation is performed. All together these elements and nodes comprise the mesh (also known as the finite element mesh).

3.4.4 Turbulence Method

In this study the slandered k-epsilon (k- ϵ model for turbulence) is used because of the fully turbulent flow and non-separated flows and that it can have stability issues due to numerical stiffness. The K-epsilon model is one of the most common turbulence models. It is a two equation model that means it includes two extra transport equations to represent the turbulent properties of the flow. This allows a two equation model to account for history effects like convection and diffusion of turbulent energy.

The first transported variable is turbulent kinetic energy, k . The second transported variable in this case is the turbulent dissipation, ϵ . It is the variable that determines the scale of the turbulence, whereas the first variable, k , determines the energy in the

turbulence. There are two major formulations of K-epsilon models. That of Launder and Sharma is typically called the "Standard" K-epsilon Model. The original impetus for the K-epsilon model was to improve the mixing-length model, as well as to find an alternative to algebraically prescribing turbulent length scales in moderate to high complexity flows.

The K-epsilon model has been shown to be useful for free-shear layer flows with relatively small pressure gradients and it is typically more accurate than the constant eddy viscosity. Similarly, for wall-bounded and internal flows, the model gives good results only in cases where mean pressure gradients are small; accuracy has been shown experimentally to be reduced for flows containing large adverse pressure gradients. One might infer then, that the K-epsilon model would be an inappropriate choice for problems such as inlets and compressors.

The iteration method is used with the these equations to calculate the pressure and velocity distribution and the equation of mass and momentum used by the cfd program for comprisable and incomparable steady flow.

3.4.4.1 The Continuity Equation

The law of mass conservation expresses the fact that mass cannot be created in such a fluid system, nor can disappear from it (J. Blazer, 2001).

$$\frac{\partial}{\partial t} \int_{\Omega} \rho d\Omega + \oint_{\partial\Omega} \rho (\vec{v} \cdot \vec{n}) dS = 0. \quad (3.1)$$

This represents the integral form of the continuity equation - the conservation law of mass.

3.4.4.2 The Momentum Equation

We may start the derivation of the momentum equation by recalling the particular form of Newton's second law which states that the variation of momentum is caused by the net force acting on a mass element we have

$$\rho \vec{v} d\Omega. \tag{3.2}$$

We can identify two kinds of forces acting on the control volume:

1. External volume or body forces, which act directly on the mass of the volume. These are for example gravitational, buoyancy, Coriolis or centrifugal forces. In some cases, there can be electromagnetic forces present as well.

2. Surface forces, which act directly on the surface of the control volume. They result from only two sources:

(a) The pressure distribution, imposed by the outside fluid surrounding

(b) The shear and normal stresses, resulting from the friction between the volume, fluid and the surface of the volume.

Hence, if they now sum up all the above contributions according to the general conservation law, they finally obtain the expression

$$\frac{\partial}{\partial t} \int_{\Omega} \rho \vec{v} d\Omega + \oint_{\partial\Omega} \rho \vec{v} (\vec{v} \cdot \vec{n}) dS = \int_{\Omega} \rho \vec{f}_e d\Omega - \oint_{\partial\Omega} p \vec{n} dS + \oint_{\partial\Omega} (\bar{\tau} \cdot \vec{n}) dS \quad (3.3)$$

3.4.4.3 K- ϵ Two-Equation Model

The K- ϵ turbulence model is the most widely employed two-equation eddy-viscosity model. It is based on the solution of equations for the turbulent kinetic energy and the turbulent dissipation rate.

$$\frac{\partial \rho K}{\partial t} + \frac{\partial}{\partial x_j} (\rho v_j K) = \frac{\partial}{\partial x_j} \left[\left(\mu_L + \frac{\mu_T}{\sigma_K} \right) \frac{\partial K}{\partial x_j} \right] + \tau_{ij}^F S_{ij} - \rho \epsilon \quad (3.4)$$

$$\begin{aligned} \frac{\partial \rho \epsilon^*}{\partial t} + \frac{\partial}{\partial x_j} (\rho v_j \epsilon^*) &= \frac{\partial}{\partial x_j} \left[\left(\mu_L + \frac{\mu_T}{\sigma_\epsilon} \right) \frac{\partial \epsilon^*}{\partial x_j} \right] + C_{\epsilon 1} f_{\epsilon 1} \frac{\epsilon^*}{K} \tau_{ij}^F S_{ij} \\ &- C_{\epsilon 2} f_{\epsilon 2} \rho \frac{(\epsilon^*)^2}{K} + \phi_\epsilon. \end{aligned} \quad (3.5)$$

The terms on the right-hand side represent conservative diffusion, eddy-viscosity production and dissipation, respectively. Furthermore, ϕ_ϵ denotes the so-called explicit wall term. The Favre-averaged turbulent stresses τ_{ij}^F and the strain-rate tensor S_{ij} . The constants, the near-wall damping functions as well as the wall term differ between the various K- ϵ models. Here, we choose the Launder-Sharma model because

it gives good results for a wide range of applications. For the Launder-Sharma model, the constants and the turbulent Prandtl number are given by

$$C_{\mu} = 0.09, \quad C_{\varepsilon 1} = 1.44, \quad C_{\varepsilon 2} = 1.92, \\ \sigma_K = 1.0, \quad \sigma_{\varepsilon} = 1.3, \quad Pr_T = 0.9.$$

CHAPTER FOUR

RESULTS AND DISCUSSIONS

4.1 Wind Speed

The results from kuala Terengganu station is used as example for the discussion on the frequency of wind speed .The overall results for standard deviation, mean wind speed energy density and annually energy density for all station is also shown in (table 4.3). The wind data is sorted into 16 intervals. They are 0.1-0.5, 0.6-1.0, 1.1-1.5, 1.6-2.0, 2.1-2.5, 2.6-3.0, 3.1-3.5, 3.5-4.0, 4.1-4.5, 4.6-5.0, 5.1-5.5, 5.6-6.0, 6.1-6.5, 6.6-7.0, 7.1-7.5, 7.6-8.0. The median of wind speed is extrapolated to the height of 25m. The extrapolated calculation is shown in the third column. A histogram is drawn using the data in Table 4.1. From figure 4.1 the highest frequency among the intervals are the interval 2.6-3.0 m/s. it is recorded as 32.73%. Most of the wind speed data are in the range of 1.1-2.5 m/s.

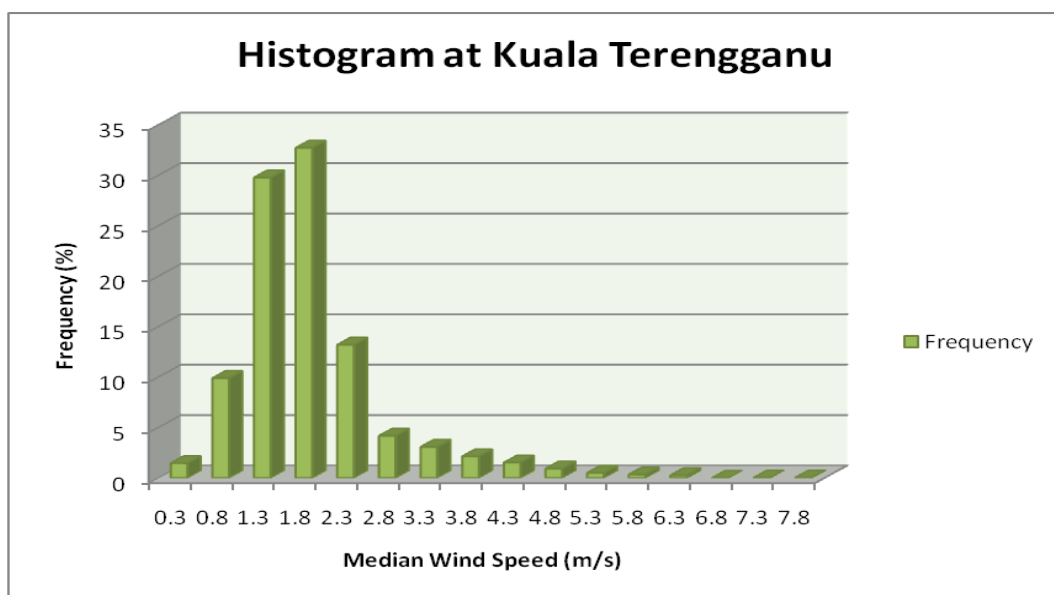


Figure 4.1: Histogram of frequency of wind speed at kuala Terengganu station

Table 4.1: frequency of wind speed for Kuala Terengganu station

| Wind (m/s) | Median (m/s) | V_M (m/s) | F | F(%) |
|-------------------|---------------------|----------------------------|-------------|-------------|
| 0.1-0.5 | 0.3 | 0.34 | 53 | 1.46 |
| 0.6-1.0 | 0.8 | 0.91 | 358 | 9.89 |
| 1.1-1.5 | 1.3 | 1.48 | 1078 | 29.78 |
| 1.6-2.0 | 1.8 | 2.05 | 1185 | 32.73 |
| 2.1-2.5 | 2.3 | 2.61 | 478 | 13.20 |
| 2.6-3.0 | 2.8 | 3.18 | 151 | 4.17 |
| 3.1-3.5 | 3.3 | 3.75 | 111 | 3.07 |
| 3.5-4.0 | 3.8 | 4.32 | 77 | 2.13 |
| 4.1-4.5 | 4.3 | 4.89 | 55 | 1.52 |
| 4.6-5.0 | 4.8 | 5.46 | 33 | 0.91 |
| 5.1-5.5 | 5.3 | 6.03 | 18 | 0.50 |
| 5.6-6.0 | 5.8 | 6.95 | 12 | 0.33 |
| 6.1-6.5 | 6.3 | 7.16 | 9 | 0.25 |
| 6.5-7.0 | 6.7 | 7.73 | 0 | 0 |
| 7.1-7.5 | 7.3 | 8.30 | 1 | 0.028 |
| 7.6-8.0 | 7.8 | 8.87 | 1 | 0.028 |
| TOTAL | | | 3620 | 100 |

Table 4.2: frequency of wind speed for Kota Bharu station

| Wind (m/s) | Median (m/s) | V_M (m/s) | F | F(%) |
|--------------|--------------|-------------|-------------|------------|
| 0.1-0.5 | 0.3 | 0.34 | 32 | 1.02 |
| 0.6-1.0 | 0.8 | 0.91 | 107 | 3.42 |
| 1.1-1.5 | 1.3 | 1.48 | 565 | 18.03 |
| 1.6-2.0 | 1.8 | 2.05 | 1002 | 31.98 |
| 2.1-2.5 | 2.3 | 2.61 | 738 | 23.56 |
| 2.6-3.0 | 2.8 | 3.18 | 303 | 9.67 |
| 3.1-3.5 | 3.3 | 3.75 | 141 | 4.50 |
| 3.5-4.0 | 3.8 | 4.32 | 84 | 2.68 |
| 4.1-4.5 | 4.3 | 4.89 | 66 | 2.11 |
| 4.6-5.0 | 4.8 | 5.46 | 48 | 1.53 |
| 5.1-5.5 | 5.3 | 6.03 | 25 | 0.8 |
| 5.6-6.0 | 5.8 | 6.95 | 15 | 0.48 |
| 6.1-6.5 | 6.3 | 7.16 | 6 | 0.19 |
| 6.5-7.0 | 6.7 | 7.73 | 1 | 0.03 |
| TOTAL | | | 3620 | 100 |

From figure 4.2 the highest frequency among the intervals 2.0-2.5m/s. It's recorded as 31.98%. Most of the wind speed data are in the range of 0.6-2.5 m/s. The frequency of wind speed above 6 m/s is only 0.22%. That back to the position of kota baru in klantan as its has smaller area contact to the sea compare to kuala turengganu.

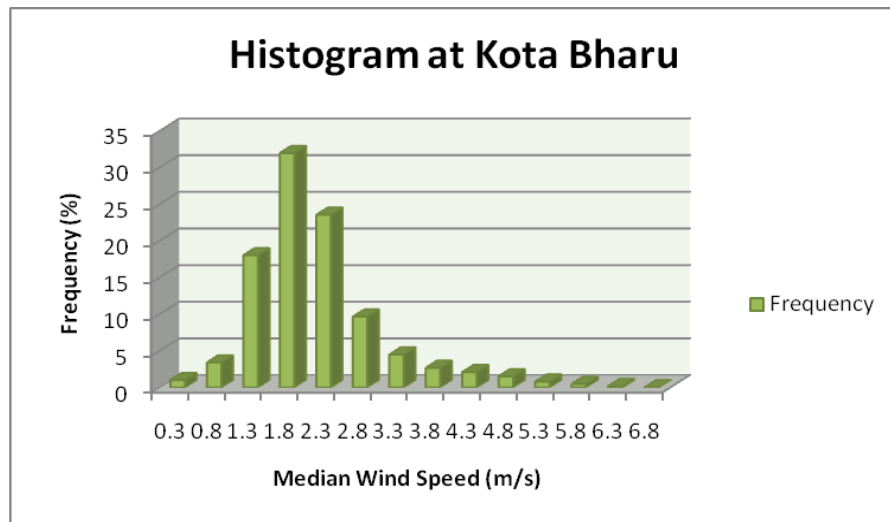


Figure 4.2: Histogram of frequency of wind speed at Kota Bharu

4.2 Wind Speed Comparison

The wind direction in Malaysia blows in the direction of 33.75o to 101.250 which is north –east-east. The highest frequency wind speed for Kota Bahru is the same which is 1.6-2.0 m/s. Kota Bahru most of the wind speed data are in the range of 0.6-2.5 m/s. While Kuala Terengganu most of the wind speed data are in the range of 1.1-2.5 m/s. As kuala terngganu has a larger area contact with the sea that make it's a bit higher than kota baru in the wind speed.

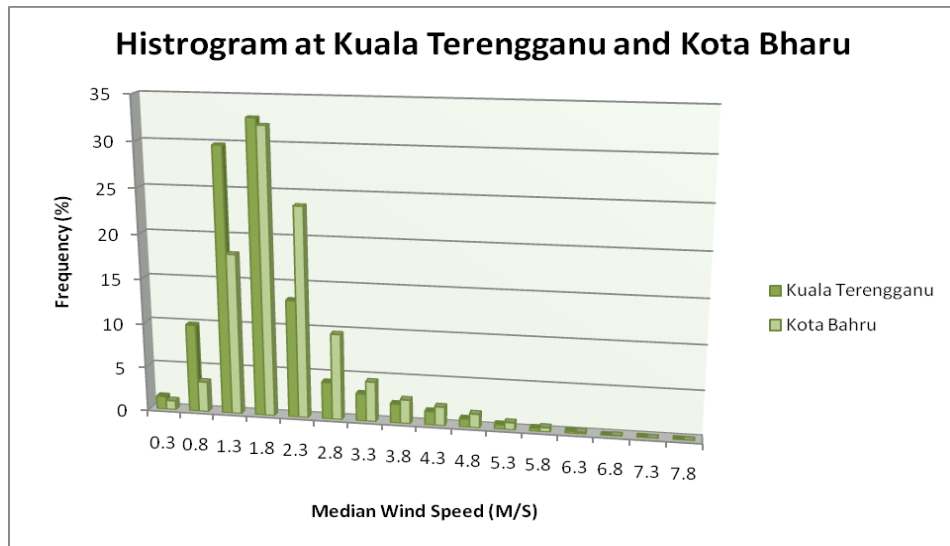


Figure 4.3: Graph of comparison of Wind speed

4.3 Mean Wind Speed and Standard Deviation

Table 4.3 shows that the mean wind speed in Malaysia is quite low which is in the range of 0-2.14 m/s. The mean wind speed in Kota Bharu station is the highest which is 2.14 m/s. Meanwhile Petaling Jaya has the lowest value. The mean wind speed in Petaling Jaya station is only 0.69 m/s as petaling jaya is far from sea shore and be in the middle of the city .

The maximum value for standard deviation is only 1.02 m/s. standard deviation for Kuala Terengganu station is the highest among the 10 stations and that back to the place as its been on the south china sea side. Petaling Jaya still the lowerest which is only 0.3 m/s as the main changes come from the the effect of the sea to kuala terngganu area compare to ptaling jaya which don't have contact to the sea around .

Table 4.3: Mean wind speed and standard deviation for all stations

| Station | Mean wind speed (V_M) (m/s) | Standard Deviation (m/s) |
|-------------------------|---|---------------------------------|
| Kota Bharu | 2.14 | 0.85 |
| Alor Star | 1.35 | 0.46 |
| Bayan Lepas | 1.75 | 0.48 |
| Ipoh | 1.07 | 0.24 |
| Kota Kinabalu | 1.87 | 0.36 |
| Kuala Terengganu | 1.79 | 1.02 |
| Kuantan | 1.69 | 0.45 |
| Kuching | 1.08 | 0.27 |
| Melacca | 1.37 | 0.58 |
| Petaling Jaya | 0.69 | 0.30 |

4.4 Prototyping

The data from the analysis is used to design the wind turbine:

4.4.1 Aspect Ratio

An aspect ratio is the ratio between the height and width of a rotor. The number denoting height comes first, and the width portion of the aspect ratio is always written as 1. And here we consider it for the blade width to the height of the rotor.

4.4.1.1 Aspect Ratio (3:1)

This turbine is 2 meter high and the blade diameter is 0.66 meter with a gap of 0.198 meter which is equal to an overlap ratio of 0.3. The turbine is designed using the pro engineer software for 3D modeling and virtual prototyping.

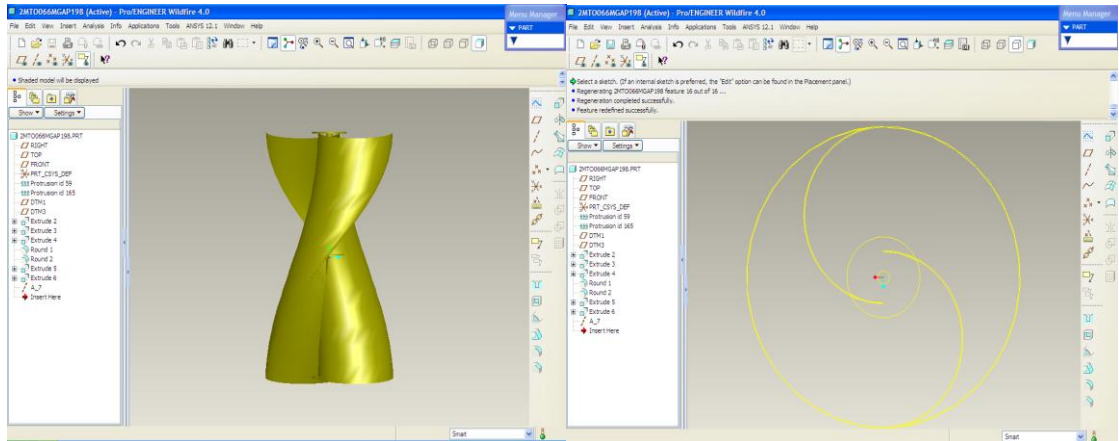


Figure 4.4: Front and Top View of Helical Wind Turbine with 3:1 Aspect Ratio

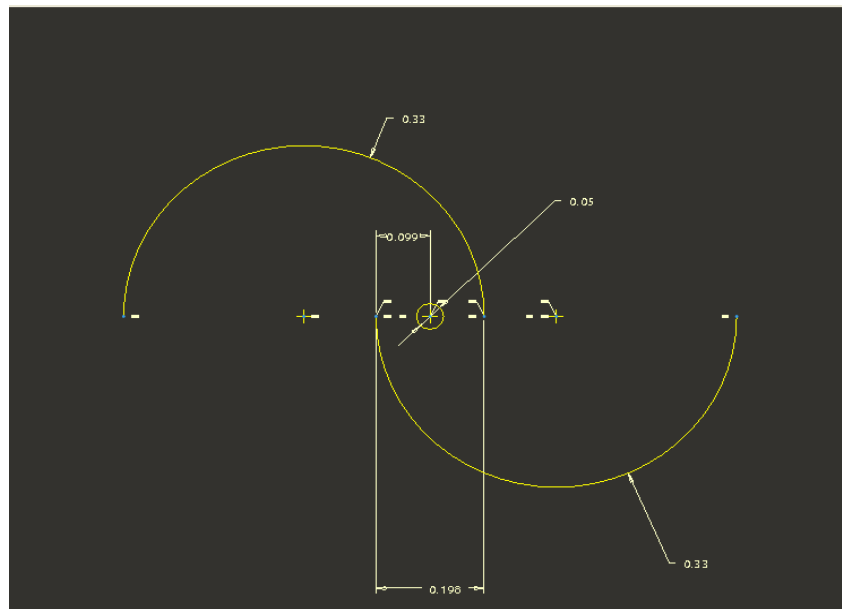


Figure 4.5: Schematic of the Helical Wind Turbine 3:1 Aspect Ratio Top View

4.4.1.2 Aspect Ratio (4:1)

In this case the turbine is 2 meter high and the blade diameter is 0.5 meter with a gap of 0.15 meter which is equal to overlap ratio of 0.3.

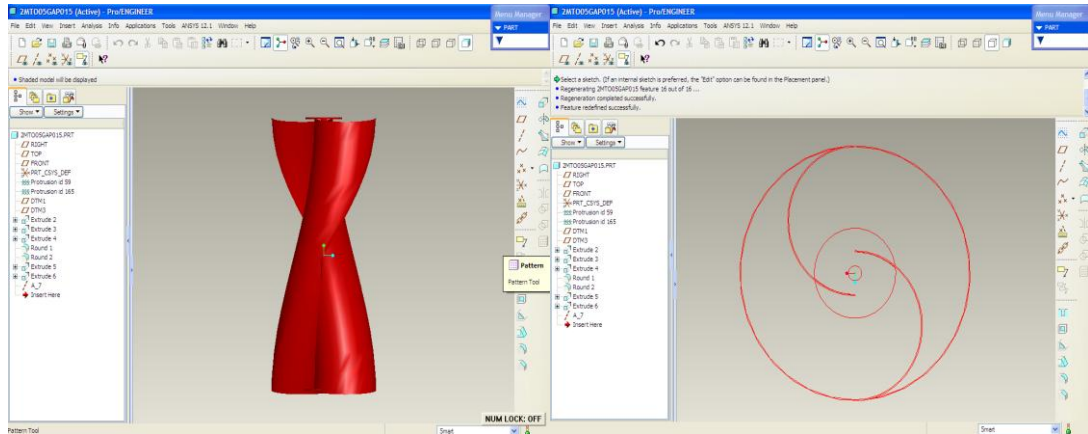


Figure 4.6: Front and Top View of Helical Wind Turbine with 4:1 Aspect Ratio

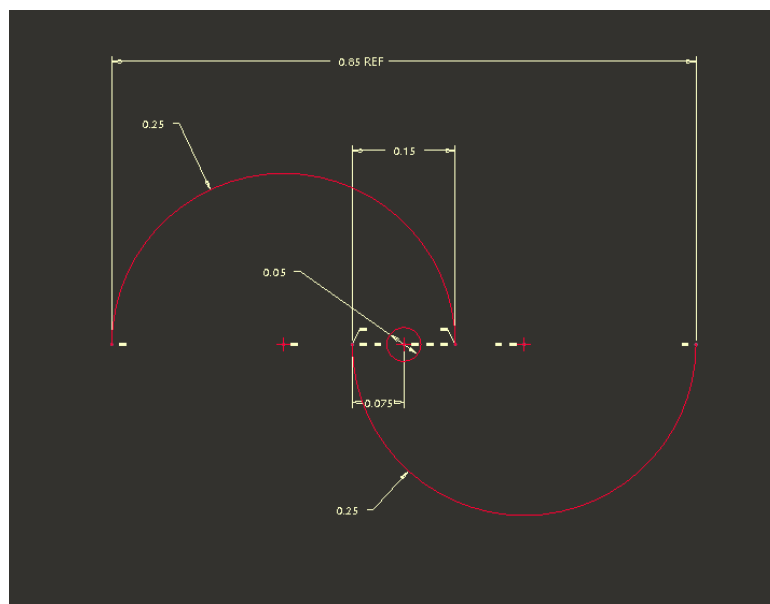


Figure 4.7: Schematic of the Helical Wind Turbine 4:1 Aspect Ratio Top View

4.4.1.3 Aspect Ratio (5:1)

This is a 2 meter high turbine and the blade diameter is 0.4 meter with a gap of 0.12 meter which is equal to an overlap ratio of 0.3.

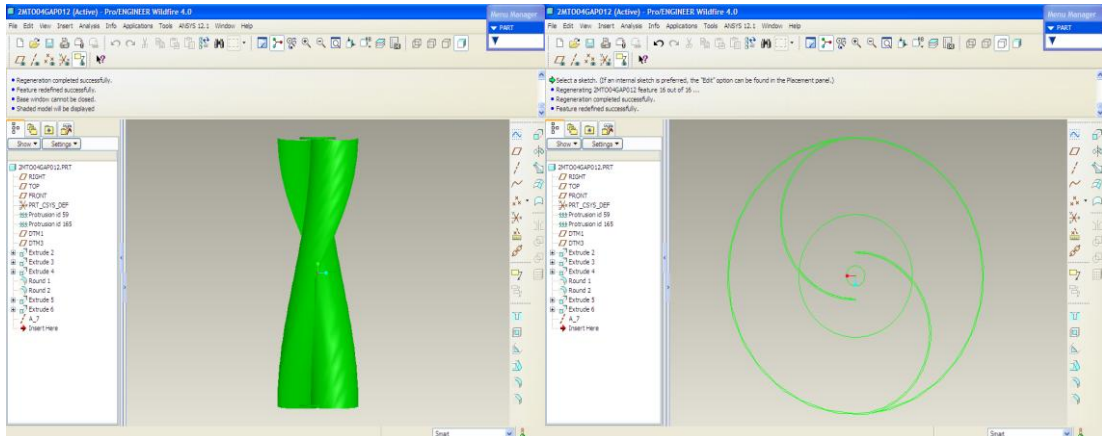


Figure 4.8: Front and Top View of Helical Wind Turbine with 5:1 Aspect Ratio

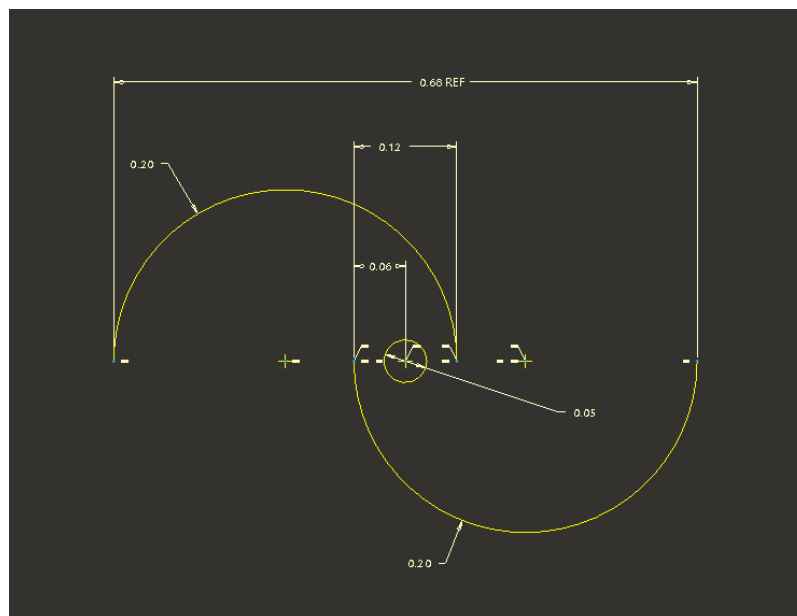


Figure 4.9: Schematic of the Helical Wind Turbine 5:1 Aspect Ratio Top View

4.4.2 Separation Gap (20mm Minus and 20 mm Plus)

A separation gap is the space between the two blades for the rotors but in the perpendicular direction of the overlap gap because this one is the distance between the faces of the blade.

4.4.2.1 Separation Gap 20mm Minus

This is a 2 meter high turbine when the gap between the blades is in a negative space of 20 mm.

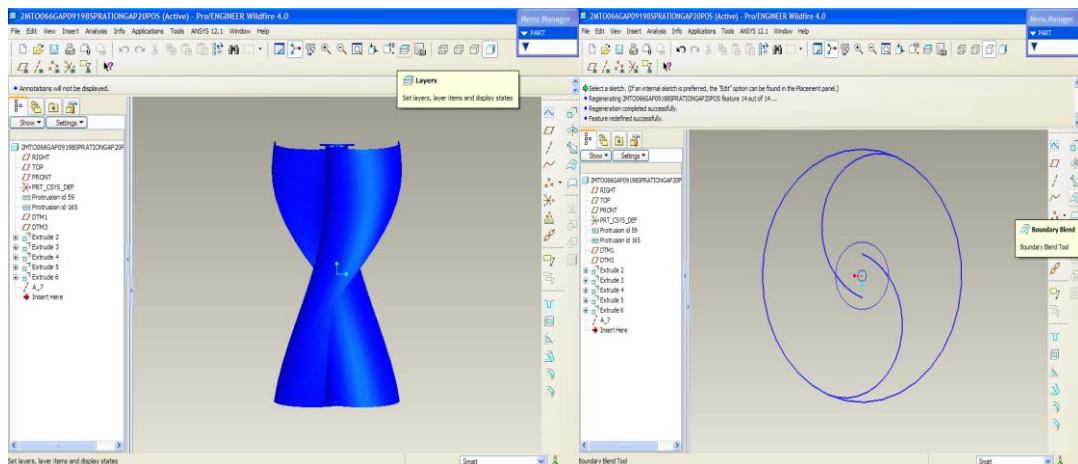


Figure 4.10: Front and Top View of Helical Wind Turbine with Minus Separation Gap

4.4.2.2 Separation Gap 20mm Plus

This is a 2 meter high turbine when the gap between the blades is in a positive space of 20 mm.

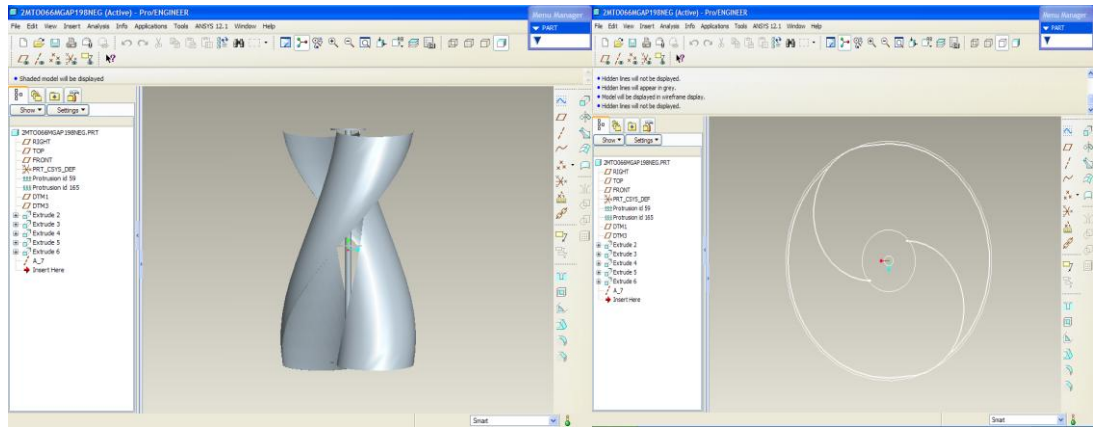


Figure 4.11: Front and Top View of Helical Wind Turbine with plus Separation Gap

4.4.3 Bach Shape for the Blade

In this design the blade is semi circular. It will be Bach and that means it is a Savonius rotor assembly which includes two blades. Each of the blades has an outer edge and an inner edge with the outer edges of the blades lying on a circle which define the diameter of the rotor. Each of the blades has a linear portion adjacent to the inner edge and a first curved portion which is substantially an arc of a circle tangent to the linear portion and tangent to the circle defining the rotor diameter. A second curved portion is substantially coincident to the circle defining the rotor diameter.

4.4.3.1 Bach Shape with Outer Edge of 20° and Inner Edge of 90°

This is when the wind will be concentrated in the inner edge of the rotor through the gap zone between the two blades.

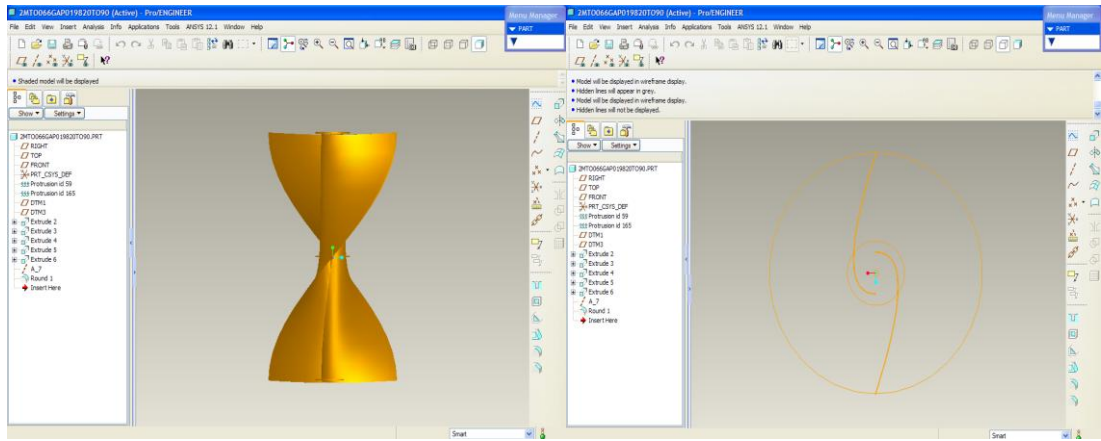


Figure 4.12: Front and Top View of Helical Wind Turbine with Bach Shape 20° to 90°

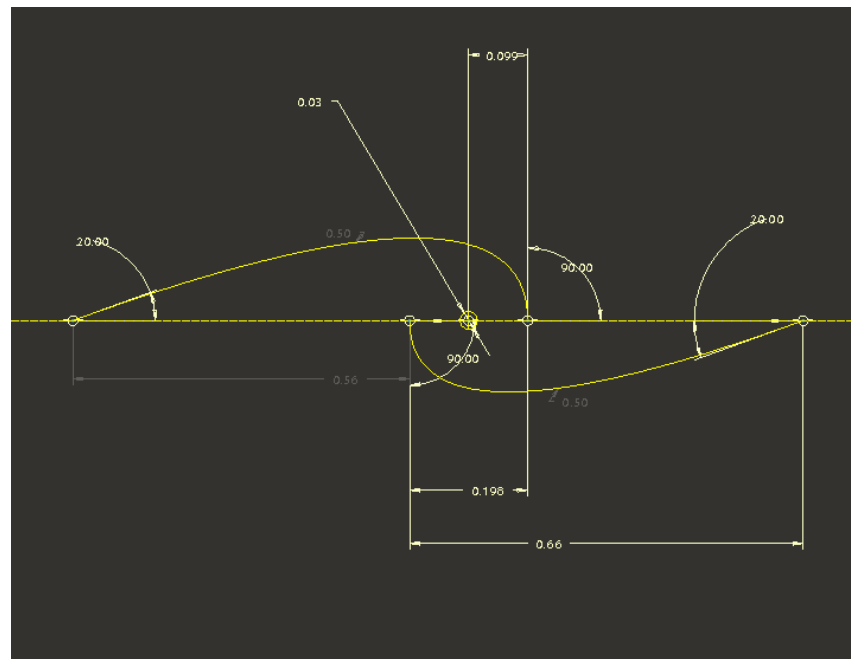


Figure 4.13: Schematic of the Helical Wind Turbine with Bach 20° to 90°

4.4.3.2 Bach Shape with Outer Edge of 40° and Inner Edge of 70°

The air speed on the outer edge is increased by increasing the angle to 40° .

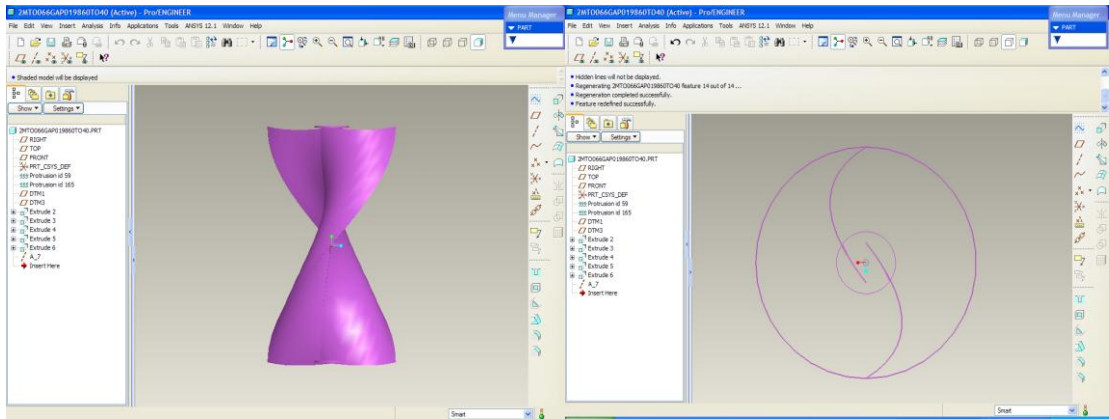


Figure 4.16: Front and Top View of Helical Wind Turbine with Bach Shape 60° to 40°

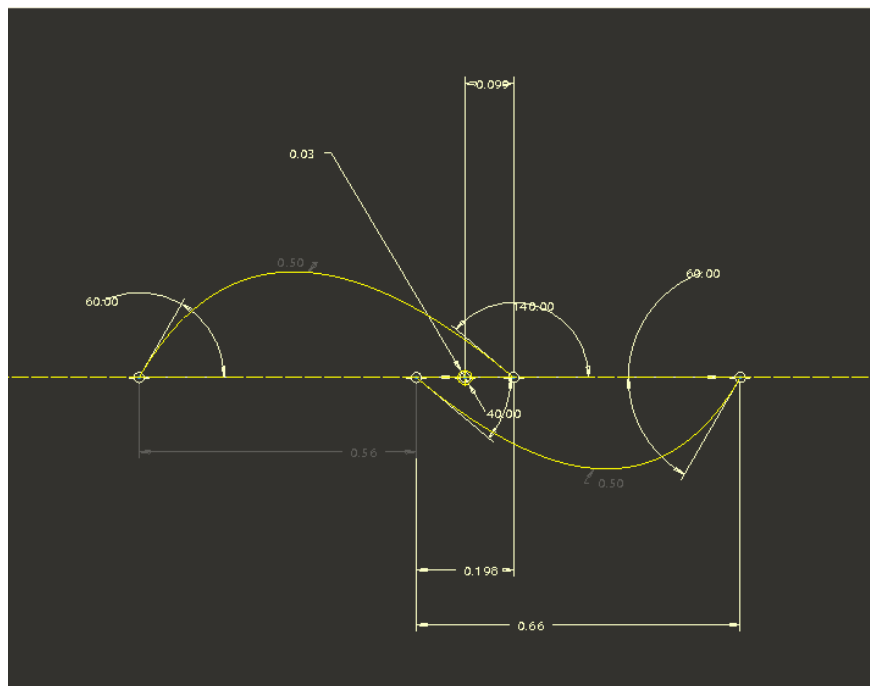


Figure 4.17: Schematic of the Helical Wind Turbine with Bach Shape 60° to 40°

4.4.3.4 Bach Shape with Outer Edge of 80° and Inner Edge of 30°

The 80° in the outer edge helps the turbine to have more torque.

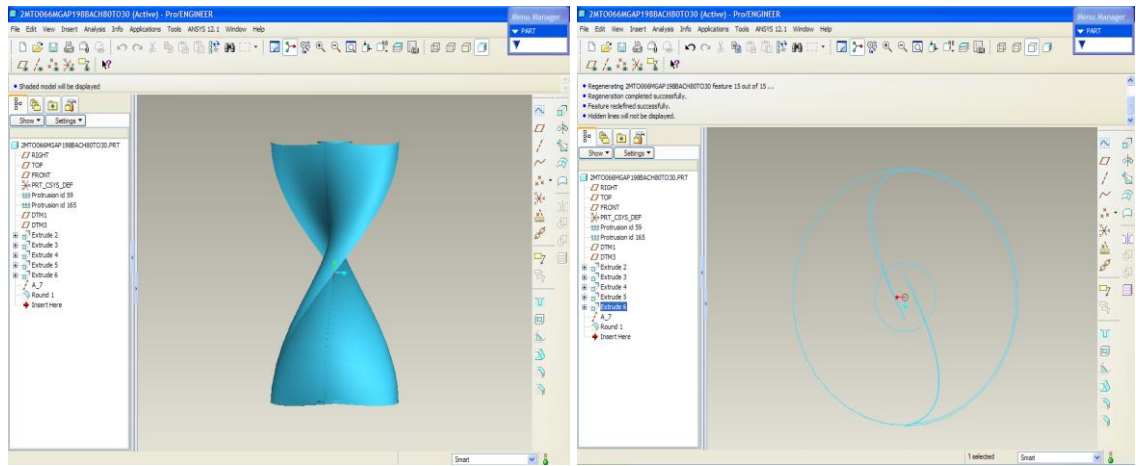


Figure 4.18: Front and Top View of Helical Wind Turbine with Bach Shape 80° to 30°

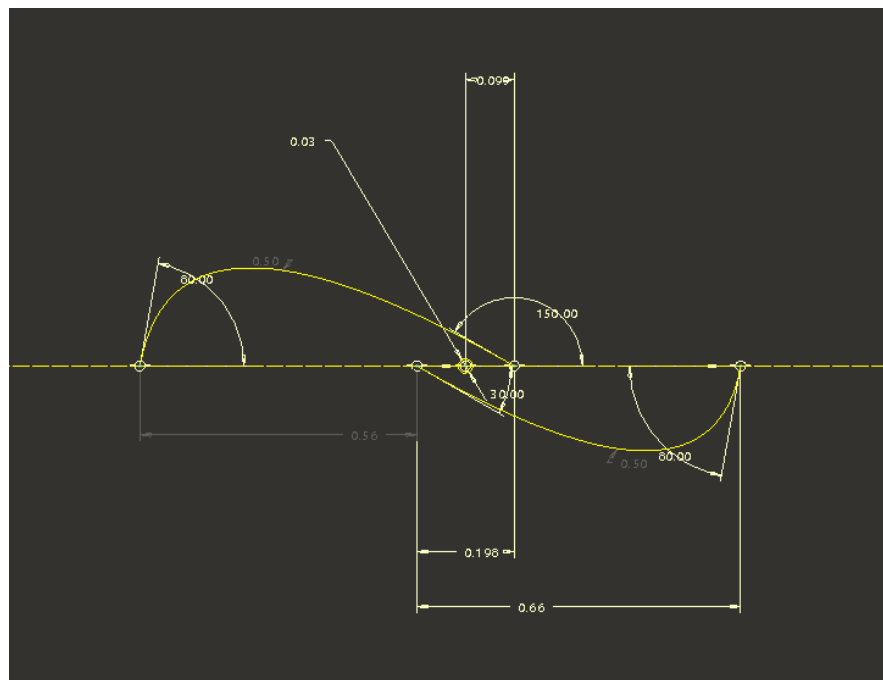


Figure 4.19: Schematic of the Helical Wind Turbine with Bach Shape 80° to 30°

4.4.3.5 Bach Shape with Outer Edge of 90° and Inner Edge of 20°

The 90° in the outer edge help the turbine to have more torque and it will increase the pressure in the outer edge.

other edges are assigned smaller element sizes which can even vary along the span of the edge as in figure 4.22.

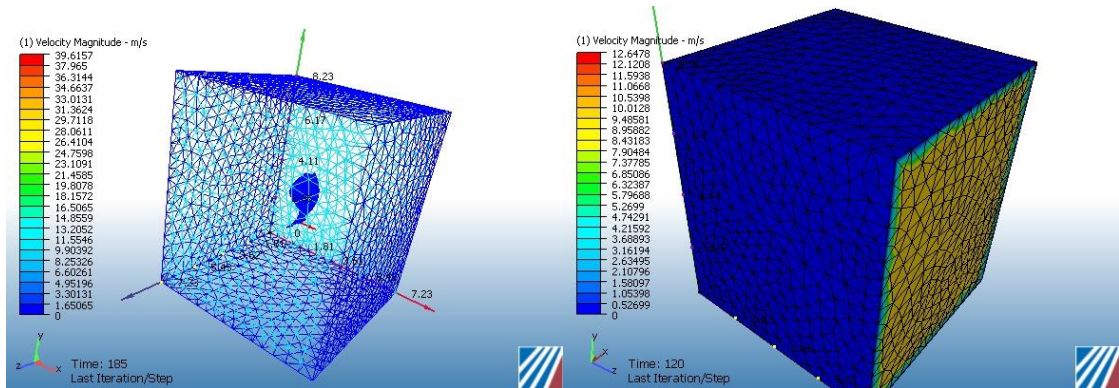


Figure 4.22: Mesh Generation for the Wind Tunnel for the Helical Wind Turbine by cfdesign Program

4.6 Wind Distribution Over The Rotor

In figure 4.23 is shown clearly that the behavior of the wind as it starts to reduce the speed when it reaches the rotor due to the conversion of the speed to mechanical energy that turns the rotor due to the friction between the wind and rotor surface and the shape of the rotor with the space gap between the blades adds a more area of contact and adds more torque to the rotor helping to generate more electricity.

As the lines in figure 4.23 show the path of the wind and also the color represents the speed of the wind.

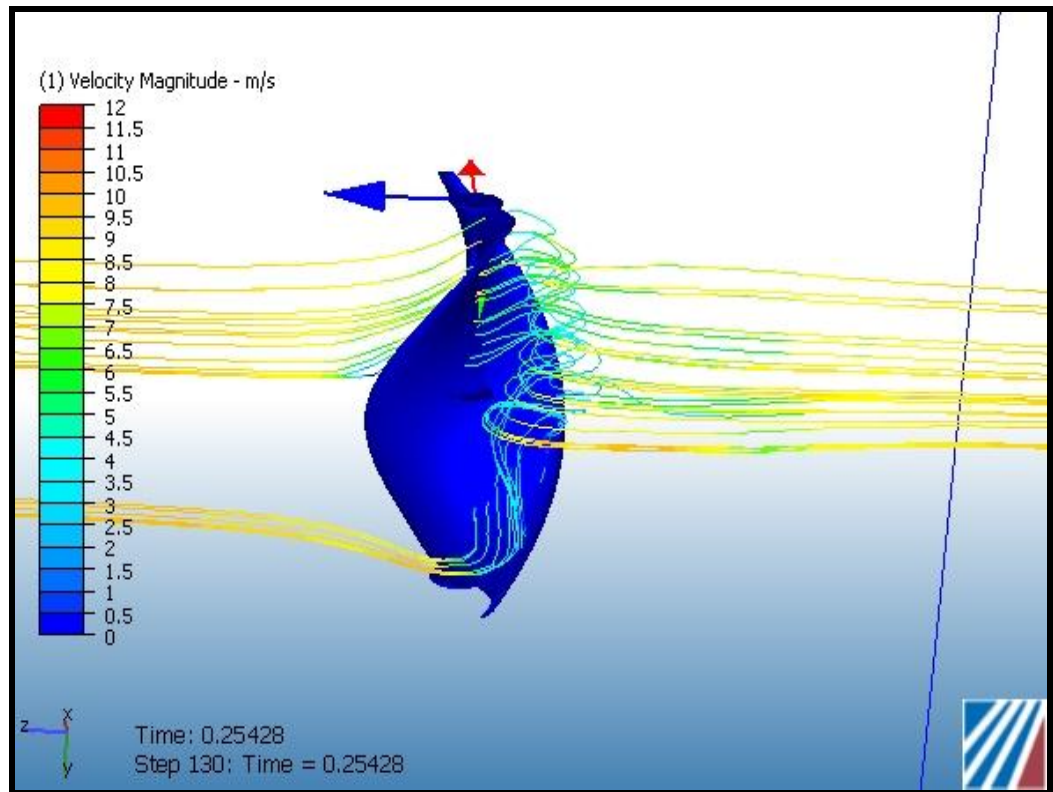


Figure 4.23: Wind Disturbution Over Bach rotor with with (90°-20°)

4.7 Coefficient of Power

The result of the cdesign program show that the one of the most important factor of the wind turbine performance is the coefficient of power which is shown in table 4.4. Figures 4.4,4.5 and 4.6 show the different performance for the different mechanical design of the aspect ratio, separation gap and Bach Cross-section profile. It shows the rate of the energy that the rotor can capture compare to the energy in the wind. The relation between the rotor rotation and the torque lead to the coefficient of power amount that generated in the rotor then due to the vary for the torque amount with the tip speed ratio for the rotor they generate a non-linear relation between the coefficient of power with the tip speed ratio in the figures 4.4, 4.5 and 4.6 .From the coefficient of power in table 4.4 we see a lot of effect due to rotor shape over the torque and RPM.

Table 4.4: Coefficient of Power for different Mechanical Design Considerations

| Helical Type | Coefficient of power(C_p) | | | | |
|--------------------|-------------------------------|-----------|-----------|----------------|-----------|
| | Aspect ratio | (3:1) | | (4:1) | |
| 0.168947 | | 0.175 | | 0.180476 | |
| Separation Gap | Minus with 20mm | | | Plus with 20mm | |
| | 0.101292 | | | 0.151206 | |
| Bach Cross-section | (20°-90°) | (40°-70°) | (60°-40°) | (80°-30°) | (90°-20°) |
| | 0.164514 | 0.122622 | 0.1965939 | 0.186317 | 0.262287 |

4.7.1 Coefficient of Power for Different Aspect Ratio

Figure 4.4 shows the coefficient of power for the helical savonius rotor with aspect ratio of (3:1), (4:1) and (5:1). The highest coefficient of power is achieved by the helical rotor with aspect ratio of 5:1 ($C_p = 0.18$) followed by the helical rotor with (4:1). The lowest value for coefficient of power is obtained by the helical rotor with aspect ratio of (3:1). The result shows that the performance of the rotor with a smaller diameter is better because it has a higher rotational speed compared to a bigger diameter. however it will affect the torque because of the smaller diameter and also in the safety matters as the smaller diameter will be harder to control in the high wind speed as the rotation will be so high and maybe reach the failure.

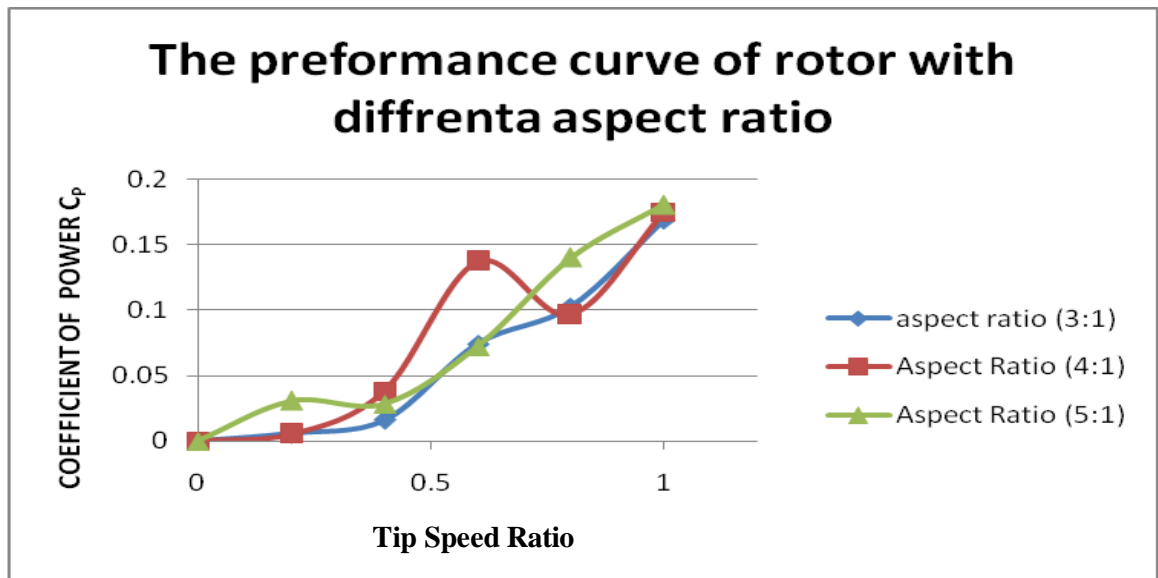


Figure 4.24: the performance curve of rotor with different aspect ratio

4.7.2 Coefficient of power for different separation gap

Figure 4.5 show the coefficient of power for the helical savonius rotor with separation gap of minus 20mm and plus 20 mm. It clearly shows a non-linear relationship between the performance of the rotor and the tip speed ratio. The highest coefficient of power is obtained with a separation gap of plus 20 mm which is ($C_p = 0.15$) followed by the helical rotor with minus 20 mm. The result show us the performance in terms of coefficient of power for a rotor with a plus gap is better because of the difference in pressure between the two blades as the minus separation gap create a negative torque due to the movement of the air to the outer side of the blade instead of the inner side which reduce the performance for the rotor.

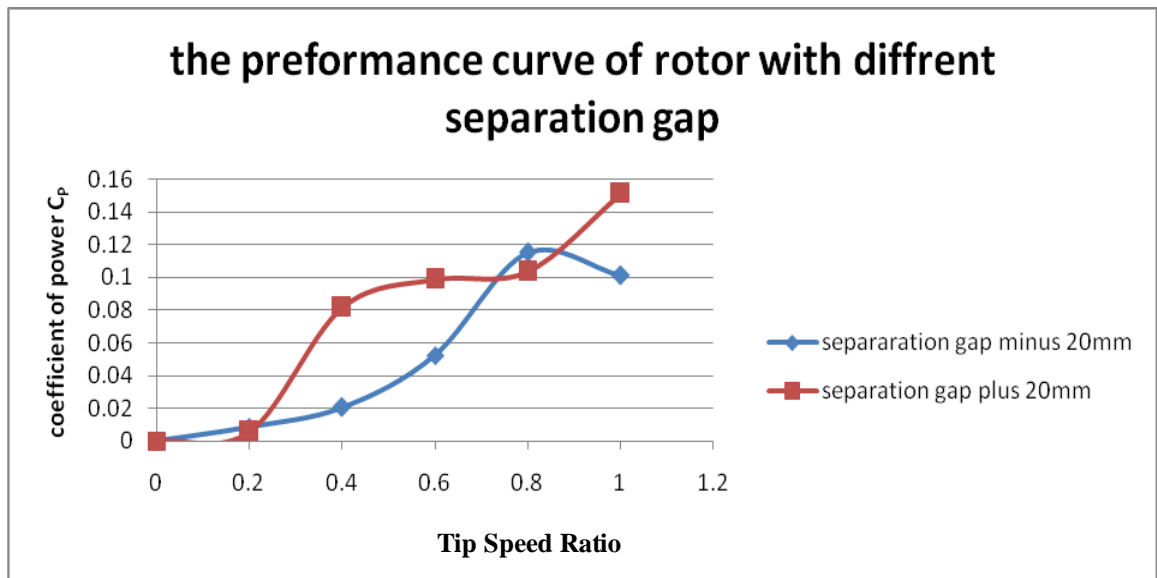


Figure 4.25: The Preformance Curve of Rotor with Diffrnet Separation Gap

4.7.3 Coefficient of power for Bach Cross-Section Profile with different inner and outer edge Angle

Figure 4.6 show the coefficient of power of the helical savonius rotor with Bach Cross-section profile with different inner and outer edge angle. In this study the values chosen are $(20^{\circ}-90^{\circ})$, $(40^{\circ}-70^{\circ})$, $(60^{\circ}-40^{\circ})$, $(80^{\circ}-30^{\circ})$ and $(90^{\circ}-20^{\circ})$. the right figure being the outer angle and the left figure the inner edge angle. It clearly shows a non-linear relationship between the performance of the rotor and the tip speed ratio. The highest coefficient of power is recorded by the helical rotor with Bach cross-section of $(90^{\circ}-20^{\circ})$ mm which is $(C_P = 0.26)$ followed by the helical rotor with Bach of $(60^{\circ}-40^{\circ})$ then $(80^{\circ}-30^{\circ})$ then $(20^{\circ}-90^{\circ})$ and the lowest performance the Bach of $(40^{\circ}-70^{\circ})$. The result shows that the performance of a rotor with a bigger outer angle is better than a bigger inner angle. It can be seen from figure 4.6 the bigger outer angle performs the best. There is a clear improvement in the coefficient in the power compare to the previous study which achieve a maximum performance of $(C_P=0.2)$ as the shape of the bach blade with $(90^{\circ}-$

20°) make the air pressure constrain in the far end of the blade and that help to create a better torque effect the whole performance.

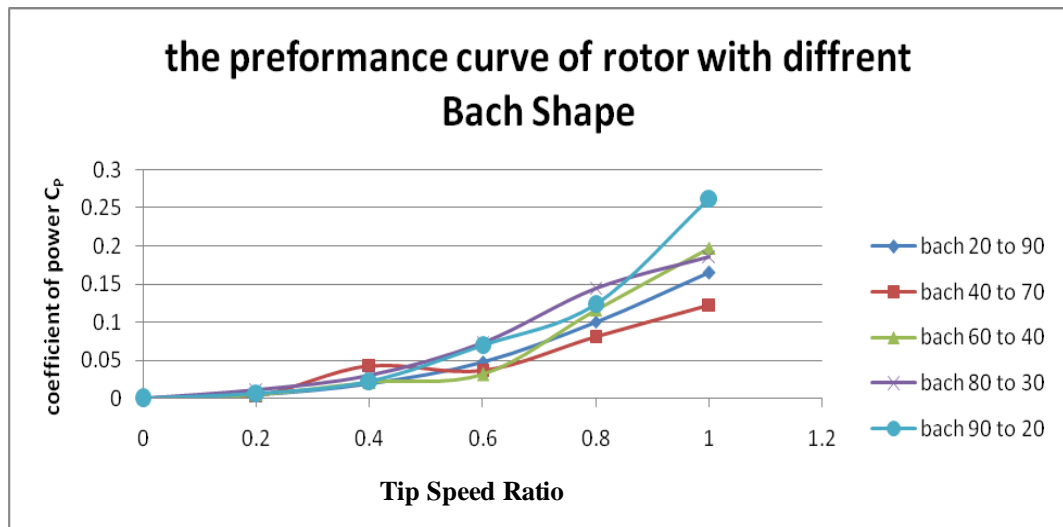


Figure 4.26: The Performance Curve of Rotor with Different Bach Shape

4.8 Coefficient of Torque

The coefficient of torque which calculated in the figures below was generated by calculate the mean torque for the rotor with rotate in 360° therefore there will be a non-linear relationship between the tips speed ratio and the coefficient of torque in figures 4.7, 4.8 and 4.9 as the torque is one of the main factor which consider in the power generation.

4.8.1 Coefficient of Torque for Different Aspect Ratio

Figure 4.7 show the coefficient of torque for the helical savonius rotor with aspect ratios of (3:1), (4:1) and (5:1). It clearly show a non-linear relationship between the coefficient of torque of the rotor and the tip speed ratio. The highest coefficient of power is

recorded for the helical rotor with an aspect ratio of (3:1) which it is ($C_T = 0.062$). This is due to the rotor diameter being the largest diameter among the rotors and that the same reason we see the (3:1) start slowly and the torque increase gradually.

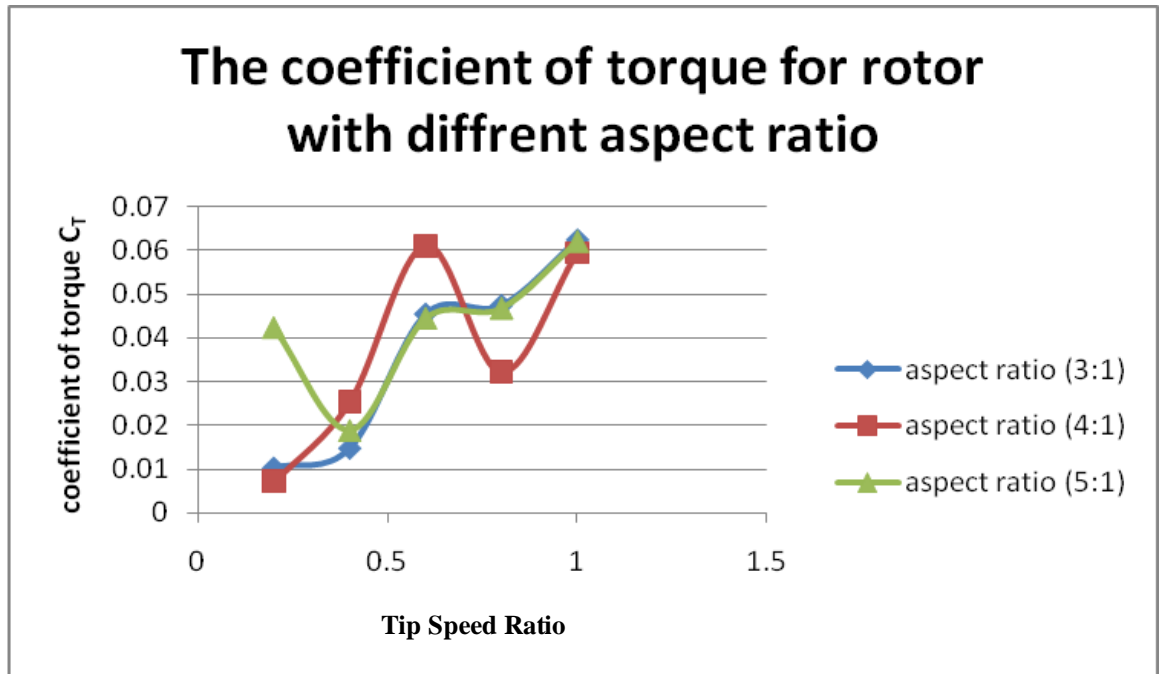


Figure 4.27: The Coefficient of Torque for Rotor with different Aspect Ratio

4.8.2 Coefficient of torque for different separation gap

Figure 4.8 show the coefficient of power for the helical savonius rotor with separation gap of minus 20mm and plus 20 mm. It clearly show a non-linear relationship between the coefficient of torque of the rotor and tip speed ratio. The highest coefficient of torque is recorded for the helical rotor with a separation gap of plus 20 mm which is ($C_P = 0.069$ at $TSR=0.6$). The result shows that the performance of a rotor with a plus gap is better and that show the effect of the torque on the performance as one of the main contributors like the rotational speed as the plus gap add more torque to the rotor.

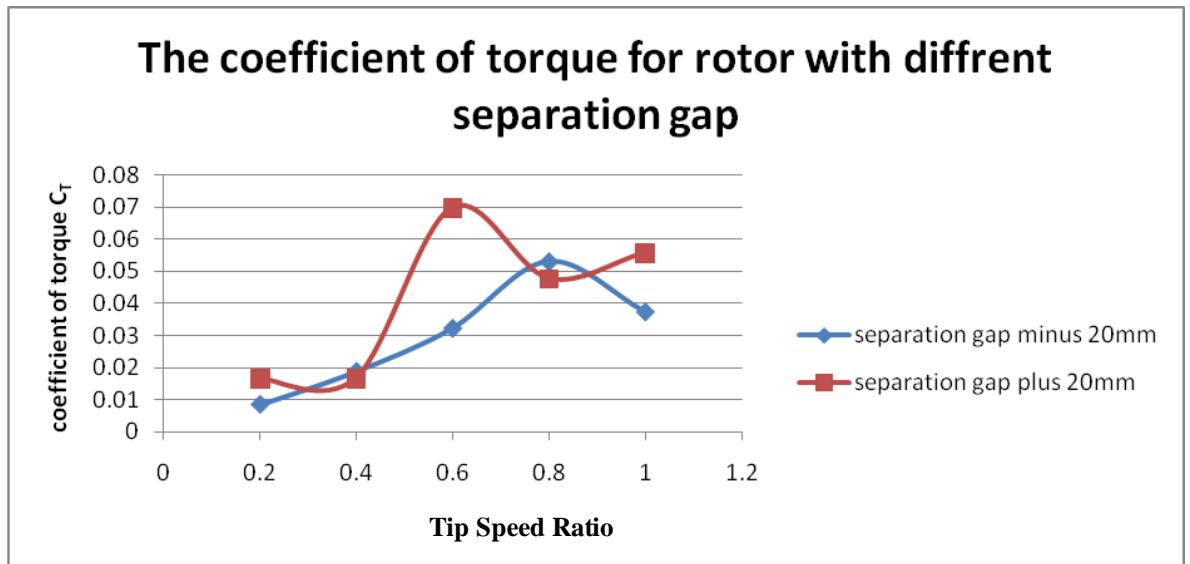


Figure 4.28: The Coefficient of Torque for Rotor with different Separation gap

4.8.3 Coefficient of Torque for Bach Cross-Section Profile with different inner and outer edge Angle

Figure 4.9 show the coefficient of torque for the helical savonius rotor with Bach Cross-section profile with different inner and outer edge angle. The values of (20°-90°), (40°-70°), (60°-40°), (80°-30°) and (90°-20°). were chosen where the first figure is the inner angle followed by the outer edge angle. It clearly show the non-linear curves between the performance of the rotor and the tip speed ratio. The highest coefficient of torque is recorded for the helical rotor with Bach cross-section of (90°-20°) mm which is ($C_t = 0.0967$) followed by the helical rotor with Bach of (80°-30°) then (60°-40°) then (20°-90°) and the minimum performance the Bach of (40°-70°) which shows a little improvement at TSR=0.4 achieving a value of ($C_t=0.0389$). The result shows that the coefficient of torque for rotor with a bigger outer angle is better than the bigger inner angle. This is because of the difference in the two blades pressure caused by the Bach shape of the blade which add more pressure to the outer edge with the velocity of the air.

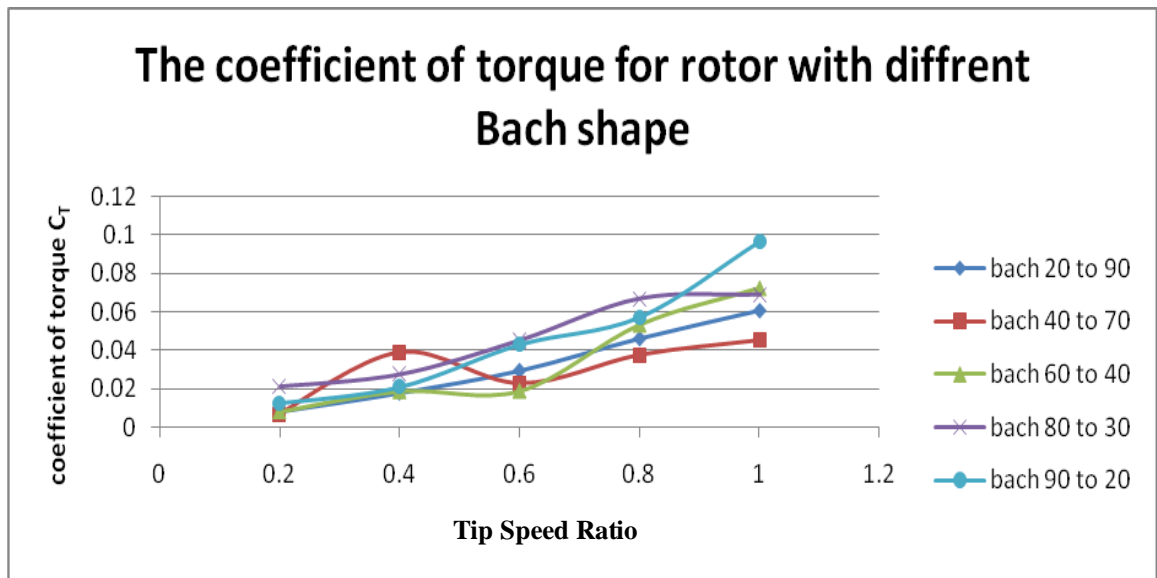


Figure 4.29: The Coefficient of torque for Rotor with Diffrnet Bach Shape

4.9 Output power

The output power is ultimately the value that needs to be the highest possible.

4.9.1 Output Power for Different Aspect Ratio

Table 4.5 show the power generated by the helical savonius rotor with aspect ratio of (3:1), (4:1) and (5:1). It clearly shows that the highest rotor generation is the one with aspect ratio of (3:1), This can be attributed to the large projected area facing the wind compared to the other rotors because of the larger diameter creating more air contacting with the rotor surface can consider to the double than the (5:1) rotor.

Table 4.5: Power Production for Helical Savonius with Different Aspect Ratio

| TSR | Power For Aspect Ratio (3:1) in Watt | Power For Aspect Ratio (4:1) in Watt | Power For Aspect Ratio (5:1) in Watt |
|------------|---|---|---|
| 0 | 0 | 0 | 0 |
| 0.2 | 6.776347995 | 4.8498 | 22.66723459 |
| 0.4 | 19.55700614 | 35.1889 | 20.86403561 |
| 0.6 | 90.69389488 | 127.27 | 53.53267 |
| 0.8 | 125.6288426 | 89.266 | 103.858121 |
| 1 | 206.6187297 | 162.29 | 134.5103637 |

4.9.2 Output Power for Different Separation Gap

Table 4.6 show the power generated by the helical savonius rotor with separation gap of minus 20mm and plus 20 mm. It clearly shows that the highest output power achieved is the one with separation gap of plus 20 mm because of the higher torque and the RPM for the plus will be higher as the diameter for the rotor will be smaller compare to the minus one.

Table 4.6: Power Production for Helical Savonius with Different Separation Gap

| TSR | Power For Minus Separation Gap in Watt | Power For Plus Separation Gap in Watt |
|------------|---|--|
| 0 | 0 | 0 |
| 0.2 | 6.6006 | 7.06735384 |
| 0.4 | 25.09730963 | 22.22239838 |
| 0.6 | 64.08814109 | 120.7459117 |
| 0.8 | 140.69588003 | 126.723292 |
| 1 | 123.8781661 | 184.9215137 |

4.9.3 Output Power for Bach Cross-section Profile with Different Inner and Outer Edge Angle

Table 4.7 show the power generated by the helical savonius rotor with Bach Cross-section profile with different inner and outer edge angle. The values chosen are (20°-90°), (40°-70°), (60°-40°), (80°-30°) and (90°-20°). The highest output is achieved by the one with Bach of (90°-20°) followed by (60°-40°) , (80°-30°) , (20°-90°) and (40°-70°) that back to the performance of the design as get both the best coefficient of power and coefficient of torque.

This show that the best design in term of output power for the helical rotor is the Bach helical rotor with outer angle of 90° and inner angle of 20° in the term of the coefficient of power and the coefficient of torque as the make it the best among all the designs.

Table 4.7: Power Production for Helical Savonius with Different Inner and Outer Edge Angle for Bach Cross-section Profile

| TSR | Power For Bach with (20°-90°) in Watt | Power For Bach with (40°-70°) in Watt | Power For Bach with (60°-40°) in Watt | Power For Bach with (80°-30°) in Watt | Power For Bach with (90°-20°) in Watt |
|------------|--|--|--|--|--|
| 0 | 0 | 0 | 0 | 0 | 0 |
| 0.2 | 5.349926452 | 4.63334268 | 5.539471674 | 14.72162881 | 8.282213843 |
| 0.4 | 23.80368816 | 52.14382642 | 25.24843364 | 37.13282534 | 28.0162454 |
| 0.6 | 54.4611582 | 45.1496412 | 37.96833183 | 90.07109721 | 85.6335189 |
| 0.8 | 122.3335432 | 99.69981584 | 141.9410383 | 176.9387104 | 152.1311833 |
| 1 | 201.1977612 | 149.9677245 | 240.4304379 | 227.8623734 | 320.772206 |

CHAPTER FIVE

CONCLUSIONS AND RECOMMENDATIONS

5.1. Conclusions

A total of 10 prototypes of helical savonius wind turbines were designed using the Pro Engineer program . 3 prototypes were designed with different aspect ratios, 2 prototypes were designed with different separation gaps and another 5 prototypes with different Bach cross-section profile. All the prototypes were designed with an overlap ratio of 0.3. The following conclusions are made based on CFD studies:

The coefficient of power increases with increasing aspect ratio however a small diameter will give a smaller torque therefore the lowest of (3:1) is chosen. For separation gap it was found that the design with a plus separation gap performs better at all TSR values except when TSR=0.8. The coefficient of torque for the minus design is better than the plus design at TSR=0.6. However in general the plus design is better than minus design and its give more power output than the minus design. For the bach cross section area its was found that the rotor with the highest coefficient of power is the one with (90°-20°) outer to inner edge angle . It also has the highest coefficient of torque . The highest power output is also achieved by the (90°-20°) with a value of (cp=0.26).

The data for the wind speed show us that the wind speed would be much higher during the evening and night. This is due to the change in weather from the morning session where the clouds seem to be building up to rain in the morning due to the calm weather when the wind speed is relatively low. The turbine needs a low start up speed to generate electric. The wind

speed data range from 2m/s to 4.7m/s during evening. On a calm day, it ranges from 0.6m/s to 2.4m/s.

5.2. Recommendations for Further Work

Further work could be done to obtain more data to improve the performance of the helical wind turbine. The following recommendations could be considered for future work to enhance the search in this area:

- 1) To study the effect of the shift size in the helical wind turbine design and its ratio to the gap.
- 2) To study the effect of use different type of material for the rotor.
- 3) Study the design in other CFD program and compare the results.
- 4) Design a prototype and test it at real wind situations to experience the real behavior of the wind turbine.

REFERENCES

- Aldo Vieira da Rosa (2005), *Fundamentals of Renewable Energy Processes*, 1st edn. United States of America, Elsevier Inc.
- Burçin Deda Altan*, Mehmet Atilgan (2009). The use of a curtain design to increase the performance level of a Savonius wind rotors. *Renewable Energy xxx* (2009) 1–9.
- Dan Chiras (2006). *The Homeowner's Guide to Renewable Energy*, 2nd edn. Canada, New Society Publishers.
- Darrieus GJM (1931). Turbine Having its rotating shaft transverse to the flow of the current. US Patent No.1835081, 1931.
- David Olson and Ken Visser (2008), *Self-Starting Contra-Rotating Vertical Axis Wind Turbine for Home Heating Applications*.
- Edwards PJ (1986). *Small scale wind power guide For New Zealand, Australia and the South Pacific*. New Zealand: New Zealand Energy Research and Development Committee. University of Auckland, November, 1986. Report No. 136.
- Eldridge, F.R., *Wind Machines*, Washington, DC, Report AER-75-12937, p. 55, 1975
- Erick hau (2006), *wind turbines fundamentals, technologies, application, economaics*, 2nd edn. Berlin Springer.
- Frank Scheurich (2009) *Small-Scale Wind Turbines for Sustainable Energy Supply in Urban Environments*. Universities 21 International Conference for Graduate Research Students Sustainable Cities for the Future University of

Melbourne and University of Queensland, Australia, 29 November – 5 December 2009.

- Gary L. Johnson (2006), WIND ENERGY SYSTEMS, 3rd edn. Manhattan.
- Gasch, R., Twele, J. (2002), Wind Power Plants, 1st edn. London, James & James.
- Ibrahim Al-Bahadly (2009), Building a wind turbine for rural home. Energy for Sustainable Development vol. 13 (2009) 159–165.
- J. Blazer (2001), Computational Fluid Dynamics: principles and applications, 1st edn. UK, Elsevier Inc.
- M.A. Kamoji, S.B. Kedare, S.V. Prabhu (2009), Experimental investigations on single stage modified Savonius rotor. Renewable Energy vol.34 (2009) 521–529
- Mazharul Islam, David S.-K. Ting, Amir Fartaj (2008), Aerodynamic models for Darrieus-type straight-bladed vertical axis wind turbines. Renewable and Sustainable Energy Reviews vol. 12 (2008) 1087–1109.
- Md. Nahidul Islam Khan, M. Tariq Iqbal, Michael Hinchey, and Vlastimil Masek (2009), PERFORMANCE OF SAVONIUS ROTOR AS A WATER CURRENT TURBINE. Journal of Ocean Technology 2009 Vol. 4, No. 2, 2009.
- Mukund R. Patel (1999), Wind and Solar Power Systems, 1st edn. United States of America, CRC Press LLC.
- Robert Y. Redlinger, er Dannemand Andersen and Poul Erik Morthorst (2002), Wind Energy in the 21st Century, 1st edn. New York: published by PALGRAVE.

- Thomas Ackermann (2005), *Wind Power in Power Systems*, 1st edn. England, John Wiley & Sons, Ltd.
- U.K. Saha, M. Jaya Rajkumar (2008), on the performance analysis of Savonius rotor with twisted blades. *Renewable Energy* vol. 31 (2006) 1776–1788.
- V. D'Alessandro*, S. Montelpare, R. Ricci, A. Secchiaroli (2010). Unsteady Aerodynamics of a Savonius wind rotor: a new computational approach for the simulation of energy performance. *Energy* xxx (2010) 1-15.
- Vaughn Nelson (2009), *WIND ENERGY Renewable Energy and the Environment*, 1st edn. United States of America, & Francis Group, LLC.
- Volker Quaschnig (2005), *Understanding Renewable Energy Systems*, 1st edn. Published by Earthscan in the UK and USA.
- Zhenzhou Zhao, Yuan Zheng, Xiaoyun Xu, Wenming Liu, Guoxiang Hu (2010). *Research on the Improvement of the Performance of Savonius Rotor Based on Numerical Study*.

APPENDIX A

PRESSURE DISTURBUTION OVER A BACH CROSS-SECTION PROFILE WITH 90° TO 20° THROUGH 360° ROTATION

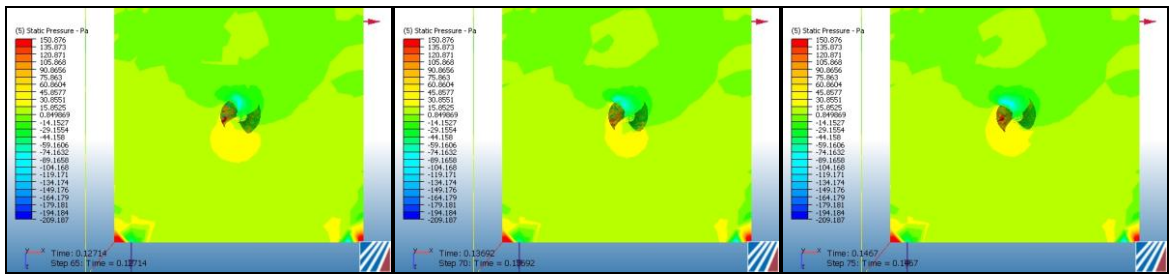
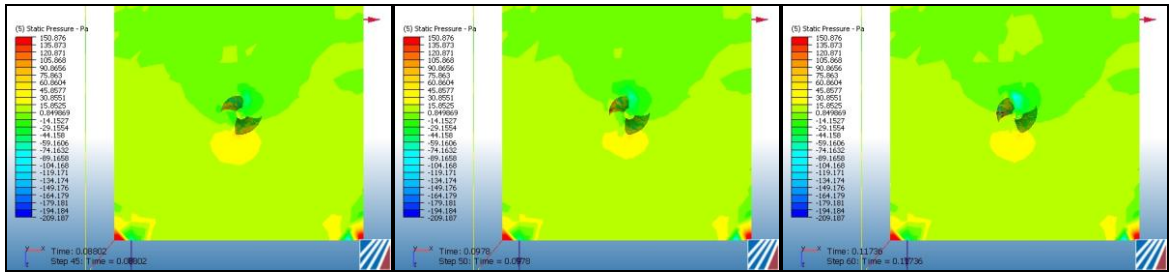
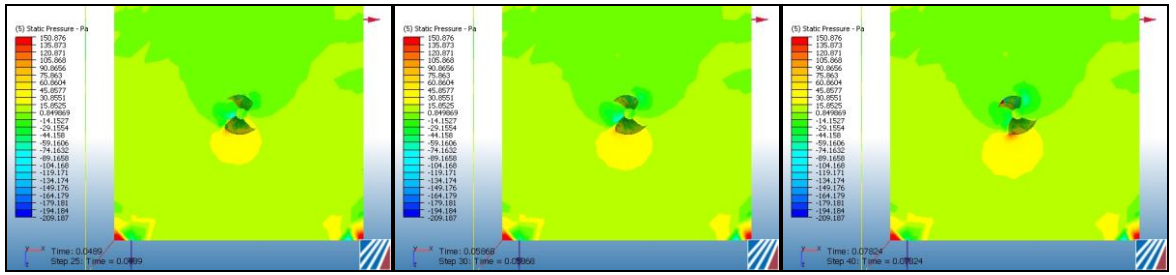
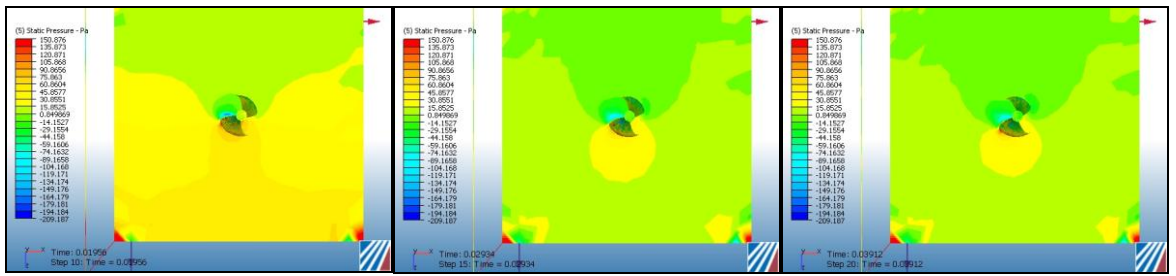


Figure A1: Pressure Distribution for Bach with (90°-20°)

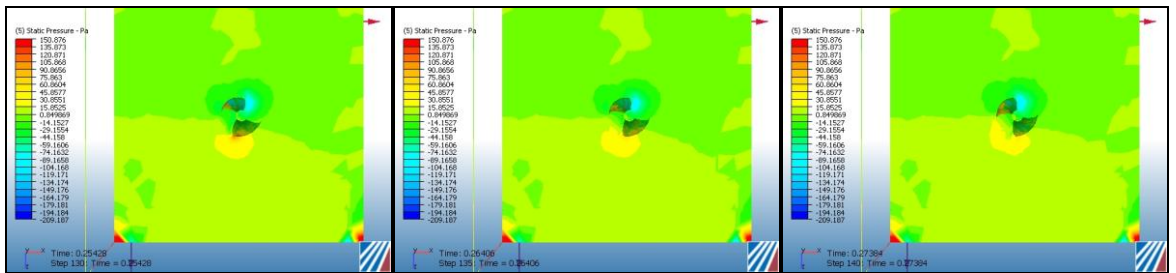
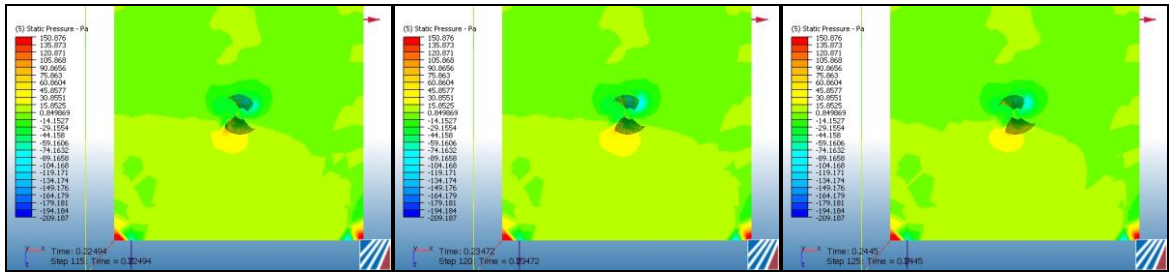
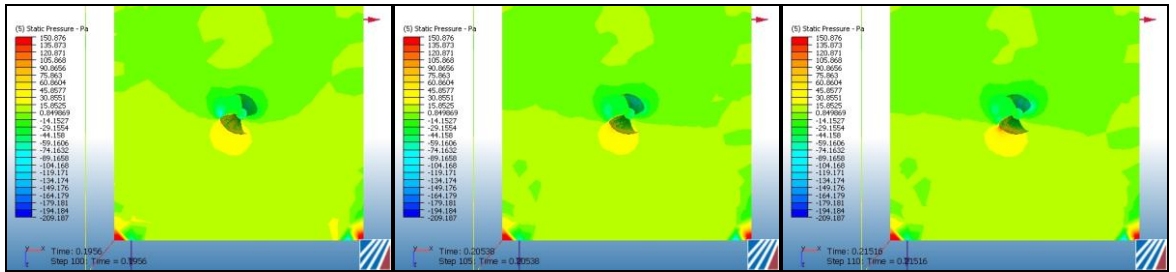
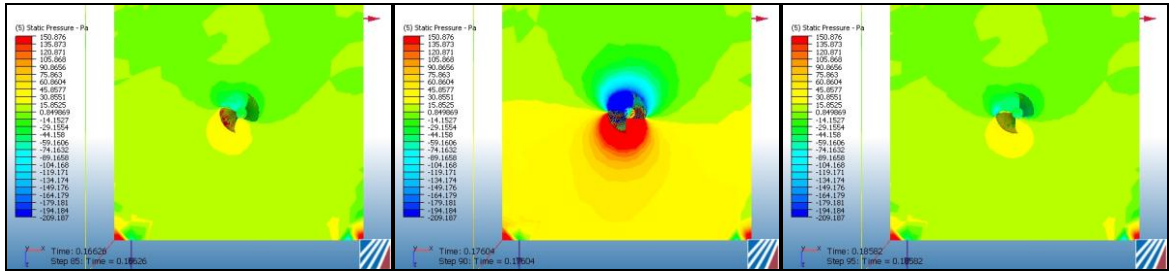


Figure A2: Pressure Distribution for Bach with (90°-20°)

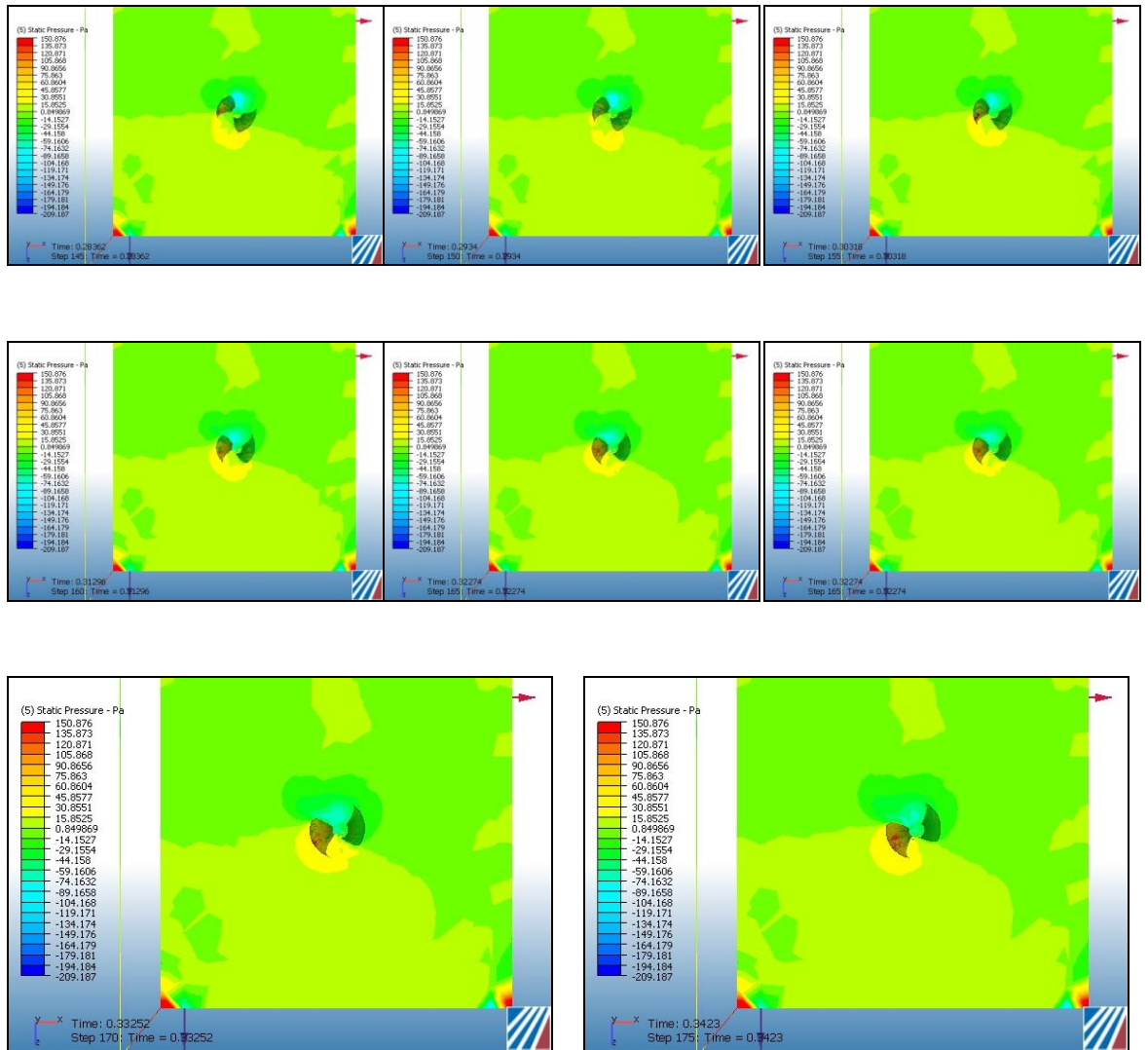


Figure A3: Pressure Distribution for Bach with (90°-20°)

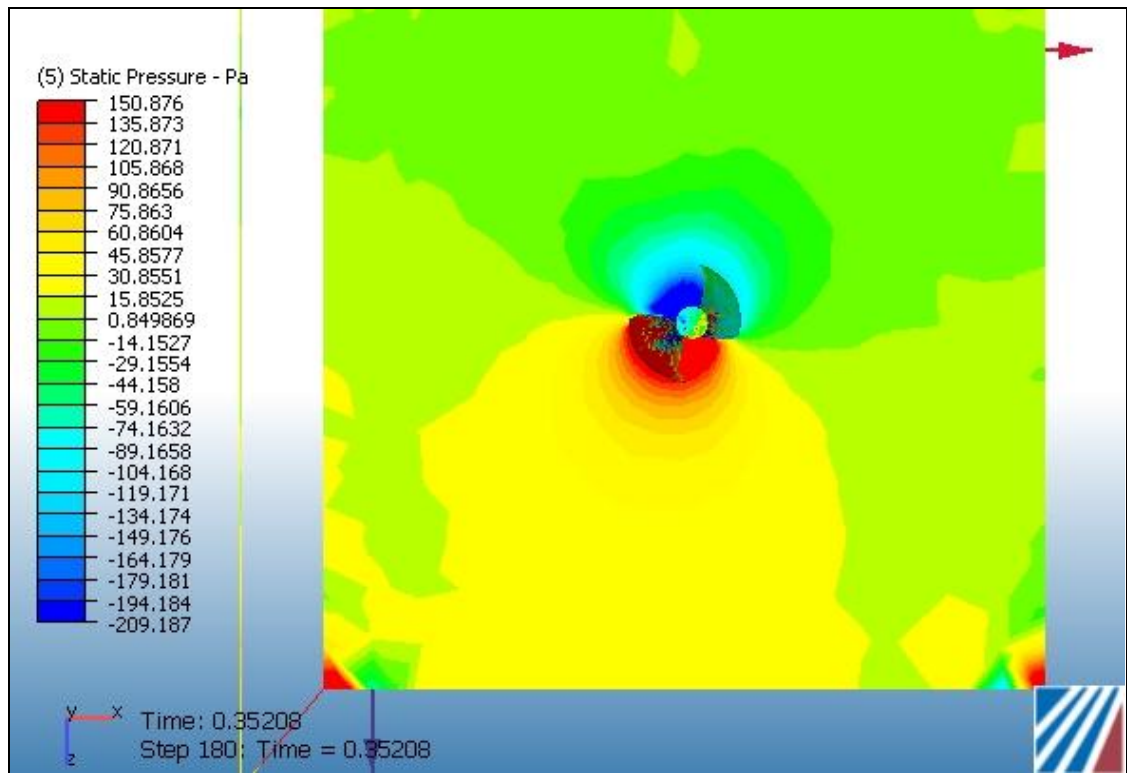


Figure A4: Pressure Distribution for Bach with (90°-20°)

APPENDIX B

VELOCITY DISTURBUTION OVER A BACH CROSS-SECTION PROFILE WITH 90° TO 20° THROUGH 360° ROTATION

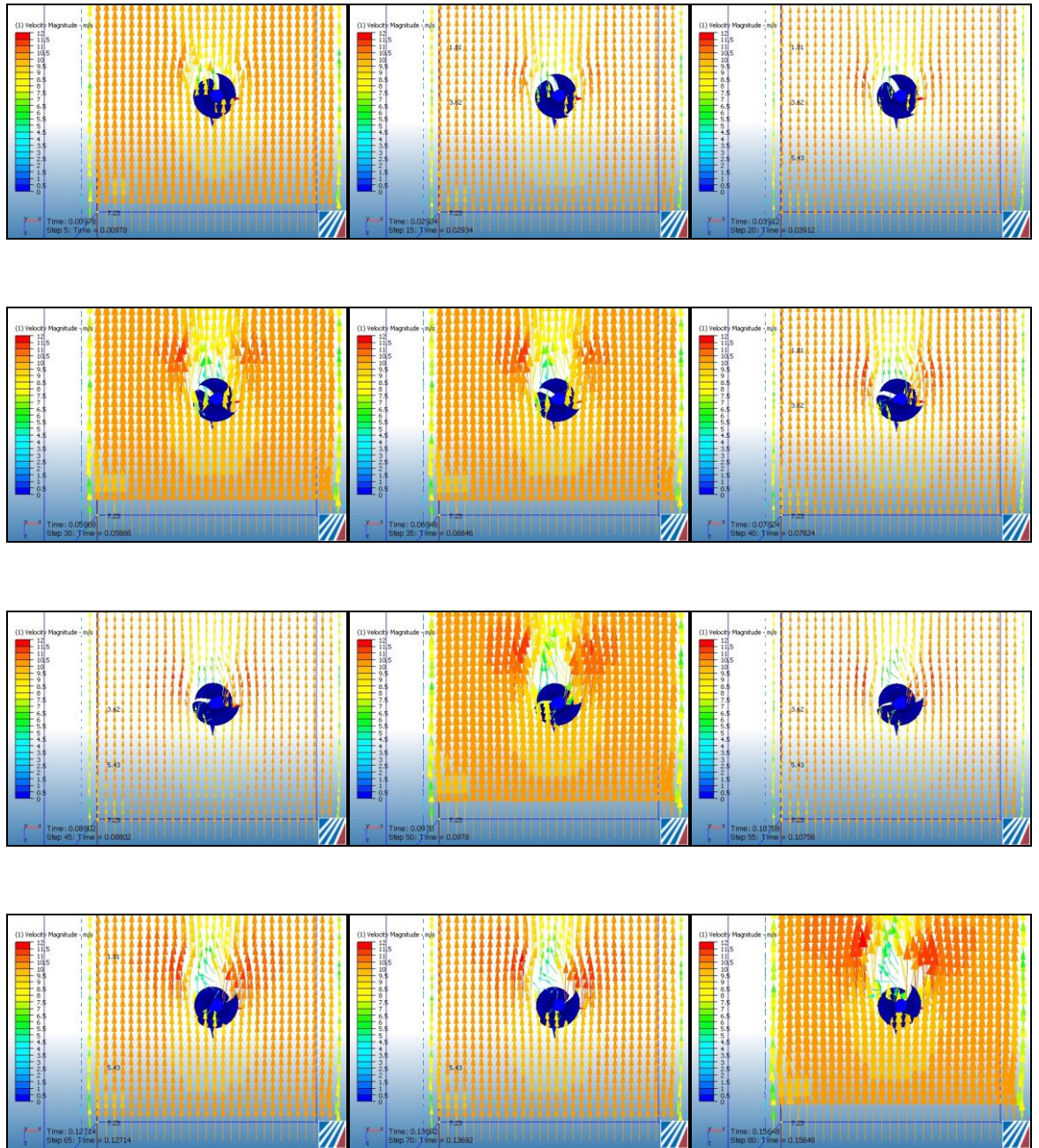


Figure B1: velocity Distribution with wind direction for Bach with (90°-20°) (Top View)

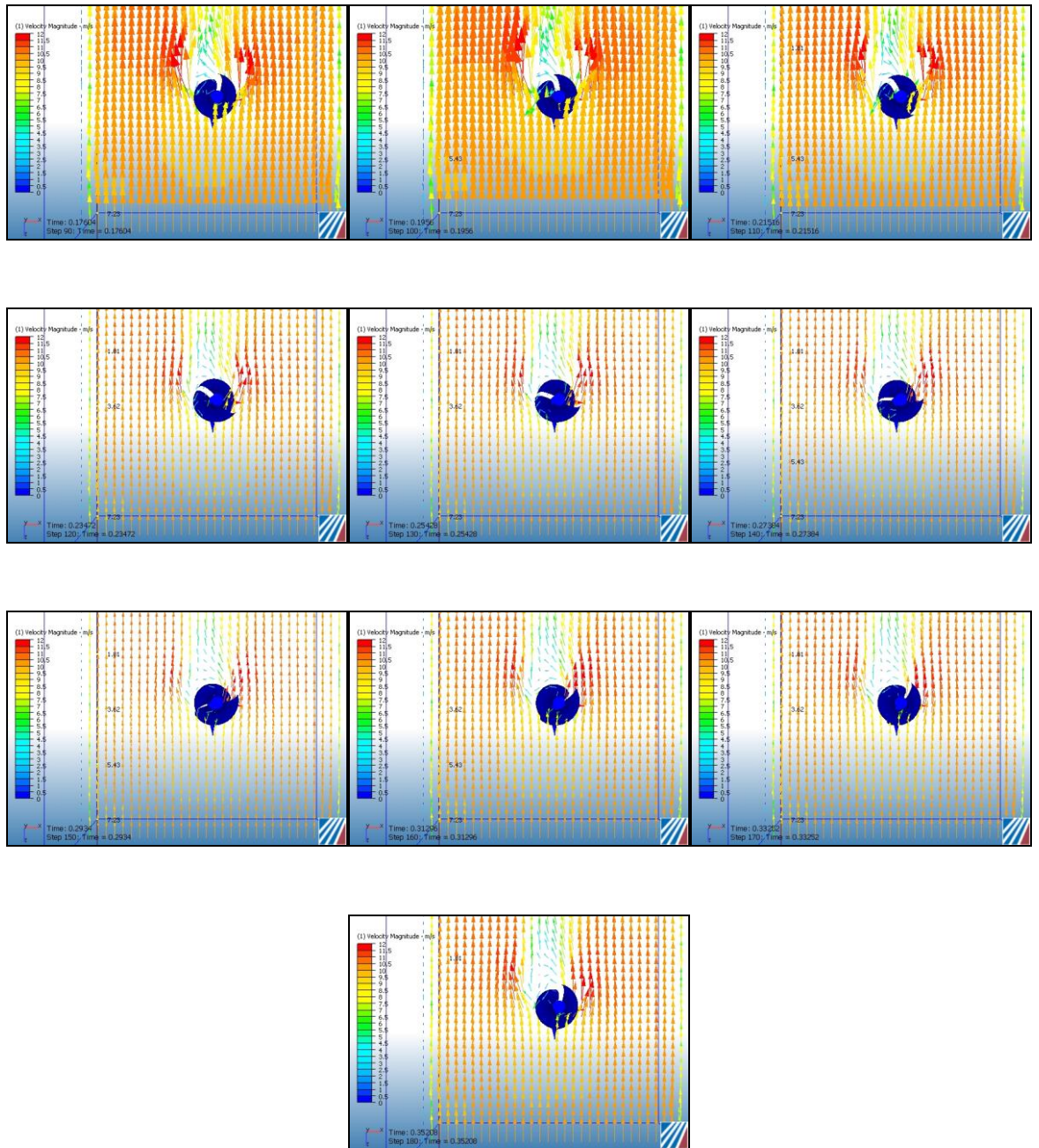


Figure B2: velocity Distribution with wind direction for Bach with (90°-20°) (Top View)

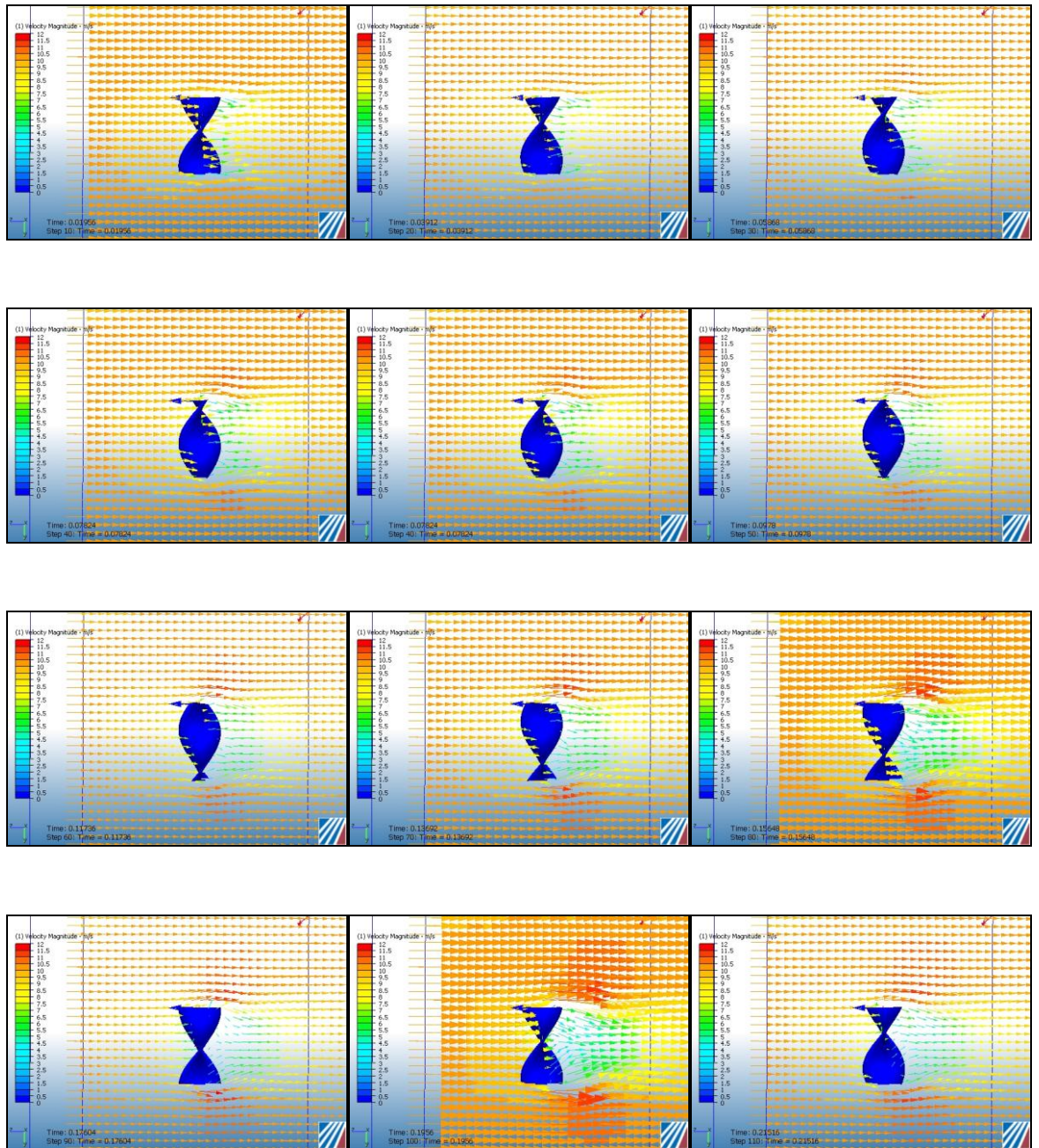


Figure B3: velocity Distribution with wind direction for Bach with (90°-20°) (side View)

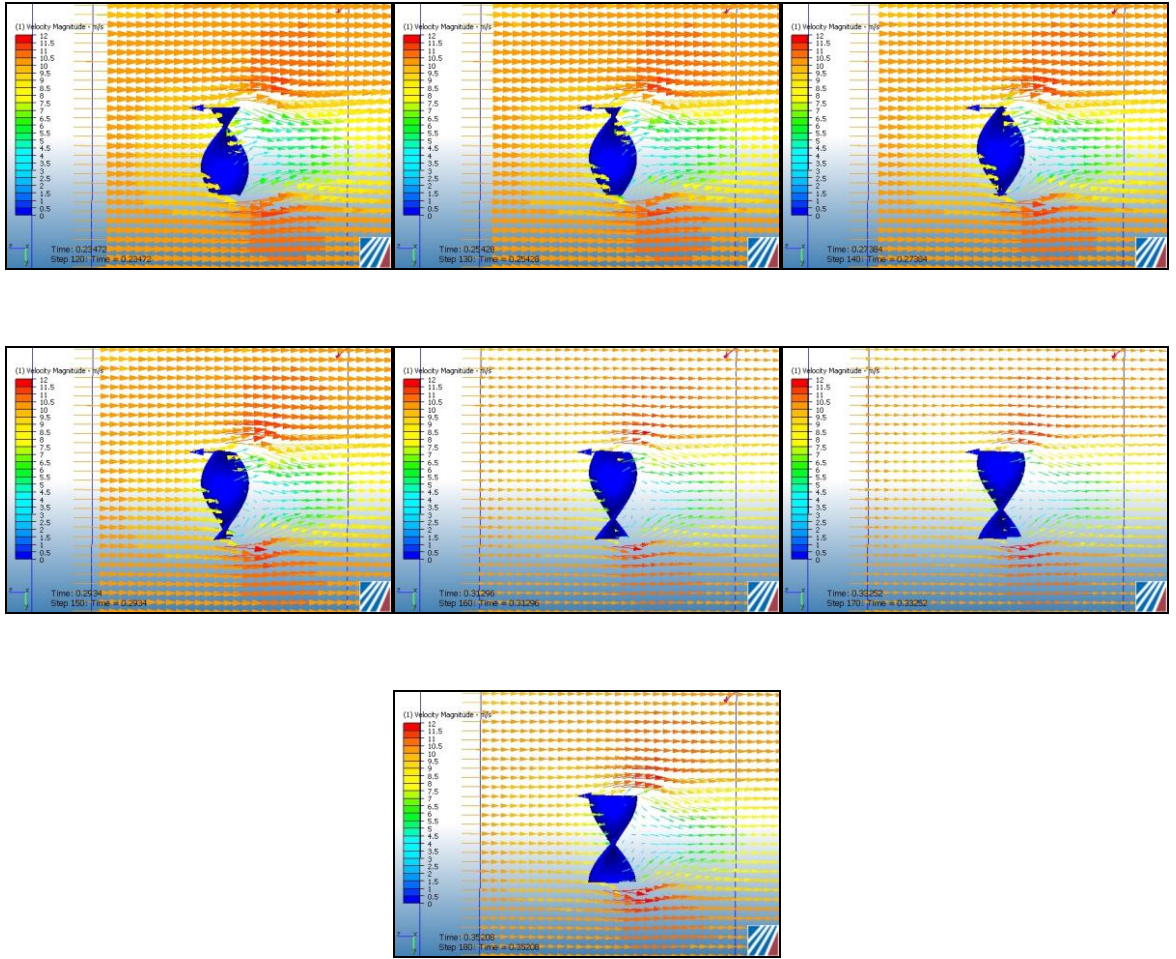


Figure B4: velocity Distribution with wind direction for Bach with (90°-20°) (Side View)

APPENDIX C

SAMPLE OF RAW DATA OBTAINED FROM MALAYSIAN METROROGICAL STATION

Table C.1: Raw data from Kuala Terengganu station 1/1/2006-30/1/2006

| | | | 24 hours | Maximum | |
|------|-------|-----|---------------|------------------------|----------------|
| Year | Month | Day | mean (M/S) | Direction in degree | Speed (M/S) |
| 2006 | 1 | 1 | 3.4 | 30 | 7.6 |
| 2006 | 1 | 2 | 3.6 | 50 | 9.1 |
| 2006 | 1 | 3 | 2.5 | 80 | 8.2 |
| 2006 | 1 | 4 | 3.0 | 80 | 9.0 |
| 2006 | 1 | 5 | 4.3 | 70 | 10.5 |
| 2006 | 1 | 6 | 2.5 | 20 | 9.3 |
| 2006 | 1 | 7 | 3.7 | 60 | 9.8 |
| 2006 | 1 | 8 | 4.3 | 60 | 11.1 |
| 2006 | 1 | 9 | 3.9 | 70 | 11.1 |
| 2006 | 1 | 10 | 4.5 | 60 | 11.0 |
| 2006 | 1 | 11 | 3.7 | 70 | 10.5 |
| 2006 | 1 | 12 | 4.3 | 40 | 8.9 |
| 2006 | 1 | 13 | 3.3 | 20 | 9.1 |
| 2006 | 1 | 14 | 3.0 | 20 | 8.9 |
| 2006 | 1 | 15 | 2.5 | 50 | 7.5 |
| 2006 | 1 | 16 | 2.4 | 30 | 7.3 |
| 2006 | 1 | 17 | 2.9 | 50 | 9.5 |
| 2006 | 1 | 18 | 3.0 | 70 | 8.1 |
| 2006 | 1 | 19 | 1.6 | 80 | 6.5 |
| 2006 | 1 | 20 | 2.2 | 70 | 8.0 |
| 2006 | 1 | 21 | 2.1 | 50 | 7.0 |
| 2006 | 1 | 22 | 2.3 | 60 | 8.2 |
| 2006 | 1 | 23 | 2.3 | 30 | 8.2 |
| 2006 | 1 | 24 | 2.5 | 10 | 8.6 |
| 2006 | 1 | 25 | 2.5 | 90 | 8.8 |
| 2006 | 1 | 26 | 4.3 | 80 | 9.6 |
| 2006 | 1 | 27 | 4.4 | 80 | 9.7 |
| 2006 | 1 | 28 | 3.7 | 80 | 8.9 |
| 2006 | 1 | 29 | 3.7 | 80 | 9.0 |

Table C.2: Raw data from Kota Bharu station 1/1/2006-30/1/2006

| | | | 24 hours | Maximum | |
|------|-------|-----|---------------|------------------------|----------------|
| Year | Month | Day | mean (M/S) | Direction in degree | Speed (M/S) |
| 2006 | 1 | 1 | 2.2 | 30 | 8.1 |
| 2006 | 1 | 2 | 1.8 | 60 | 8.1 |
| 2006 | 1 | 3 | 2.4 | 60 | 7.9 |
| 2006 | 1 | 4 | 2.6 | 40 | 10.1 |
| 2006 | 1 | 5 | 3.2 | 70 | 6.2 |
| 2006 | 1 | 6 | 2.4 | 90 | 10.0 |
| 2006 | 1 | 7 | 3.5 | 60 | 10.5 |
| 2006 | 1 | 8 | 3.4 | 90 | 10.3 |
| 2006 | 1 | 9 | 3.5 | 60 | 10.6 |
| 2006 | 1 | 10 | 3.9 | 40 | 9.9 |
| 2006 | 1 | 11 | 3.0 | 60 | 9.5 |
| 2006 | 1 | 12 | 2.2 | 30 | 8.5 |
| 2006 | 1 | 13 | 1.6 | 60 | 7.4 |
| 2006 | 1 | 14 | 1.6 | 40 | 7.9 |
| 2006 | 1 | 15 | 1.9 | 70 | 8.5 |
| 2006 | 1 | 16 | 2.4 | 50 | 8.2 |
| 2006 | 1 | 17 | 2.7 | 30 | 9.0 |
| 2006 | 1 | 18 | 2.8 | 70 | 9.6 |
| 2006 | 1 | 19 | 1.8 | 80 | 7.3 |
| 2006 | 1 | 20 | 1.8 | 50 | 9.0 |
| 2006 | 1 | 21 | 1.3 | 30 | 6.9 |
| 2006 | 1 | 22 | 1.8 | 40 | 9.6 |
| 2006 | 1 | 23 | 1.6 | 50 | 8.1 |
| 2006 | 1 | 24 | 1.3 | 20 | 6.7 |
| 2006 | 1 | 25 | 2.1 | 70 | 9.5 |
| 2006 | 1 | 26 | 4.2 | 80 | 11.0 |
| 2006 | 1 | 27 | 4.1 | 70 | 11.6 |
| 2006 | 1 | 28 | 2.9 | 60 | 9.6 |
| 2006 | 1 | 29 | 3.1 | 70 | 10.3 |

